PRIMATE ANTERIOR INSULAR CORTEX REPRESENTS ECONOMIC DECISION VARIABLES POSTULATED BY PROSPECT THEORY

by

You-Ping Yang

A dissertation submitted to the Johns Hopkins University in conformity with the requirements for the degree of Doctor of Philosophy

Baltimore, Maryland

January 2021

Abstract

Humans and animals need to make decisions under various degrees of uncertainty. These decisions are strongly influenced by an individual's risk attitude. Substantial studies have demonstrated that one's risk attitude can vary substantially across different behavioral contexts. For instance, humans and animals show different risk attitudes when facing risky gains versus risky losses. The abundance of resources in the environment and the current wealth of subjects also modulate an individual's risk attitude. Prospect theory, the most successful and wide-ranging descriptive model of decision-making under risk, explains these behavioral effects using the concepts of a reference point and loss aversion.

However, at present, prospect theory cannot be clearly interpreted in terms of neuronal mechanisms. None of the known structures or processes involved in decision-making in the primate brain has been convincingly related to the two key concepts: reference point-dependence and loss aversion.

Based on human imaging and lesion studies, we hypothesized that the anterior insular cortex (AIC) may be the candidate that represent the current state of the subject (the reference point) as well as reference-dependent value signals that differ in loss or gain context (asymmetrical value functions in loss and gain) suggested by prospect theory.

Using a new token gambling task, we found that macaques, like humans, change their risk attitude across wealth levels and gain/loss contexts. In addition, monkeys' risk behaviors were well explained with a wealth-dependent prospect theory model. Furthermore, neurons in the primate AIC monitor contextual factor that influence monkey's risk attitudes. Many AIC neurons encoding the wealth level of the monkey as well as the expected value of options in a gain/loss-

specific manner. A subset of AIC neurons can further predict inter-trial fluctuations of the monkey's risk attitude. These findings suggest a role of the primate AIC in representing economic gain and loss relative to a reference point and in influencing the likelihood of accepting a risk during uncertain decisions. We anticipate our finding to be a starting point for thoughtful investigation of neural implementation of core components in the prospect theory.

Primary Reader and Advisor:

Veit Stuphorn, Associate Professor

Zanvyl Krieger Mind/Brain Institute

Solomon H. Snyder Department of Neuroscience, School of Medicine

Johns Hopkins University

Secondary Reader:

Daeyeol Lee, Bloomberg Distinguished Professor

Department of Psychological and Brain Sciences, Krieger School of Arts and Sciences

Solomon H. Snyder Department of Neuroscience, School of Medicine

Zanvyl Krieger Mind/Brain Institute

Johns Hopkins University

Acknowledgments

Earning this Ph.D. is definitely a remarkable milestone in my life. Looking back on my journey to Ph.D., I feel it resemblant to the classic story "*Journey to the West*"- not only in that in order to achieve the goal, one must face her inner challenges and overcome obstacles with firm confidence and perseverance, but most of all, that I was not alone along the way. Had it not been for the help from many people around me, I would never be able to make it.

First of all, I would like to thank my advisor Dr. Veit Stuphorn for all his guidance and help. I will definitely miss the time when I "fight with Veit" in scientific discussion. His patience and tolerance provide a very friendly environment where I can express my thoughts without fear of making mistakes, which has great influence on my development as an independent researcher. Being a scientist studying decision-making, I know little about how an "optimal" decision is made, but I do believe joining the Stuphorn lab is one of the best decisions I have ever made.

I would also like to express my gratitude to my committee members, Dr. Patricia Janak, Dr. Daeyeol Lee, and Dr. Christopher Fetsch for all their suggestions and comments on my research. I much enjoyed all our brainstorming discussions. I am especially grateful to my committee chair, Dr. Ernst Niebur, who is also my closest collaborator. In the countless meetings we had, he was always so kind and being ready to give me a hand whenever I needed it. I would also like to thank Dr. Shreesh Mysore, Dr. Christopher Honey, and Dr. Kishore Kuchibhotla for their provocative feedbacks every time I presented my research. Knowing that people cared about your research is encouraging, and it is an important drive that motivates me forward.

I am very fortunate to have great lab members like Dr. Erik Emeric, who was extremely patient in teaching me everything about primate research; and Jacob Elsey, who helped me not only in the lab, but more about the life in U.S. in general. Thank you both for making my days in

the Stuphorn lab so enjoyable. And many thanks to the members of the MBI/PBS family: Ofelia Garalde, Bill Quinlan, Bill Nash, Susan Soohoo, Eric Potter, and Charles Meyer – not only for their administrative and technical supports but also their warm-hearted friendliness; Elissa Zurbuchen, Julie Bullock, Laura Dalrymple, Rebecca Swisdak – their administrative assistance indeed made my Ph.D. life much earlier.

I would also like to say thank you to many of my friends in Baltimore and in Taiwan, for their blessings and supports. Those include (but not limited to): Chia-Hsuan, Feng-Wei, Yen-Lin and Chin-Fu – the time spent with them is a major enrichment in my Ph.D. life; and especially my best friend Hsiao-Yun – the words she gave me as we both decided to pursue a Ph.D. abroad turned to be the force that supported me through. I would also like to thank my previous mentors – Dr. Keng-Chen Liang, Dr. Chun-I Yeh, and Dr. Yu-Cheng Pei, who inspired and encouraged me to embark on my journey in academia. .

Thanks to my family – my mother (A-Mu), sister (A-Ciao) and lovely dog (little-ke). Only with their unconditional love and support, I can pursue my dream without any hesitation. Thanks to my aunt and uncle (and their family) for always taking care of me no matter I am in Taiwan or overseas. Thanks to Chia-Hung (Kampanat), my husband and also my travel agent, who helps me literally everything other than research. Without him, it was not possible for me to complete the degree.

As the story of the classic novel, my “journey to the west” also have some major characters in company. At the very end, I would like to thank Wen-Kai, who have influenced me the most, Ke-Hsin and Ting-Yu. I am grateful for having their company for years in the exploration of science and career in academia, and I wish to have them in the journey ahead.

Contents

List of Tables

List of Figures

Chapter 1

Introduction

1.1 Background and significance

Humans and animals need to make decisions under various degrees of uncertainty. These decisions are strongly influenced by an individual's risk attitude. Risk attitude is often seen as a fundamental, stable personality trait (Gilaie-Dotan et al., 2014b). However, recent studies have demonstrated that one's risk attitude can vary substantially across different behavioral contexts(Pedroni et al., 2017; E. U. Weber et al., 2002). For instance, humans show different risk attitudes when facing risky gains versus risky losses(Canessa et al., 2013). The abundance of resources in the environment and the current wealth of subjects also modulate an individual's risk attitude(Juechems et al., 2017; Stephens, 2008; Vermeer et al., 2014; Yamada et al., 2013). These findings suggest that risk attitude is not a stable personality trait, but rather emerges during the process of decision-making in a context-dependent manner(Farashahi et al., 2018; Payne et al., 1992; Slovic, 1995).

Prospect theory(Tversky & Kahneman, 1979), the most successful and wide-ranging descriptive model of decision-making under risk, explains these and other behavioral effects using the concepts of a reference point and loss aversion. Prospect theory first assumes that possible future outcomes ('prospects') are evaluated relative to a reference point (reflecting current wealth and resources), either as gains or as losses. Second, losses are assumed to weigh stronger than gains, which leads to an aversion to loss.

Evidence from Capuchin monkey trading behavior indicates these primates displayed several hallmark biases like humans, including reference dependence and loss aversion (Chen et al.,

2006). It may suggest that there is an evolutionarily ancient decision-making system in the primate brain dealing with these risk preference characteristics shared by humans and animals. However, at present prospect theory cannot be clearly interpreted in terms of neuronal mechanisms. None of the known structures or processes involved in decision-making in the primate brain has been convincingly related to the two key concepts of reference point-dependence and loss aversion.

Human imaging experiments and lesion studies have identified a network of brain areas that are active during decision-making under risk(Breiter et al., 2001; Hsu et al., 2005, 2009; Huettel et al., 2006; Jung et al., 2018; Krain et al., 2006; Kuhnen & Knutson, 2005; Rao et al., 2008). Of particular interest is the anterior insular cortex (AIC), a large heterogeneous cortex in the depth of the Sylvian fissure. Human fMRI studies have suggested a crucial role of AIC in promoting risk-averse behavior(Kuhnen & Knutson, 2005), representing the current internal state(Craig & Craig, 2009), and influencing the level of loss aversion(Canessa et al., 2013). Patients with lesions in the insular cortex are less risk-averse(Clark et al., 2008; Shiv et al., 2005). These findings suggest a wider role of AIC in representing both the current state of the self (reference point) and aversive signals that strengthen the tendency for risk-averse choices (loss aversion). However, due to the limited spatial and temporal resolution of the BOLD signal, human imaging studies are limited in terms of the interpretation of the underlying neuronal activities. Thus, neuronal mechanisms underlying these fundamental features of risk-preference are not well understood.

To address this issue, we recorded neural activity in the AIC of monkeys during a token-based gambling task developed to test their risk attitude in the gain and loss domain and as a function of starting token number (i.e., wealth level or reference point). We hypothesized that

AIC neurons represent behaviorally relevant contextual information that influences the probability of choosing a risky reward option. We first examined behavioral data to test if and how monkeys changed risk attitudes in varying behavioral contexts (gain or loss outcomes; different starting token assets). Next, we tested a series of models to predict monkey's choice based on decision-related variables. Then we identified AIC neurons representing factors that influence risk attitudes, such as start token number, gain or loss outcome, the value of the option, and uncertainty. Finally, we determined whether the AIC neurons encoding these factors also predict the monkey's choice or risk attitude.

The current research is one of only a few studies (<5) to examine animal's risk attitude in the "loss" domain. With the development of the token-based gambling task, it helped us to find that monkeys' risk attitudes were not always constant across context but adjusted by various contextual factors. In addition, comparing to substantial studies focus on animals' responses to aversive stimuli like intense light/sound, air-puff, foot-shock, bitter taste, or omission of reward delivery, this task allowed us to examined animal's risk attitude when facing an "economic loss", which was investigated by only a few studies. Moreover, through the token-based gambling task developed here, we can explore important effects in economic theory, such as status quo bias, loss aversion, the endowment effect (subjects are more likely to keep an object they own than acquire the same object if they do not own it), and the framing effect (subject tends to avoid risk when a positive frame is presented but seek risk when a negative frame is presented). By combining the behavioral paradigm with electrophysiological recording, this research has the power to discover, for the first time, the specific coding of value signal in the gain and loss domain and at different wealth levels in the primate brain (specifically in the anterior insular cortex in this dissertation). The anterior insular cortex is clearly highly important for decision-

making under risk. Nevertheless, with respect to single-unit studies of cognitive functions, it is complete terra incognita. The insular cortex is clearly an understudied brain region that likely participates in many different functions. Specifying its functional role in one context in detail will provide a great impetus for the further study of this important brain region.

1.2 Decision making under risk

We make a lot of decisions every day: some simple, some complicated. Sometimes we can be quite certain that our actions will result in a given outcome, while at other times we can only know that our choice will result in a given outcome with a specific probability. When, in a given decision scenario, the outcomes of potential choices are uncertain, it is called a decision under risk. When making decisions under risk, our preference toward risk will strongly influence our choices. Imagine that you have won a prize with $1000 in an event, and now the host offers you a choice to directly get the $1000 or toss a coin to double the prize or return it to zero. Your choice between the safe option and the risky option will be highly affected by your risk attitude. A risk-averse person will prefer to get $1000 for sure because it is safer, while a person who is risk-prone will be more likely to toss the coin because it provides a chance to win more bonus (though loss the prize as well).

Since the outcomes of most of our choices are uncertain, decisions under risk are central to our daily lives. Decision-making under risk has been extensively studied in several scientific fields, such as economics, finance, psychology, and neuroscience. However, across these disciplines, different conceptual frameworks have been used for describing risk (Glimcher, 2008). This has led to ambiguity and confusion. Thus, it is important to understand the meaning of terms such as risk, risk attitude, value, and utility in distinct perspectives.

1.3 Risk attitude

1.3.1 Classical economic theory -- Expected value theory

Consider a gambler faced with two options: (1) throwing a single six-sided die, which wins $1500 if an odd number appears and wins $500 if an even number appears, or (2) getting $1000 certainly without throwing a die (see Table1). The classical economic theory began with the work of Pascal (1670/1966), who proposed that people deal with this problem by maximizing expected value. That is, people should calculate the expected value (EV) of each option and choose the one with the highest EV. The EV of each option is defined as the magnitude of each possible outcome multiplied by its probability summed over all possible outcomes:

$$EV = x1p1 + x2p2 + \cdots + xnpn \quad = \sum_{i=1}^{n} xipi\,,$$

where x_i is the (monetary) outcome of the state i and p_i is the probability of state i.

Table 1.1 shows how the expected value can be computed in the above example. Doing this shows that the EV of option 1 and option 2 is both $1000. Thus, if choices are selected by maximizing EV, a decision-maker should have no preference between these two options since the EV of these two options are identical. This example suggests two important things about Pascal's Expected Value theory. First, the decision-maker is expected to care only about the EV of options but to be not sensitive to the variance of outcomes (i.e., risk). Thus, the decision-maker is assumed to be risk-neutral. Second, the subjective value of each option is a direct linear function of its objective value (**Figure 1.1A**). This function is indifferent to a global scaling operation. Thus, the relative advantage of one option over another is not changed, if a certain amount is added or subtracted evenly from all options. Therefore, no matter what the current wealth level of a subject is (i.e., the momentary reference point), the subject should make the same consistent decisions.

1.3.2 Classical economic theory -- Expected utility theory

The theory of expected value is mathematically influential and allows people to calculate their long-run average payoffs in many decision-making contexts. However, it is severely limited as a descriptive theory of human decisions under risk, because of its inability to account for risk-seeking or risk-averse behavior. For instance, it cannot explain why people would prefer getting $49 for sure over getting $100 by chance or why people would purchase insurance. In all of these scenarios, people prefer the safe over the risky option even so the EV of the safe option is lower than the EV of the risky option. Daniel Bernoulli (1738) dealt with this problem by replacing objective (e.g., monetary) values with subjective values, that is, the 'utility' or pleasantness one (expect to) experience following that particular decision (Stearns, 2000). Instead of maximizing the expected value (EV) of options, Bernoulli's model suggests people tend to choose the option with the highest expected utility (EU):

$$EU = u(x1)p1 + u(x2)p2 + \cdots + u(xn)pn = \sum_{i=1}^{n} u(xi)pi,$$

where u(x_i) represents the utility of outcome of state i (x_i) and p_i is the probability of state i. In this model, the main difference from Pascal's expected value formulation is that there is a nonlinear mapping between the monetary outcomes (x_i) and their corresponding internal utility (u(x_i)).

$$u(xi) = xi^{\alpha},$$

where u(x_i) is an exponential function of monetary outcomes (x_i) with a free parameter α.

In Bernoulli's original formulation, he used a logarithmic transformation. In modern versions, it is common to use a power law, as indicated above. This mathematical formulation is identical to Stevens's Power Law (Stevens, 2017) that specifies the psychophysical function that

transforms the strength of a sensory stimulus into a subjective human level of perception. Likewise, the utility function transforms the objective state of the world (e.g., the monetary amount that is lost or gained) into an internal subjective value. The parameter α controls the curvature of the utility function and therefore the subjective mapping of the objective outcome. Moreover, the expected utility model of decision under risk links the curvature of the utility function naturally to an individual's risk-attitude (Von Neumann & Morgenstern, 1947). If α is one, it results in a straight line as described in the expected value model (**Figure 1.1A**). (Therefore, Pascal's expected value model is contained in expected utility theory as a special case.) If α is less than one, the utility function is a concave curve so that the internal utility-scale is compressed (**Figure 1.1B**). That means that subjective value becomes less sensitive to changes in objective magnitude as it increases. This leads to less sensitivity to large outcome magnitudes and thus to risk-averse behavior. On the other hand, if α is larger than one, the utility function is a convex curve, indicating that subjective value becomes more sensitive to changes in objective magnitude as it goes up (**Figure 1.1C**). This leads to risk-seeking behavior.

To illustrate the relationship between risk attitude and utility function curvature, we first consider a person with a concave utility function (e.g., α = 0.92; **Figure 1.1B**). The utility difference between an outcome of \$50 and of \$100 can be calculated as: u (\$*100*) – u (\$50) = $\$100^{0.92} - \$50^{0.92} = \$32.62$. To examine the effect of outcome magnitude on utility we study next another option set [\$150, \$200] with an expected value difference that is identical to the first set [\$50, \$100], but with an overall increased magnitude of the outcomes. The utility difference between these two options is: u (\$*200*) – u (\$150) = $\$200^{0.92} - \$150^{0.92} = \$30.44$. This demonstrates that for a person with a concave utility function the subjective wealth increment between two options decreases (from \$32.62 to \$30.44), as the overall wealth level across both

options increases (from 50 to 100). When such a subject faces a choice between: (1) getting \$100 for certain or (2) getting either \$200 or \$0 with equal probability 0.5, the EU of the sure option will be $\$100^{0.92} * 1 = 69.18$ and the EU of the risky option will be $\$200^{0.92} * 0.5 + \$0 * 0.5 = 65.45$ (**Table 1.2**). Thus, the subject with a *concave* utility function will be more likely to choose the sure option and behave in a *risk-aversive* manner.

Next, we consider a subject with a convex utility function (e.g., $\alpha = 1.08$; **Figure 1.1C**). The utility differences (ΔEUs) of the two option sets [\$50, \$100] and [\$150, \$200] for this subject are: $\$100^{1.08} - \$50^{1.08} = \$76.17$ and $\$200^{1.08} - \$150^{1.08} = \$81.61$, respectively. Thus, for this subject, the subjective wealth increment increases, as the overall wealth level increases. If the subject faces the same choice between getting \$100 for certain or getting \$200 with a winning probability of 0.5, the EU of the sure option will be $\$100^{1.08} * 1 = \$144.54$ and the EU of the risky option will be $\$200^{1.08} * 0.5 = \$152.79$ (**Table 1.3**). Thus, the subject with a *convex* utility function will prefer the risky option over the sure option behave in a *risk-seeking* manner.

The expected utility (EU) theory extended the expected value (EV) theory in at least two aspects. First, in contrast to EV theory, which assumes people make decisions in a risk-neutral manner, EU theory allows people to exhibit risk-seeking or risk-aversive behavior. Specifically, the EU model assigns a free parameter α to describe the risk attitude through a nonlinear utility function. This modification makes the EU theory a better predictor of human choice behavior. Second, this nonlinear utility function also leads to an effect of wealth level on risk attitude. People are predicted to have different levels of risk preference with changing starting wealth points since the marginal utilities are modulated by the curvature of the utility function. For two subjects with the same concave utility function, an identical gamble offer will be more attractive

to the subject that owns nothing than to a subject that is a millionaire, because the marginal increase in utility for the poor subject is higher than for the rich subject.

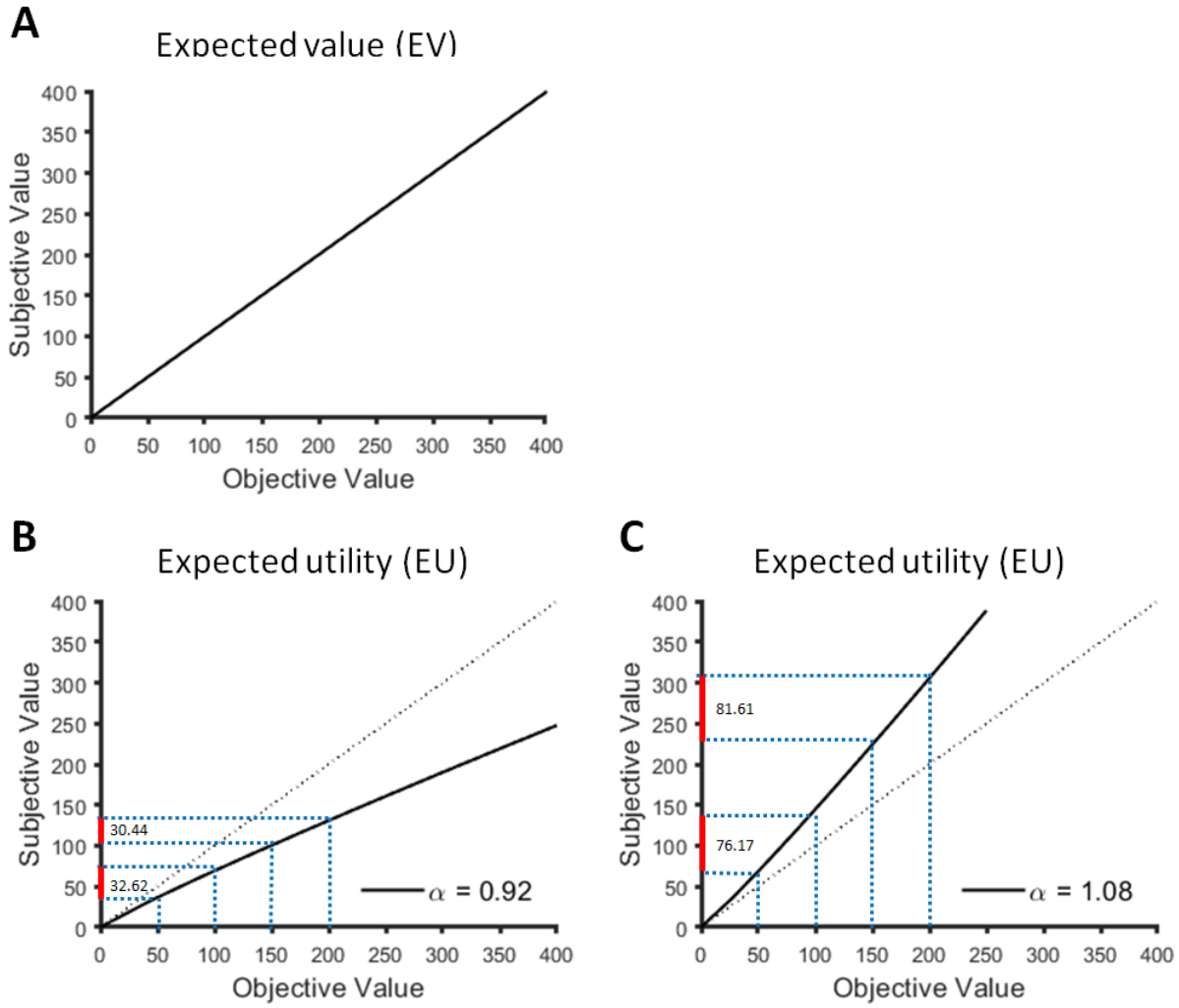

Figure 1.1. Expected value and expected utility functions. (A) Value function in expected value formulation, demonstrating a linear relationship between objective value and subjective value. Plotted as the black dotted (diagonal) line in panels (B) and (C). (B) Utility function with $\alpha = 0.92$ in expected utility formulation, demonstrating a concave relationship between objective value and subjective value. (C) Utility function with $\alpha = 1.08$ in expected utility formulation, demonstrating a convex relationship between objective value and subjective value.

Table 1.1. The decision matrix for the example gambler computing Expected Value (EV)

	Option 1: Risky Option			Option 2: Sure Option
Value (x_i)	\$200	\$0		\$100
Probability (p_i)	0.5	0.5		1
$x_i * p_i$	\$100	\$0		\$100
Expected value (EV)	\$100		=	\$100

Table 1.2. The decision matrix for an example gambler with a concave utility function ($\alpha = 0.92$)

	Option 1: Risky Option			Option 2: Sure Option
Value (x_i)	\$200	\$0		\$100
Utility ($u(x_i)$)	$\$200^{0.92}$	$\$0^{0.92}$		$\$100^{0.92}$
Probability (p_i)	0.5	0.5		1
$u(xi) * p_i$	\$65.45	\$0		\$69.18
Expected utility (EU)	\$65.45		<	\$69.18

Table 1.3. The decision matrix for an example gambler with a convex utility function ($\alpha = 1.08$)

	Option 1: Risky Option			Option 2: Sure Option
Value (x_i)	\$200	\$0		\$100
Utility ($u(x_i)$)	$\$200^{1.08}$	$\$0^{1.08}$		$\$100^{1.08}$
Probability (p_i)	0.5	0.5		1
$u(xi) * p_i$	\$152.79	\$0		\$144.54
Expected utility (EU)	\$152.79		>	\$144.54

1.3.3 Allais Paradox that violates expected utility theory

Expected utility theory has been developed as a normative model of rational choice under risk (Von Neumann & Morgenstern, 1947). This model proposes that any individual who makes a decision under risk by maximizing expected utility should satisfy certain axioms of rational behavior. The four axioms of the von Neumann-Morgenstern utility theorem include (1) completeness, (2) transitivity, (3) continuity, and (4) independence of irrelevant alternatives. *Completeness* assumes that an individual has well-defined preferences and is always able to make choices between any two alternatives. *Transitivity* assumes that the preference of an individual is consistent across any three options. *Continuity* assumes that when there are three lotteries (with the individual preferring A to B and B to C), there should exist a probability *p* such that the individual is indifferent between lottery B and the combination of A and C ($pA + (1-p)C$). *Independence of irrelevant alternatives* assumes that the preference of an individual should maintain the same order of preference between two alternatives when adding an irrelevant third alternative or when the two are presented independently of the irrelevant alternative. In this context, 'irrelevant' means of lower value than the other options and thus never chosen. In general, human subjects agree that all of the four axioms embody reasonable guidelines of rational behavior. However, several decades of studying human decision-making have revealed numerous classes of choices among risk options in which humans systematically violate the axioms of expected utility theory.

Allais (1953) proposed an example that shows an inconsistency of actually observed choices with the prediction of expected utility theory (Allais, 1953). In the Allais Paradox, there are two separate decision problems.

In the first problem, the subject chooses between two lotteries:

Lottery A: $100 million with certainty (100%)

Lottery B: $ 500 million with a probability of 10%

$100 million with a probability of 89%

Nothing with a probability of 1%

In the second problem, the subject chooses between other two lotteries:

Lottery C: $100 million with a probability of 11%

Nothing with a probability of 89%

Lottery D: $ 500 million with a probability of 10%

Nothing with a probability of 90%

According to the axiom of independence of irrelevant alternatives in expected utility theory, a common consequence added to each of the two alternatives can be discarded and should not affect the preference of one alternative over the other. In the example, we can find the 89% of winning $100 million is a common consequence of the two decision problems. Lotteries C and D can be converted into lotteries A and B by replacing 89% of getting nothing ($0) with 89% of winning $100 million. The preference of an individual should be consistent across the two decision problems (i.e. choose either A and C or B and D) if he makes a decision based on the expected utility theory entails axiom of independence. Nevertheless, in actually observed choices, most rational people chose A over B and D over C, even though the expected value of each option can be easily calculated. Thus, the Allais Paradox demonstrates a violation of expected utility theory, especially the *independence* axiom. Examples of this behavior have led many behavioral economists and mathematical psychologists to formulate other models of

economic choices that can better explain these systematic choice biases and thus are better descriptive models than expected utility theory (Machina, 1987).

1.3.4 Financial theories

In classical decision theory, the risk is commonly considered to reflect the variation of the distribution of possible outcomes, their likelihood, or their subjective value. In the expected utility theory, a subject's risk-attitude is estimated by the nonlinearities in the revealed utility for monetary outcomes. It implicitly presupposes that one's risk-attitude is primarily reflected by the mapping of monetary outcome (u(x), utility). Then people make a choice by integrating both the utility of a possible outcome (x) and its probability of occurrence (p) (i.e. the expected utility).

However, risk can be determined as one of the attributes of an option along with its expected value by calculating the variance of the probability distribution of possible gains and losses associated with a particular option (Arrow, 1965). In a financial context, the asset allocation problem requires an investment strategy that balances between the demand for reward maximization (average return of investment) and risk minimization (standard deviation of the investment's return, σ). In the risk-return model, Markowitz (1952) estimated risk as to the variance of the distribution around the mean, or its range, and further extended the use of mean-variance analysis (Markowitz, 1952). In this way, the preference of an individual between two extreme options (one with lowest σ and one with highest σ) in asset allocation can reveal a degree of risk aversion (Sharpe, 1964). Recently, Weber and Shafir (2004) suggested the use of a different variable, the coefficient of variation (CV), as a risk estimator, based on its better fit to human and animal choice behavior (E. U. Weber et al., 2004).

1.3.5 Risk for negative outcomes

While all theories discussed so far use different definitions of risk, a common assumption used in all of them is that the likelihood of choosing a risky option is affected by the variability of the option's possible outcome. However, risk can also be assessed in a very different way. In 1987, March and Shapira proposed that risk as a psychological variable in decision making is related to the probability and severity (i.e., magnitude) of potential losses (March & Shapira, 1987). That is, the risk is not primarily related to the variability of outcomes independent of valence, but rather specifically to the probability distribution of negative outcomes. Thus, they defined a risky choice as one with the threat of a negative outcome. A similar concept has been suggested by Loewenstein et al. (2001)(Loewenstein et al., 2001).

It should be notice here that the following discussion of risk is in the framework of economical or financial theory, so that risk mentioned below refers to the likelihood of choosing a risky option with specific variability of the potential outcome, rather than the preference for negative outcomes.

1.4 Risk attitude as a stable trait or a context-dependent variable

So far, we have reviewed differences in the basic concepts or models used to define and explain risk attitude. A commonality among all of these models is that they treat risk preference as a stable personality trait. However, this assumption has been questioned recently, based on evidence that an individual's risk attitude might be context-dependent.

1.4.1 Risk attitude as a stable personality trait

Risk attitude is often seen as a fundamental, stable personality trait. Specific types of people are presumed to be more risk-prone in general, while other types of people are more risk-avoiding. This perspective underlies research in which risk attitudes of people belonging to

different classified groups are compared (**Figure 1.2**, left). For example, an individual's risk preference can be related to specific personality dimensions, developmental stage, culture, neuroanatomy, and neurophysiology.

The concept of a trait-like risk attitude is supported by a large number of studies. Lauriola and Levin (2001) showed that specific personality factors (the Big Five) can predict risk-taking behavior in the gain domain (Lauriola & Levin, 2001). People with high scores on 'Openness to Experience' are associated with greater risk-taking, while people with high scores on 'Neuroticism' are associated with less risk-taking. People with personality traits such as sensation-seeking, impulsivity, and low self-control have also been associated with a risk-taking attitude (E. U. Weber et al., 2002). Dohmen et al., (2011) found that demographics factors like gender, age, height, and parental background had a significant impact on an individual's willingness to take risks (Dohmen et al., 2011). Importantly, the individual risk attitudes were relatively stable across different contexts. The importance of demographic factors has been further supported by studies that have shown that females are less risk-seeking than males (Eckel & Grossman, 2008; Powell & Ansic, 1997). Age has also been confirmed to be a factor modulating risk attitude, in that risk aversion increases slowly between childhood and adulthood (Levin & Hart, 2003; Weller et al., 2011). Individuals from different cultures or countries often are differed in their risk preference (M. Wang et al., 2017; E. U. Weber & Hsee, 1998). All these findings suggest the presence of a stable underlying personally trait that determines an individual risk preference.

These behavioral studies are further supported by a large number of neuroscientific studies that have linked specific features of human brains to individual risk attitudes. First, some anatomical characteristics are a stable biomarker for risk preference at the individual level. In

particular, people with a larger gray matter volume in the right posterior parietal cortex (PPC) have a greater tolerance for financial risk (Gilaie-Dotan et al., 2014a).

Second, neural activity levels in many brain areas predict risk preference. In an fMRI study, the degree to which neural activity in both the ventral striatum and prefrontal cortex (PFC) responded to loss predicted individual differences in sensitivity to losses and gains, which is closely related to risk preference (Tom et al., 2007). Individual differences in risk-taking behavior are correlated with resting-state slow-wave electroencephalographic (EEG) activity in the PFC (Gianotti et al., 2009; Schutter & Van Honk, 2005) and with neural activity in PPC (Huettel et al., 2006).

Third, several lesion and stimulation studies demonstrate a causal relationship between specific brain regions and risk-based decision behavior. Patients with damage in the orbitofrontal (OFC) and ventromedial prefrontal (VMPFC) cortex display impaired decision-making behavior and risk-taking behavior in the Iowa Gambling Task (Bechara et al., 1996; Manes et al., 2002, p. 2). They persist in selecting more cards from very risky decks even so they were disadvantageous because of infrequent, catastrophic losses. These patients also placed higher bets on simple probabilistic decisions (Bechara et al., 1996; Manes et al., 2002). In normal subjects, repetitive transcranial magnetic stimulation (rTMS) was used to disrupt neural activity in the right dorsolateral PFC (DLPFC). Following this manipulation, subjects became more risk-seeking and were more likely to choose a larger potential reward even at a greater risk of penalty (Knoch et al., 2006). Likewise, another study used transcranial alternating current stimulation (tACS) to disrupt the theta-band (4-8Hz) oscillatory activity in the left dorsolateral prefrontal cortex (DLPFC) and also found that subjects exhibited more risk-seeking behavior (Sela et al.,

2012). In contrast, disrupting neural processing of the Intraparietal sulcus (IPS) with rTMS resulted in suppressed risk-taking behavior (Coutlee et al., 2016).

While these studies establish a relationship between brain activity in certain brain areas and the likelihood of accepting a risky option, it is less clear, if they reflect a stable neural trait, or if they reflect context-dependent conditions that might influence brain activity and through it behavior dynamically.

1.4.2 Risk attitude as a context-dependent variable

As outlined above, many studies have described risk attitude as a constant within an individual. However, the risk attitude of individuals can vary substantially across different behavioral domains (**Figure 1.2**). When the risk attitudes of individuals in five content domains (financial decision, healthy/safety, recreational, ethical, and social decisions) were assessed, respondents' degree of risk-taking was always consistent within each domain but highly domain-specific (Blais & Weber, 2006; E. U. Weber et al., 2002). Also, the methods for measuring risk preference, i.e. the properties of the choice architecture strongly affect how individuals make a decision under risk (Pedroni et al., 2017). These findings suggest that risk attitudes of humans and animals are not always a stable personality trait, but rather a propensity that emerged during the process of decision-making in a context-dependent manner (Farashahi et al., 2018; Payne et al., 1992; Slovic, 1995).

Internal factors related to energetic states and metabolic processes strongly influence risk-preferences (Pietras & Hackenberg, 2001). A number of studies found that an organism's sensitivity to risk is systematically influenced by its energy budget (metabolic reference point, i.e. the balance sheet of energy income against energy expenditure). Stephens (1981) suggested that an animal aiming to maximize survival probability should prefer safer options with lower

variance when above a metabolic reference point but should prefer risky options with higher variance when below a metabolic reference point. The metabolic reference point is determined by an equilibrium between metabolic costs and available energy (Stephens, 1981). Caraco et al., (1990) showed that a foraging bird tends to become more risk-seeking, when its metabolic energy requirement is increased by changing the ambient temperature or when its stored metabolic energy level is decreasing by fasting (Caraco et al., 1990). In contrast, monkeys are typically risk-seeking in laboratory gambling tasks but become more risk-averse when they are thirsty because of lower water levels (Yamada et al., 2013). The metabolic state can also alter economic decision-making under risk in humans. An individual's choice is generally risk-averse with a higher than expected impact of the meal while becoming risk-prone with a lower signal of nutrient intake (Symmonds et al., 2010). Moreover, human monetary decisions under risk are also systematically influenced by more abstract budget considerations, such as monetary assets. Pietras and Hackenberg (2001) found that humans' risk preference is a function of their monetary assets: people are risk-averse if their momentary earnings decrease below a minimum level and risk-prone if their earnings exceed the minimum requirement level(Pietras & Hackenberg, 2001). This effect of current wealth levels on an individual's risk-attitude has been confirmed in other studies (Juechems et al., 2017).

External factors related to environmental richness also shift risk tolerance (Stephens, 2008). Since stochasticity in the availability of resources, such as food and water, is ubiquitous in natural environments, the risk-sensitivity of an organism to environmental richness reflects likely a phylogenetically conserved adaptation. In a rich environment, in which a foraging bird can expect to gain more energy than the minimally required rate, it behaves risk-averse and avoids options with high variance. In contrast, the foraging bird becomes risk-seeking and prefers

options with high variance in a poor environment, when it can expect an energetic deficit (Caraco, 1981).

In addition, the size of the stakes also shifts risk-attitudes in humans and animals. People are less risk-averse when the stakes are small (Markowitz, 1952; Weber & Chapman, 2005). This effect is known as the "peanuts effect". Similarly, animals are more risk-seeking when reward quality or amount is low (Craft et al., 2011; Hayden et al., 2008). Other external contextual factors that influence an individuals' risk attitude include whether a choice is part of a series of repeated gambles or a one-shot gamble (Hayden & Platt, 2007) and whether probabilities and rewards are learned through experience or written description (Barron & Erev, 2003; Hertwig et al., 2004).

In addition to these internal and external contextual influences on risk preference, there is one more very important factor that does not fall clearly in either category. Instead, the effect is related to the framework used by decision-makers to determine subjective value. As explained in greater detail in the next section, humans and other animals estimate the utility of an option not on an absolute scale, but rather as a relative gain or loss relative to a standard reference point. This standard reference point is typically the momentary relevant state (e.g., internal metabolic state or in the case of humans the more abstract state of current monetary assets). Humans show different risk-attitude for risky gains versus risky losses (Canessa et al., 2013; Vermeer et al., 2014). Furthermore, how the problems are framed can also influence an individual's risk preference. People tend to avoid risks if possible outcomes are presented in a way that highlights positive aspects, while more likely to take risks when the same outcomes are presented in a way that highlights their negative aspects (Gonzalez et al., 2005; Tversky & Kahneman, 1979). The

effect of positive (received reward) or negative (received punishment) feedback has also been shown to influence the subject's risk preference (Vermeer & Sanfey, 2015).

To sum up, there is a large amount of evidence both supporting that risk-attitude can be thought of as a stable trait (**Figure 1.2 left**) and that it can be thought of as state-dependent (**Figure 1.2 right**). The risk was initially seen as a trait, but recent evidence has shown this is not true. It turns out to show that humans (and possibly animals) can both show a systematic variance of risk across identifiable groups and simultaneously, each of the individuals can have contextual variations in risk attitude (i.e., both frameworks capture part of the truth).

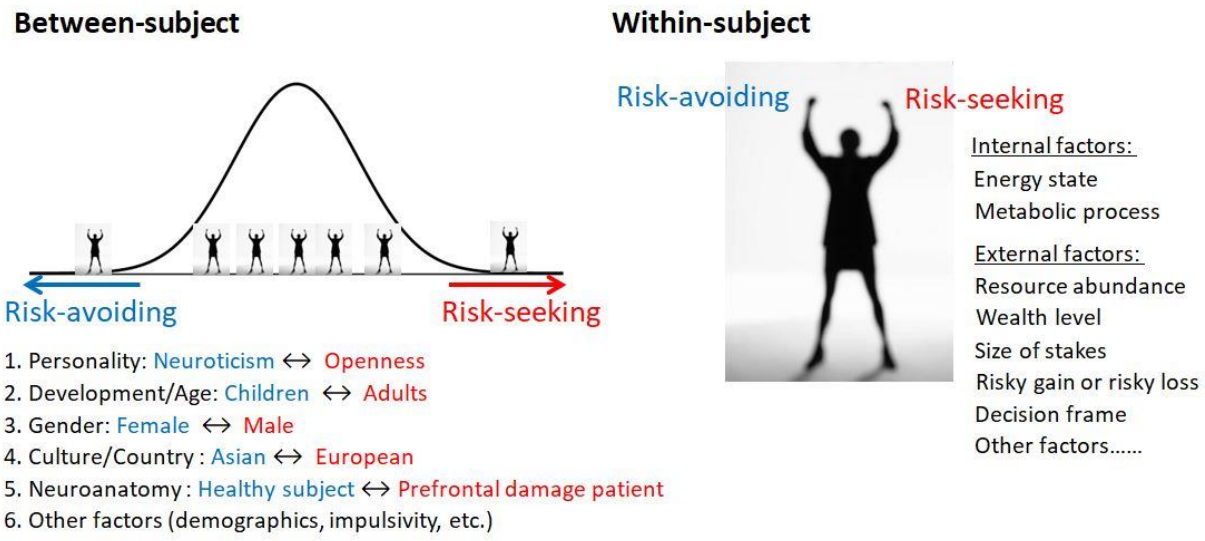

Figure 1.2. Risk attitude can be seen as a stable trait at the between-subject level or a context-dependent preference at the within-subject level. Left, different groups of people can exhibit systematically different risk-preference. Right, internal and external factors can influence an individual's momentary risk attitude.

1.5 Prospect theory

The difficulty of interpreting human choice behavior based on the predictions of expected utility theory and lead to the development of several alternative decision theories. The most successful and wide-ranging of these descriptive models is the Prospect theory (Tversky & Kahneman, 1979). Prospect Theory was originally developed as a model of decision-making under risk and makes several assumptions about the way utility and probability are represented that differ from expected utility theory. These assumptions are necessary to explain human decision-making behavior.

First, Kahneman and Tversky (1979) found strong evidence of what they referred to as the "reflection effect". That is, decision-makers do not always exhibit a similar risk attitude when facing a risky gain or risky loss. Instead, people tend to be risk-averse in the gain domain while risk-seeking in the loss domain. To illustrate this, imagine that there are two separate decision problems.

In the first problem, the subject chooses between two lotteries:

Lottery A: A 100% chance of *winning* $3000

Lottery B: An 80% chance of *winning* $4000, and a 20% chance of *winning* nothing

In the second problem, the subject chooses between two other lotteries:

Lottery C: A 100% chance of *losing* $3000

Lottery D: An 80% chance of *losing* $4000, and a 20% chance of *losing* nothing

The empirical behavioral result shows that majority of people will be more likely to choose the sure option rather than the risky option in the first problem while being more likely to choose the risky option rather than the sure option in the second problem. Thus, most people prefer a

certain gain in the positive prospect but are strongly aversive to a certain loss in the negative prospect. Importantly, gains and losses are coded relative to a reference point, as indicated above. Thus, an individual's utility function changes curvature close to the reference point (it is 'reflected'; see **Figure 1.3A**) and consequently risk preference reverses (i.e. risk-seeking for risky losses and risk-averse in risky gains). A change of reference point can further alter the preference order for prospects. It needs to be noted that the concept of the 'reference point' is somewhat unspecified in classical Prospect Theory. While it normally refers to a person's current status quo, it can also refer to some future level of aspiration, or some other 'psychological' construct. In addition to the "reflection effect", Kahneman and Tversky also suggested that subjects are more sensitive to losses than to gains. This effect is referred to as "loss aversion".

Second, to explain the behavioral pattern seen in for example the Allais Paradox, Prospect Theory proposes the "certainty effect". It assumes that people tend to overweigh outcomes that are certain, relative to outcomes that are merely probable. This is part of the more general idea that decision-makers use a distorted probability representation with biased (non-linear) weightings. For most subjects, an 'inverted-S' shape of the probability weighting function describes behavior best (**Figure 1.3B**). This function leads to an overweighting of small probabilities, an underweighting of large probabilities, and a sharp rise for certainty. This predicts that when winning probabilities are low, people should choose options that offer a larger gain (because they overestimate the probability of obtaining the gain). In this way the results of the Allais Paradox can be explained, where subjects accept a small but certain outcome over an uncertain outcome of a larger gain, despite the large probability of winning (A>B), while simultaneously choosing the option with the larger gain (D>C) when both options have a low probability of winning.

The core concepts of prospect theory -- certainty effect, refection effect, the encoding of utility relative to a reference point, and loss aversion --not only successfully predict the choice in the Allais Paradox (as well as many other choice biases) but also well describe many contextual effects on risk attitude (e.g. outcomes are encoded as risky gains or risky losses relative to the current wealth level or the choice problem is represented in a positive or negative framework).

1.5.1 Prospect theory model

The main mathematical components of the Prospect Theory model are the utility function and probability weighting function, which are both non-linear. Separate utility functions describe the gain and loss domain:

$$u(x) = x^{\alpha}, \qquad when\ x \geq 0$$

$$u(x) = -\lambda.(-x)^{\alpha}, \qquad when\ x < 0$$

The parameter α controls the curvature of the utility functions in both the gain and loss conditions. The loss aversion effect is incorporated by adding a loss aversion parameter to the utility function in the loss domain (**Figure 1.3A**).

The probability weighting function permits probabilities to be weighted nonlinearly. There are a number of different functions that have been suggested in the literature. Here we show the probability weighting function in a Prelec form with a single parameter:

$$w(p) = exp(-(-ln(p)^{\gamma}))$$

The parameter γ allows the probability weighting curve to be S (or inverse-S) shaped (**Figure 1.3B**). That is an initially concave (convex) then convex (concave) curve, so that small

probabilities are overweighted (underweighted) while large probabilities are underweighted (over-weighted).

By fitting this model to empirical data, Kahneman & Tversky (1979) found that most people are best described by an S-shaped value function ($0<\alpha<1$) with loss aversion ($\lambda>1$). It indicated that people are risk-averse in the gain domain while risk-seeking in the loss domain. In addition, most people show an inverse S-shaped probability weighting function ($0<\gamma<1$). This leads to low probabilities to be overweighed and high probabilities to be underweighted.

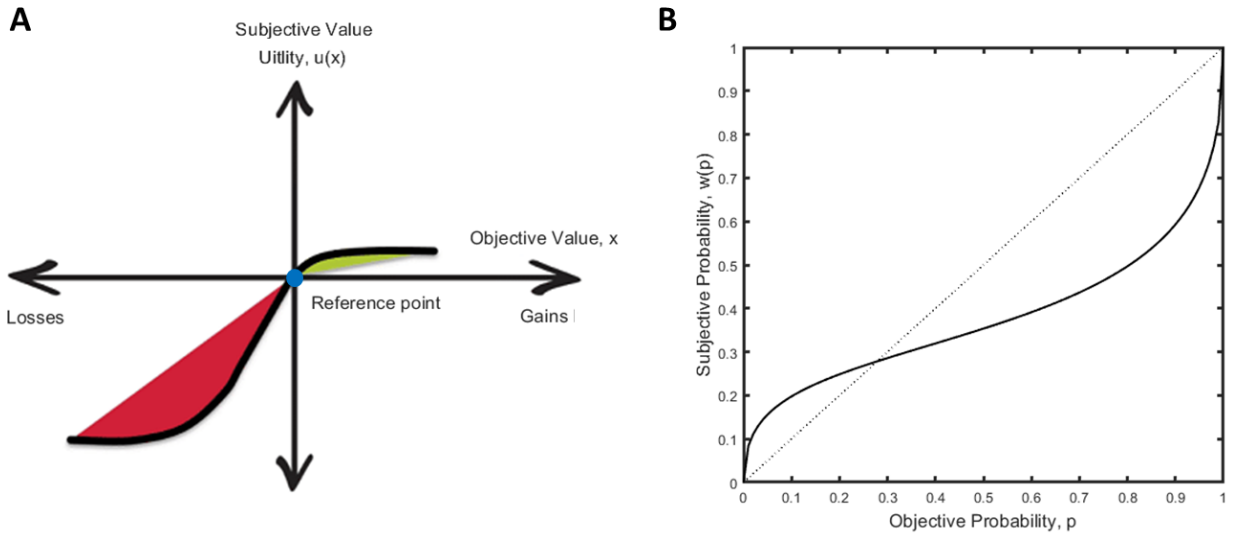

Figure 1.3. The utility function and probability function in the prospect theory. (A) Utility u(x) is a concave utility of gains ($x\geq0$) and a convex function of losses ($x<0$). (B) Probability weighting function w(p) is a four-fold nonlinear function of p. Smaller probabilities are overestimated and larger probabilities are underestimated.

1.5.2 Neurophysiological basis of Prospect theory

Prospect theory has dominated the analysis of decision-making under risk for decades. Non-human primates, such as Capuchin monkeys and Rhesus monkeys show several hallmark biases underlying Prospect Theory, just like humans, including reference dependence and loss aversion (M. K. Chen et al., 2006; Stauffer et al., 2015). This suggests that there is an evolutionarily ancient decision-making system in the primate brain responsible for generating these risk preference characteristics shared by humans and animals (for a review see, Trepel et al., 2005). Nevertheless, the assumptions of Prospect Theory remain ad-hoc and it is not known if they reflect any underlying brain mechanism. Modern cognitive neuroscience has therefore used imaging, lesion, and stimulation studies to investigate possible links between neural mechanisms and Prospect Theory. The various findings are listed in **Table 1.4**.

Human imaging studies

With the rise of modern neural activity imaging techniques (e.g. PET, fMRI), researchers have begun to investigate the neural mechanisms of risky decision making. Some studies have searched more generally for brain regions that encode behaviorally relevant variables, such as risk, uncertainty, or variance of the possible outcome. These studies have identified a distributed network of brain areas. An early positron emission tomography (PET) study found that OFC and anterior cingulate cortex (ACC) were implicated in coding risk in terms of increased uncertainty of potential gains or losses (Ernst et al., 2002). This finding was confirmed and extended by reports that the fMRI signal in the OFC, ACC, as well as insular cortex (IC), responded to different levels of risk in a gambling task (Critchley et al., 2001; Paulus et al., 2003).

Several fMRI studies showed that activities in separate neural systems are correlated with risk-avoiding and risk-seeking behavior, respectively. One study showed that a risk-seeking

attitude was positively correlated with activity in the medial part or (OFC), while a risk-averse attitude was strongly associated with the activity in the lateral OFC (Tobler et al., 2007). A similar anatomical division with respect to risk-attitude was also found in the prefrontal cortex (PFC). The BOLD signal in the dorsomedial PFC was negatively correlated with risk-seeking while the BOLD signal in the inferior frontal gyrus (IFG, adjacent to DLPFC) was positively correlated with risk-averseness (Christopoulos et al., 2009; Xue et al., 2009).

Other studies have more specifically tested the conceptual assumptions underlying the Prospect Theory model. They have searched for the neural basis of gain/loss-specific value encoding, the reference point, loss aversion, probability distortion, and the predicted effects of these factors on risk attitude.

First, a critical assumption underlying Prospect Theory is the idea that utility is represented differently for gains and losses and that both utility representations are using a relative framework for encoding value. Whether or not gains and losses are encoded separately is a contested issue in the field. Several regions including striatum, VMPFC, ventral ACC, and medial OFC, increase their activation with an increased size of the potential gain. Importantly, the same network of areas also decreases activity as the size of the potential loss increased (Tom et al., 2007). This supports the idea of a distributed circuit that encodes uniformly value-increases and decreases. On the other hand, potential gains and losses should elicit different emotional and behavioral responses. A potential gain should elicit positive arousal and promote approach behavior, while a potential loss should elicit negative arousal and promote avoidance behavior (Knutson & Greer, 2008). This hypothesis is supported by accumulating evidence that qualitatively and quantitatively different processes may be engaged in risk-taking to obtain gains and to avoid losses (Levin et al., 2012). The anterior IC and the amygdala are suggested to be the

node encoding anticipation of loss, while the ventral striatum is suggested to be the node encoding anticipation of gain (Breiter et al., 2001; Canessa et al., 2013; Kahn et al., 2002; Knutson, Adams, et al., 2001; Kuhnen & Knutson, 2005; Yacubian et al., 2006). This model suggested that risky decision-making in the gain and loss domain may be processed in separate systems that are highly involved in positive or negative emotional arousal. This finding supports the general assumptions of Prospect Theory.

Second, substantial effort has also been spending on attempts to find the neural representation of the probability weighting function. Human fMRI studies have found neural responses that are involved in the representation of nonlinear probability mapping (Berns et al., 2008; Hsu et al., 2009). Smith et al., (2009) found that several brain regions including the insula, amygdala, and posterior cingulate cortex elicited more activation for higher reward magnitude while the anterior cingulate cortex elicited more activation for higher reward probability (Smith et al., 2009). A PET study in humans also found that the availability of striatal dopamine D1 receptor is correlated with the degree of nonlinearity in the probability weighting function that best fits behavior across subjects (Takahashi et al., 2010).

Lesion and stimulation studies

Case studies from patients with brain injury allow the investigation of the causal relationship between different brain regions and decision-related functions. Amygdala damage eliminates monetary loss aversion (De Martino et al., 2010). Patients with insula damage showed fewer risky choices than healthy controls in the gain domain and also became less sensitive to differences in expected value between options (Weller et al., 2009).

Another population that allows for causal experiments is Parkinson's patients. When these patients are off their dopamine medication that reverses an abnormally low level of dopamine,

they are more sensitive to negative outcomes (punishments) than positive outcomes (rewards) in a learning task. The application of dopamine medication reverses this bias(Frank et al., 2004). A followed study showed that administration of a dopaminergic drug (a D2/D3 receptor antagonist) modulated humans' subjective weighting probabilities in the gain domain (Ojala et al., 2018). These studies show that dopamine plays an important, but differential, role in gain and loss-specific feedback mechanisms.

In healthy subjects, transcranial direct current stimulation (tDCS) of a specific brain region changes activity in the affected region. When tDCS was applied over the right and left prefrontal cortex to include its cortical excitability, the subjects became more risk-seeking in the gain domain, but more risk-averse in the loss domain (Ye et al., 2015, 2016). This further supports the idea that the gain and loss domain engage at least partially separate circuits, even in the same brain region.

Table 1.4. Summary of neural systems hypothesized to be involved in the major aspects of prospect theory from human image studies.

Prospect thoery		Brain areas
Utility function	Anticipation of gains	**Ventral striatum (+)**
		VMPFC (+)
		ACC (+)
		OFC (+)
		AIC
	Anticipation of losses	Ventral striatum (-)
		VMPFC (-)
		ACC (-)
		OFC (-)
		AIC
		Amygdala
	Loss aversion	**Amygdala**
		AIC
Probability weighting function	Linear mapping	**ACC**
		Striatum
		MPFC
		Parietal cortex
		Temproal cortex
		Motor cortex
		Cerebellum
	Nonlinear mapping	**Cingulate cortex**
		Striatum
		Motor cortex
		Cerebellum
Reference point		OFC
		Amygdala

Animal models and associated challenges

Human imaging studies and non-invasive stimulation techniques have started to map the network of brain areas responsible for decisions under risk. Nevertheless, the interpretations of the neuronal activity pattern are limited due to the limits of spatial and temporal resolution of the techniques available in humans. Therefore, to truly understand the mechanisms underlying decision-making, it is necessary to investigate and manipulate brain activity on the level of neuronal circuits. This is only possible in animal models. Thus, it is of critical importance to develop find out corresponding behavioral paradigms in animals to help us further investigate the underlying neural mechanism.

Accumulating evidence has shown that animals show specific behavior characteristics in line with prospect theory. As mentioned above, capuchin monkeys were found to exhibit trading behavior based on a nonlinear utility and probability weighting function (M. K. Chen et al., 2006). Similar behavioral effects have also been found in rhesus macaques. Stauffer et al., (2015) first demonstrated that macaque monkeys exhibit probability distortion similar to the inverse S-shaped probability function proposed in the prospect theory (Stauffer et al., 2015). Farashahi et al., (2018) found that macaque monkeys' risk attitudes differed in the gain and loss domain based on a nonlinear and asymmetric utility function (Farashahi et al., 2018). Macaque monkeys are also found to behave like humans and flexibly adjust their risk preference with changing satiation levels (Fujimoto & Minamimoto, 2019).

Reward magnitude, reward probability, risk (outcome variance), and risk-attitude are important factors for decision-making under risk. Recent studies in macaques have shown that all these decision-related variables are encoded in a distributed network throughout the brain at the level of single neurons.

Neural correlates of subjective value have been found in numerous brain areas. By training monkey in a matching task, Sugrue et al., (2004) found the activity of LIP neurons parametrically track the subjective value of saccades in a trial-by-trail fashion, suggesting lateral intra-parietal (LIP) neurons carry information related to the probability that a saccade to each target would result in a reward (Sugrue et al., 2004). Similar action-value signals have been found in SEF neurons (X. Chen & Stuphorn, 2015; So & Stuphorn, 2010). Amiez et al., (2006) found that ACC responses reflected expected juice quantity, which is related to both reward (juice) quantity and reward probability. Inactivation of the ACC impaired the monkey's ability to choose the optimal target and reduced it to chance level (Amiez et al., 2006).

Neural correlates of reward probability or corresponding outcome variance are also found in various subcortical and cortical areas. An electrophysiological study in non-human primates found that dopaminergic neurons in the midbrain encode not the only reward but also its variance (Fiorillo et al., 2003). O'Neill and Shultz, (2010) found a distinct group of neurons in the orbitofrontal cortex that reward risk, independently from reward value (O'Neill & Schultz, 2010). Orbitofrontal neurons that encode reward probability also have been found in rodents performing an olfactory discrimination task (van Duuren et al., 2009). Posterior Cingulate Cortex neurons also increase their activity when monkeys make more risky choices (McCoy & Platt, 2005). This might indicate that they encode the degree of risk. However, it might also reflect increased subjective value, because the monkeys preferred riskier options.

Several brain regions have been proposed in controlling risk attitude. Reversible inactivation of the anterior insular cortex (AIC) in rats promotes risk-taking (Ishii et al., 2012), indicating that AIC is causally involved in risky decision making. Conversely, inactivation of SEF reduces the monkey's risk-seeking behavior (Chen & Stuphorn, 2018).

1.6 Aims, approaches, and chapter overview of this dissertation

As the literature we reviewed above indicates, a large body of work has aimed to identify the neural mechanisms of decision-making under risk. Recent interest centered on understanding the neuronal computations underlying the core concepts used in prospect theory. Neuroimaging experiments have identified a wide range of brain regions encoding signals expected by prospect theory. However, a barrier to a deeper mechanistic understanding is the lack of an animal model allowing to investigate gain/loss-specific value signals, probability (or risk) signals, as well as reference-point-related signals at a neuronal level.

To this end, we recorded neuronal activity in monkeys performing a token-based gambling task developed to test their risk attitude in a gain or loss domain with different starting token assets. We were particularly interested in the anterior insular cortex (AIC), since human fMRI studies have suggested its crucial role in signaling risk-aversive behavior (Kuhnen & Knutson, 2005), the current state of the self (Craig & Craig, 2009) and loss aversion (Canessa et al., 2013). We hypothesized that AIC may be a central node within the *risk-attitude network***,** which monitors the contextual factors that influence risk attitudes. We proposed that neurons in the AIC encode the behavioral context of the decision and shape risk attitude by modulating activities in the *risk-decision network* which selects between seeking or avoiding a risky option.

To investigated these issues, we (**Aim 1**) designed a token-based gambling task that allowed us to observe monkeys' changing risk attitude in varying behavioral contexts (outcomes represent gain or loss; different starting token assets) (Chapter 2), (**Aim 2**) developed computational models to predict monkey's risk attitude or behavioral choice based on the decision-related variables (Chapter 3), and (**Aim 3**) found neuronal correlates of decision-related variables (e.g. token asset, gain/loss context, as well as expected values and risk of options) and

neuronal responses reflect prospect theory model components in AIC with an electrophysiological recording (Chapter 4).

Finally, the dissertation will close with a conclusion, proposing a possible role of AIC in decision-making under risk, highlighting the innovation and contribution of these works, and suggestions of future directions.

Chapter 2

Behaviors of monkeys performing the token-based gambling task

2.1 Methods

2.1.1 General

Two male rhesus monkeys (Monkey G: 7.2 kg, Monkey O: 9.5 kg) were trained to perform a token-based gambling task in this study. Monkeylogic software (Asaad & Eskandar, 2008) (https://www.brown.edu/Research/monkeylogic/) was used to control task events, stimuli, and reward, as well as monitor and store behavioral events. During the experimental sessions, the monkey was seated in an electrically insulated enclosure with its head restrained, facing a video monitor. Eye positions were monitored with an infrared corneal reflection system, EyeLink 1000 (SR Research) at a sampling rate of 1000 Hz. All analyses were performed using self-written Matlab code unless noted otherwise.

2.1.2 Token-based gambling task

To investigate risk attitude in the gain and loss context with different wealth levels, two monkeys were trained in a token-based gambling task. The task was based on a previously published task design (Seo & Lee, 2009) and consisted of two types of trials: choice trials and no-choice trials. In choice trials, two targets (a sure option and a gamble option) were presented on the screen. Monkeys were allowed to choose one of the options by making a saccade to the corresponding target. Choice trials allowed us to measure the monkey's risk attitude by testing their propensity to choose the gamble option across different combinations of the expected value of the gamble and sure option (**Figure 2.1**). In no-choice trials, only one target (either a sure option or a gamble option) was presented on the screen so the monkey was forced to make a

saccade to the given target. Comparing the neuronal activity in choice and no-choice trials allowed us to identify neuronal signals specifically related to decision-making. The choice and no-choice trials were pseudo-randomly interleaved in blocks so that each block consisted of all 24 choice trials and 13 no-choice trials.

2.1.2.1 Visual Cues that indicate token outcome and outcome probability

All options in this task were represented by sets of colored squares, with the color of the square indicating the token amount that could be gained or lost (token outcome) and the proportion of the square filled by a given color indicating the probability that this event would take place (outcome probability) (**Figure 2.1**). The sure options were single-colored squares indicating a certain outcome (gain or loss of token). There were 7 different colors used for sure options representing the number of tokens that were gained or lost ([-3, -2, -1, 0, +1, +2, +3]). The gamble options were two-colored squares indicating two possible outcomes and their probabilities. Six gamble options were used in this task. Three of the gambles resulted in either a gain of 3 or 0 token(s), but with different outcome probabilities (i.e. token [+3, 0] with the probability combination of [0.1, 0.9], [0.5, 0.5], or [0.75, 0.25]). Another three gambles resulted either in a loss of 0 or 3 token(s) with different outcome probabilities (i.e. token [0, -3] with probability combination of [0.1, 0.9], [0.5, 0.5], or [0.75, 0.25]). The choice trials were divided into a gain domain and a loss domain (**Figure 2.1**).

2.1.2.2 Context of gain and loss

The choice trials were divided into a gain context and a loss context (**Figure 2.1**). In the gain context, the three gamble options that resulted in either a gain of +3 or 0 tokens with different outcome probabilities were paired with four sure options that spanned the range of gain outcomes (i.e. [0, +1, +2, +3]). These resulted in 12 possible combinations of sure and gamble

options. In the loss context, the gamble options resulting either in a loss of 3 or 0 tokens were paired with the four sure options that spanned the range of losing outcomes (i.e. [0, -1, -2, -3)). Thus, the loss contexts comprised another 12 possible combinations of sure and gamble options. This resulted in a total of 24 different combinations of reward option combinations (half in the gain context and the other half in the loss context) that were offered in choice trials. In the no-choice trials, all 13 different reward options (7 sure and 6 gamble options) which were used in the choice trials were presented in isolation.

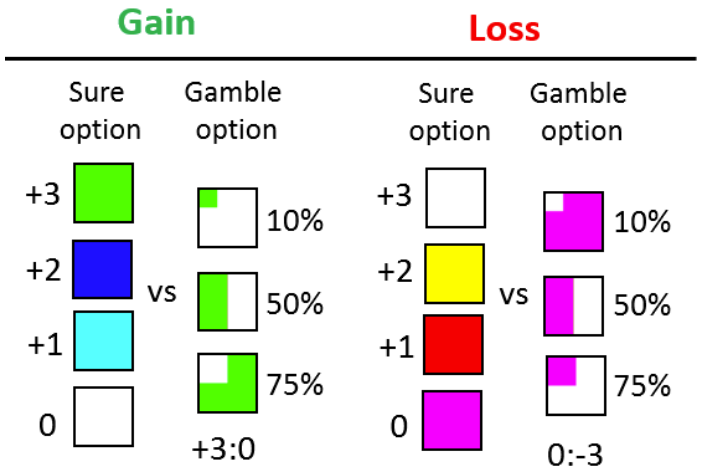

Figure 2.1. Set of choice options in the gain and loss context. Each option is a square (x degree), of which the color(s) indicated the possible outcome(s) (-3 to +3, in units of token change), and the portion of the colored area indicated the probability (10%, 50%, 75%, 100%) of the corresponding outcome to be realized. The choice trials consisted of two types (gain vs. loss context), and there was always a sure option paired with a gamble option – i.e., only the combination of [sure gain vs. gamble gain] and [sure loss vs. gamble loss] was available. In forced-choice trials, only one option was presented, which could be either a sure option or a gamble option (gain or loss).

2.1.2.3 Token as a secondary reinforcer

To investigate how critical contextual factors including the context of gain/loss and current token asset affect the risk attitude of monkeys, it required us to introduce the token system so that the monkey could experience losses, that is a reduction of welfare from its current state. In our version of the token-based gambling task, the monkey had to acquire multiple tokens (say six in this research) before he receives the immediate reward (600 μl water). In each trial, the currently owned token number was presented by a token cue. The token cue consisted of 6 circles whose number of filled circles represented the token number the monkeys owned in the current state. After each outcome, the token cue was updated to indicate the new token number.

2.1.2.4 Task procedure

A choice trial began with the appearance of a fixation point surrounded by the token cue. After the monkey had maintained its gaze at the central fixation point (±1° of visual angle) for a delay period (0.5-1s), two choice targets were displayed on two randomly chosen locations among the four quadrants on the screen. The monkey indicated its choice by shifting its gaze to the target. Following the saccade, the token cue moved to surround the chosen target and the unchosen target disappeared from the screen. The monkey was required to keep fixating the chosen target for 450-550ms, after which the chosen target changed either color or shape. If the chosen target was a gamble option, it changed from a two-colored square to a single-colored square to indicate the outcome of the gamble. The color represented the amount of gained or lost tokens in the present trial. If the chosen target was a sure option, the shape changed from a square to a circle, serving as a control for the change in the visual display that occurred during gamble option choices. Finally, after an additional delay (500ms) the token cue was updated. If the owned token number was equal to or more than 6 at this stage, the monkey received a

standard fluid reward after an additional 450ms waiting time. At the beginning of the next trial, the remaining tokens were displayed with filled circles. Otherwise, if the owned token number was smaller than 6, the monkey did not receive a fluid reward and the updated token cue was displayed at the beginning of the next trial. If the owned token number was smaller than 0, the inter-trial-interval (ITI) for the next trial would be prolonged (300 ms per owed token).

The monkey was required to maintain fixation on the point until it disappeared for reward delivery. If the monkey broke fixation in either one of the two time periods, the trial was aborted and no reward was delivered. The following trial repeated the condition of the aborted trial, contingent on the time of fixation break. A trial in which the monkey broke fixation *before* the choice was followed by a trial in which the same choice targets were presented, but at different locations. This ensured that the monkey sampled every reward contingency evenly and could not prepare a saccade in advance. On the other hand, a trial in which the monkey broke fixation *after* the choice was followed by a no-choice trial in which only the chosen target was presented. If the monkey broke fixation following a gambling choice, but before the gamble outcome was revealed, the same gamble cue was presented. If the monkey broke fixation following a sure choice or after a gambling outcome was revealed, the same sure cue was presented. This ensured that the monkey could not escape a choice once it was made and had to experience its outcome. All trials were followed by a regular 1500-2000ms ITI. The schedule of the token-based gambling task is shown in **Figure 2.2**.

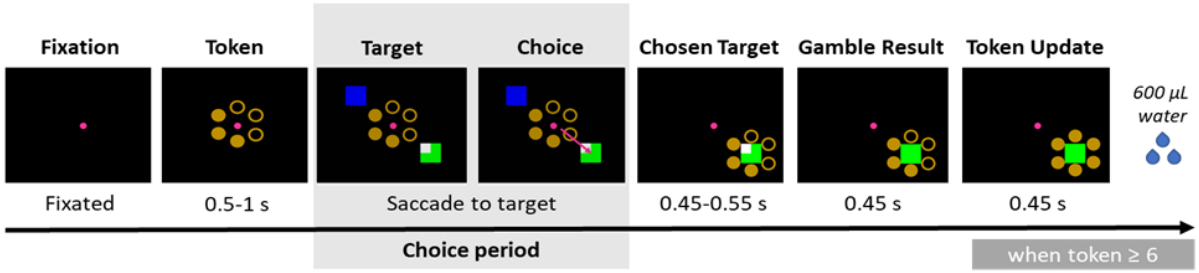

Figure 2.2. Schematic of the token-based gambling task. Each trial starts with a fixation dot at the center of the screen. Upon the monkey fixated to the central dot, the current number of tokens it has was presented (filled circles of the hexagonal placeholder). Following 0.5-1s delay, one ('forced-choice' trial) or two ('choice' trial) options were presented (detailed in (b)), and the monkey indicated its choice by making a saccade to the target. The unchosen option then disappeared, and the current number of tokens was presented again in the surround of the chosen target. The outcome of the chosen target revealed after a delay (0.45-0.55 s), indicated by the color change of the square, and the number of tokens that the monkey possessed was updated accordingly. The monkey was rewarded (600uL of water) whenever it collected six tokens or more at the end of the trial. The Shadowed area indicated the choice period during which the neuronal data were analyzed.

2.1.2.5 Saccade detection

Eye movements were detected offline using a computer algorithm (saccade detection function) that searched first for significantly elevated velocity (30°/s). Saccade initiations were defined as the beginning of the monotonic change in eye position lasting 15ms before the high-velocity gaze shift. A valid saccade for the choice was further admitted to the behavioral analysis if it started from the central fixation window (1° x 1° of visual angle) and ended in the peripheral target window (2.5° x 2.5° of visual angle).

2.1.3 Description of monkeys' behavior

Fixation behavior: We examined whether and how monkeys' motivations to initiate a new trial were influenced by the outcome of the previous trial and the start token number of the current trial. We used two behavioral signals as indications of the monkey's motivational state: (1) fixation latency (i.e., the time from fixation point onset until fixation by the monkey) and (2) fixation break ratio (i.e., the frequency with which the monkey failed to fixate on the fixation point long enough to initiate target onset). We used linear regression models to test if there was a significant relationship between each of the two variables describing the motivational state and the variables describing the history and current state.

Response time: We examined whether and how response times were influenced by different decision-related variables. For each trial, response time was defined as the period between target onset and saccade initiation estimated by the saccade detection function. The response time dataset in each condition (e.g. trials from the context of gain or loss, trials with different start token numbers, trials with different expected values of the chosen option (chosen EV), or trials with different absolute values of difference of expected values among the gamble and sure option (|ΔEVgs|)) was fitted with an ex-Gaussian distribution algorithm (Zandbelt, 2014)

(https://doi.org/10.6084/m9.figshare.971318.v2). It returned three besting-fitting parameter values of the ex-Gaussian distribution: the mean μ, the variance σ, and the skewness τ of the distribution. We used a permutation test to determine if the mean RTs of trials from the gain and loss context. We used linear regression models to test whether there was a significant relationship between mean RTs and start token number, chosen EV, or |ΔEVgs|.

2.2 Results

2.2.1 General behavior

In this task, the monkey had to collect a sufficient number of tokens (≥6) to receive a standard fluid reward (600μl water). Because the maximum number of tokens that could be earned in a single trial was three, the monkeys had to accumulate the necessary tokens over multiple trials. The modes of inter-reward-trial number for the two monkeys were 3 and 5, respectively (**Figure 2.3**), suggesting the monkeys usually needed to work for 3-5 trials to earn enough token (secondary reward) to exchange for the fluid reward (primary reward).

Both monkeys learned the use of tokens, as indicated by the observation that their fixation behavior was strongly influenced by their token assets. Monkeys fixated faster and were less likely to break their fixation (resulting in abortion of the trial) (**Figure 2.4**) when they had larger token assets at the start of the trial, and when they received more tokens from the previous trial. These results suggest that monkeys understood the use of tokens as secondary reinforcers, and thus were more motivated when they owned more and received more tokens before they earned the primary reinforcer (the fluid reward).

Both monkeys were sensitive to the expected value (EV, i.e. the product of potential gaining/losing tokens and its corresponding probabilities) of the option, as indicated by the observation that their response time (RT) was strongly influenced by the expected value of

options. The RTs were longer when the EV differences between options were smaller, suggesting monkeys took more time to make the decision when the task difficulty increases (**Figure 2.6e-f**). Besides, the RTs were shorter when the EV of chosen options was larger, suggesting monkeys are more vigilant when deciding to choose an option with a higher EV (**Figure 2.6g-h**).

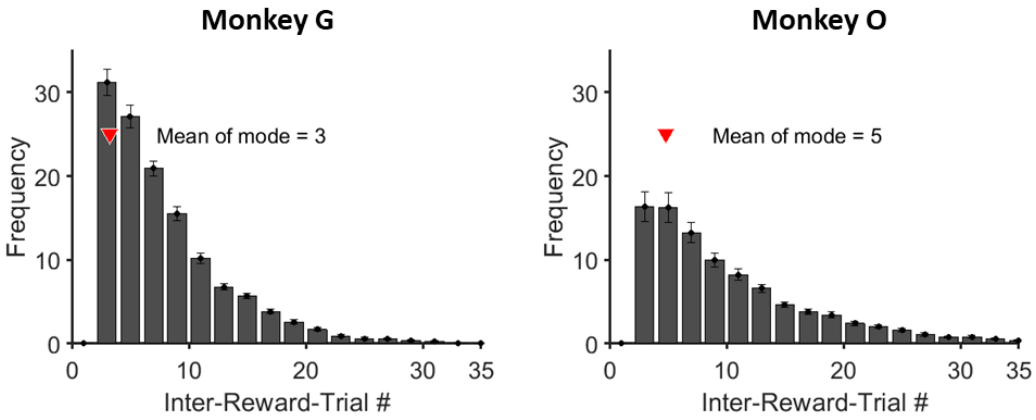

Figure 2.3. The Inter-Reward-Trial number for each monkey. Monkeys used to accumulate the necessary (6) tokens for 3-5 successive trials. Error bars indicate SEM or estimates across sessions (session number = 37 for each monkey).

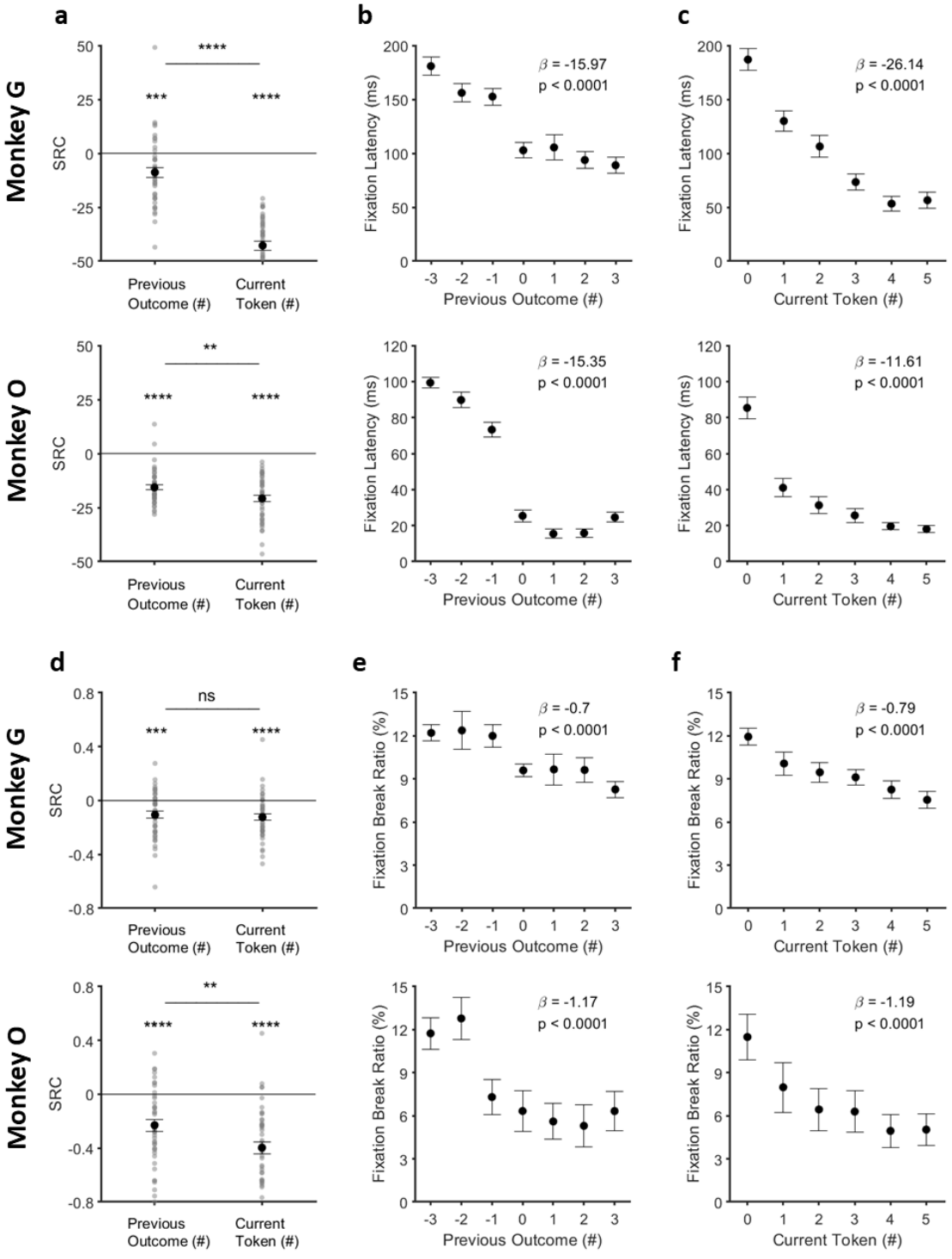
a
b
c
d
e
f
Monkey G
Monkey O
SRC
Previous Outcome (#)
Current Token (#)
Fixation Latency (ms)
Fixation Break Ratio (%)
Previous Outcome (#)
Current Token (#)
β = -15.97
p < 0.0001
β = -26.14
p < 0.0001
β = -15.35
p < 0.0001
β = -11.61
p < 0.0001
β = -0.7
p < 0.0001
β = -0.79
p < 0.0001
β = -1.17
p < 0.0001
β = -1.19
p < 0.0001
ns
**
****
***

Figure 2.4. Effect of current token asset and token outcome history on fixation latency and fixation break ratio.

(a) Standardized regression coefficients (SRCs) for fixation latency (latency to fixate on the center point at the beginning of the trial before the token cue appears). Error bars indicate SEM of SRCs across sessions.

(b) Fixation latency as a function of the previous outcome. Regression coefficient (β) between fixation latency and the token number won or losses of the previous trial.

(c) Fixation latency as a function of the current token asset. Regression coefficient (β) between fixation latency and the start token number of the current trial.

(d) Standardized regression coefficients (SRCs) for fixation break ratio (failure to hold fixation on the center point long enough for token cues to appear). Error bars indicate SEM of SRCs across sessions.

(e) Fixation break ratio as a function of the previous outcome. Regression coefficient (β) between the percentage of trials with fixation breaks and the token number won or losses of the previous trial.

(f)Fixation break ratio as a function of the current token asset. Regression coefficient (β) between the percentage of trials with fixation breaks and the start token number of the current trial.

Error bars indicate SEM or estimates across sessions (session number = 37 for each monkey).

ns, no significant, ** $p<10^{-2}$, *** $p<10^{-3}$, **** $p<10^{-4}$ (t-test or paired t-test).

2.2.2 Monkeys' risky choices were influenced by the context of gain and loss and current wealth level

We found that monkeys' choices were influenced by the context of gain and loss. Both monkeys were more likely to choose the gamble option than the sure option (**Figure 2.5 left**; t-test; Monkey G, P(Gamble)=59%, $p<10^{-4}$; Monkey O, P(Gamble)=67%, $p<10^{-4}$) and were even more likely to do so in the gain context than in the loss context (**Figure 2.5 left**; paired t-test, $p<10^{-4}$ for both Monkey G and Monkey O).

We have also found that monkeys' choices were influenced by the number of tokens they had upon the trial start ('start token', or 'asset'), and an interaction between the context of gain and loss and the start token number. Specifically, in the gain context, the probability of which the monkey chose the gamble option (P(Gamble)) decreased as the start token number increased (**Figure 2.5 right**; green dashed line; regression analysis; Monkey G, $\beta = -0.044$, $p<10^{-4}$; Monkey O, $\beta = -0.035$, $p<10^{-4}$). While in the loss context, the P(Gamble) exhibited a tendency to increase as the start token number increased (**Figure 2.5 right**; red dashed line; regression analysis; Monkey G, $\beta = 0.028$, $p<10^{-4}$; Monkey O, $\beta = -0.001$, $p = 0.8$). These results suggested that, as the monkey had more tokens in hand, it became more conservative (i.e., less willing to gamble) for a greater win; but was more willing to take a risky gamble to avoid a potential loss. This is in line with the observation of humans that human subjects tend to be more risk-aversive when facing a potential gain, and more risk-seeking when facing a potential loss as their asset increases[1].

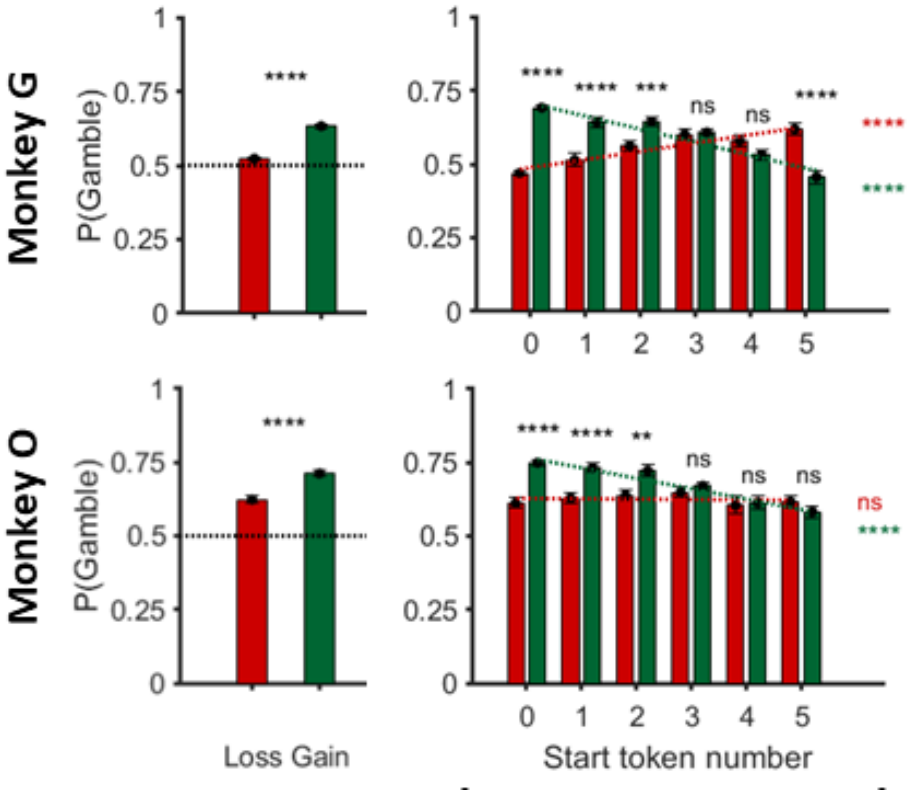

Figure 2.5. Choice probability under different contextual factors. Left. The probability of monkey choosing gamble option in gain/loss contexts. The Upper and lower panels represent data from two different monkeys, respectively. Green: gain context; Red: loss context. Error bars: S.E.M; **** $p<10^{-4}$, paired t-test. Right. The probability of monkey choosing gamble option, plotted by context and the start token number. Green: gain context; Red: loss context. Error bars: S.E.M; n.s.: not statistically significant ($p>0.05$), ** $p<10^{-2}$, *** $p<10^{-3}$, **** $p<10^{-4}$ in paired t-test (black), **** $p<10^{-4}$ in regression analyses (green or red).

2.2.3 Monkeys' response times were influenced by the context of gain and loss and current wealth level

Monkeys' response times (RTs, the interval between stimulus onset and the saccade initiation) were also influenced by these contextual factors. Both monkeys responded slower in the loss context than in the gain context (**Figure 2.6a-b**; permutation test; monkey G: RT_{gain} = 204.79ms, RT_{loss} = 246.51ms, $p < 10^{-3}$; monkey O: RT_{gain} = 175.07ms, RT_{loss} = 206.00ms, $p < 10^{-3}$), and when they had more tokens (**Figure 2.6c-d**; regression analysis; monkey G: $\beta_{StartTkn}$ = 2.83, p = 0.19; monkey O: $\beta_{StartTkn}$ = 3.50, $p < 10^{-2}$). These suggest that monkeys are more vigilant when facing a potential loss, and when they are getting closer to the water reward.

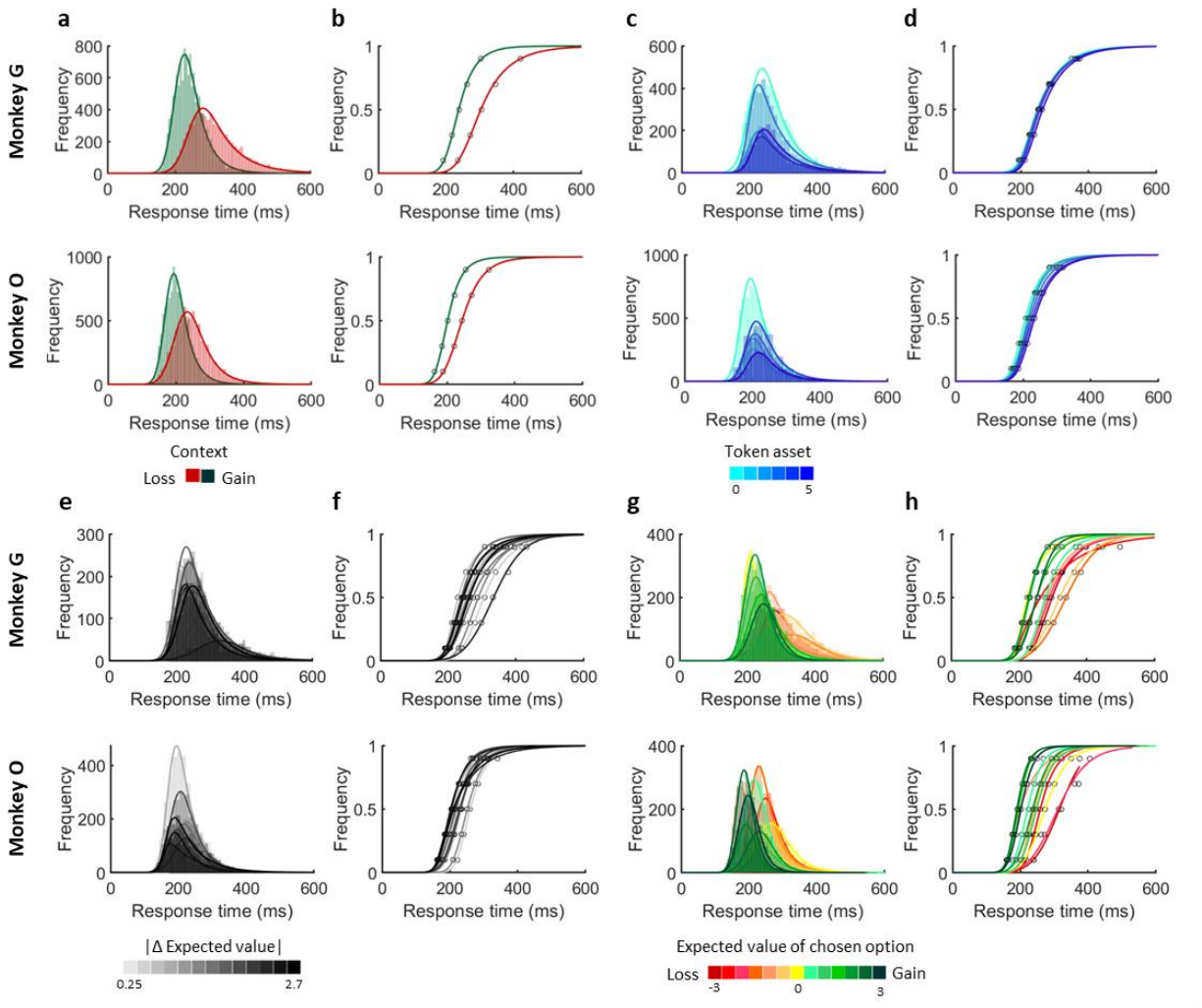
a
b
c
d
e
f
g
h
Monkey G
Monkey O
Frequency
Response time (ms)
Context
Loss
Gain
Token asset
0
5
| Δ Expected value |
0.25
2.7
Expected value of chosen option
Loss
Gain
-3
0
3

Figure 2.6. Response time of monkey's choice. (a) Distribution of response times when monkeys made decisions in the gain (green) and loss (red) context for each monkey. Histograms with light color indicate the raw data distribution and curves with dark color indicate the best-fitting (ex-Gaussian) distribution.
(b) Cumulative distribution function (CDF) of response times in the gain (green) and loss (red) context.
(c) Distribution of response times when monkeys made decisions with different start token numbers. The color gradients from light to dark blue indicate token numbers from 0 to 5.
(d) CDF of response times with different start token numbers.
(e) Distribution of response times when monkeys made decisions with different absolute values of expected value difference between a gamble and sure option (|ΔEVgs|s). The black color gradients indicate |ΔEVgs| from small to large.
(f) CDF of response times with different |ΔEVgs|s).
(g) Distribution of response times when monkeys made decisions with different EVs of the chosen option. The color gradients indicate chosen values from small to large.
(h) CDF of response times with different EV of the chosen option.
One monkey took more time to make a choice when the difference expected value between options was small (**Figure 2.6**e-f; regression analysis; monkey O: $\beta_{RT\_|\Delta EVgs|} = -5.11$, $p < 10^{-3}$), indicating a task-difficulty dependent response time. Yet another monkey showed no significant difference to this variable (**Figure 2.6**e-f; regression analysis; monkey G: $\beta_{RT\_|\Delta EVgs|} = -0.50$, $p = 0.74$). Furthermore, Both monkeys made faster choices as the expected value of chosen option increased (**Figure 2.6**g-h; regression analysis; monkey G: $\beta_{RT\_StartTkn} = 2.83$, $p = 0.19$; monkey O: $\beta_{RT\_StartTkn} = 3.50$, $p < 10^{-2}$). This likely reflects an elevated motivation for high-value options.

2.2.4 Value evaluation in a relative framework

The fact that monkeys were sensitive to the context of the decision and their risk preference changed across contexts suggests that monkeys evaluate each available option not thoroughly depending on the final status it may result (the 'prospect', i.e., the number of tokens at the end of the trial), but also depending on how the final status will be reached (by gaining or losing tokens). This is best demonstrated by the contrast of trials whose end token number were identical, but were resulted from either gaining or losing tokens (**Figure 2.7**; paired t-test; monkey G & O: $p<10^{-2}$ for all end token numbers, except end token numbers 2&5 for monkey G, and number 5 for monkey O). Given the 'prospect' (end state) was the same, monkeys chose more gambles when such prospect was offered as a gain, as compared to when it was offered as a loss.

These results support that monkeys used the relative framework -- option value was defined as token changes relative to a reference point (the starting token number) but not the absolute framework -- option was defined purely by the token number at the end of the trial (which reflect how close the monkey is to collect enough token and reap a fluid reward) for option evaluation in this task.

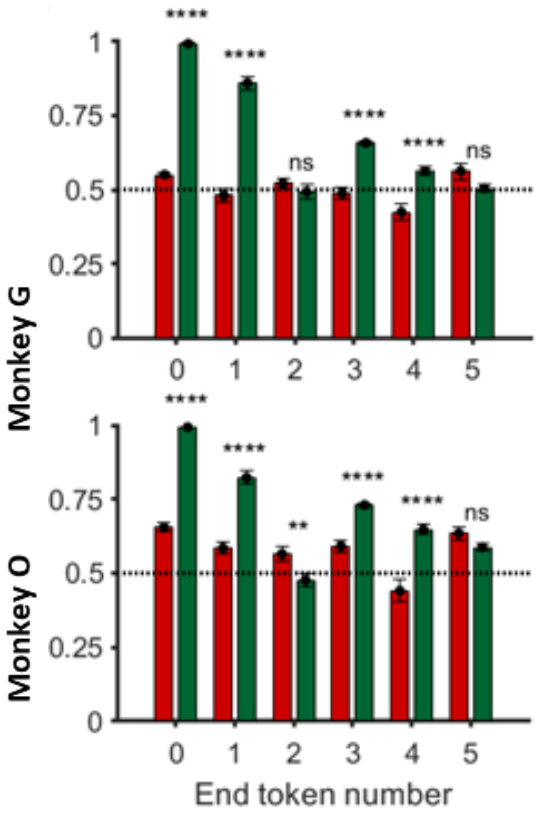

Figure 2.7. Monkeys had different risk attitudes when the identical end token states were results from gaining or losing token(s). The probability of monkey choosing gamble option, plotted by context and the end token number. Green: gain context; Red: loss context. Error bars: S.E.M; n.s.: not statistically significant ($p>0.05$), ** $p<10^{-2}$, *** $p<10^{-3}$, **** $p<10^{-4}$ in paired t-test (black), **** $p<10^{-4}$ in regression analyses (green or red).

2.3 Discussion

The behavioral results shown above confirmed that the monkeys understand the meaning of the visual cues indicating the change in token number and outcome probability as well as the goal of the task (i.e. gambling to collect token for exchanging water reward). In the task, we found that the monkeys' attitudes toward risk differed in the gain and loss context. The monkeys showed an overall tendency of risk-seeking in both the gain and loss domains. However, they were more inclined to the gamble choices when facing a risky gain than when facing a risky loss. Furthermore, we showed that the token assets, i.e., the number of already owned tokens at the beginning of the trial, influenced the monkey's risk attitude. This effect varied in the gain and the loss domain. With increasing token assets, monkeys are prone to choose the gamble option less often in the gain domain, but more or equally often in the loss domain. Thus, we found both the context of gain and loss and the wealth level (token assets) were important variables that can modulate monkeys' risk attitudes.

2.3.1 Relative framework in the token-based gambling task

Monkeys' behaviors were sensitive to both the initial wealth level and potential gaining or losing outcomes (**Figure 2.5**) demonstrating that they made decisions based on the potential gain or losses relative to their current wealth (the reference point) rather than in absolute terms. Further analysis found that monkeys displayed different preferences to risky choices when the same final wealth levels resulted from different starting points (**Figure 2.7**) again in favor of a relative rather than an absolute framework.

This relative framework is one of the core concepts of prospect theory (Tversky & Kahneman, 1979) and can provide several insights. First, the starting point can strongly influence how people subjectively evaluate a specific outcome. For example, if two workers both receive a

bonus of $1,000, the one whose regular salary was $1,000 will be much happier than the one whose regular was $10,000. The same increments (or decrements) can be evaluated as dramatically different in value, when their starting points are different. This is consistent with our finding that monkeys became less risk-seeking when their current wealth level increased (in the gain context). Second, people are most interested in their relative change in wealth as opposed to their actual final wealth. Thus, people tend to feel better when their income gets raised from $500 to $2,500 than when it is raised from $2,000 to $2,500. That is, two options that resulted in the same final state can be evaluated differentially when they have different starting points. Third, the outcome of an option can be evaluated as a gain or a loss relative to a starting point. Suppose there are two people, both receiving a salary of $2,500. For the one whose previous salary was $2,000, the new salary would be seen as a gain, while for the other whose the previous salary was $3,000, the new salary would be a loss. This is consistent with our finding in **Figure 2.7** that monkeys were sensitive to gains and losses relative to a start token number rather than the end token state, so that monkeys exhibited different risk preferences when the identical end token state resulted from a gain or a loss. Finally, how the outcomes of gains and losses are framed by subjects strongly influence their risk-attitudes. People tend to avoid risk and choose the option that guarantees a positive outcome when two offered choices are both framed as positive (i.e., a gain). On the flip side, people will be more likely to take risky choices rather than the option that guarantees a negative outcome when two offered choices are both framed as negative. This behavioral phenomenon is well known as the 'framing effect'. This effect has not been examined clearly in our present study yet. It will be interesting to design a task that well controls how animals 'frame' the same choice situation in a positive or negative way to see how the frame influences their choice behaviors. These behavioral phenomena

described above can be applied to a diverse range of situations in economics, financial, politics, or marketing fields.

2.3.2 The effects of outcome history and working memory on the decision process

The token gambling task requires the monkey to collect tokens in successive trials to obtain a primary reward. Therefore, the starting point of each trial is the result of past trials, which means that the trials are dependent on each other. As described above, the monkeys' fixation behavior systematically changes based on the past token outcome and current token number (**Figure 2.4**). It not only shows that monkeys paid attention to the token cue and were aware of their progress in obtaining rewards but also shows that monkeys were sensitive to the outcomes of previous trials. Notably, the visual cue that represented token information was not present in the early fixation period. Thus, the fact that monkeys' fixation behaviors were biased by the token asset suggests that the monkeys can hold the currently owned token number in working memory. These results suggest that working memory of recent choice and outcome history did play a role in the token gambling task.

To sum up, the new token-based gambling task that we developed helped us to investigate whether and how monkeys' risk attitudes were modulated by different contextual factors, specifically whether the outcome was a gain or loss and current wealth (i.e., token assets). Next, we used modeling techniques to test possible cognitive mechanisms underlying these behavioral phenomena.

Chapter 3

Behavior modeling of risky choices in the token-based gambling task

In the descriptive behavioral results, we found that for both monkeys their probabilities of choosing gamble (P(Gamble)) were influenced by multiple contextual factors, such as the context of gain and loss and token asset (**Figure 2.5**). This result, however, just indicated that monkeys' choices were influenced by these individual decision-related variables (including the context of gain or loss, the expected value of gamble option, expected value of the sure option, start token number, risk (outcome variance of the option), or expected end token number, etc.). It remains unclear how these decision-related variables interact with each other and how the subjective value of each option is calculated given a specific combination of these decision-related variables. Thus, we test a series of models to predict the risk attitude or choices of our subjects (two monkeys) based on various decision-related variables.

3.1 Methods

3.1.1 Model-based subjective value estimation

A model-based analysis requires first constructing a range of alternative models that embody different ways in which value could be constructed given the option attributes (here possible reward amounts and their respective probability). We included classical economic models (expected value model, expected utility model, prospect theory model), financial models (risk-value model), optimal models that aimed to maximize the probability of getting a reward (reward proximity model), and models that hybrid the best model among classical economic and financial model with the reward proximity model. Furthermore, to find out how the wealth level

influences monkey's risk attitude, we extended these basic models with the term of start token number (Token) in different ways. By fitting these wealth-dependent models to monkey's choice behavior, we can better know how the monetary assets modulate monkeys' behavior in a cognitive framework.

3.1.1.1 Expected value model

The Expected value (EV) model computes the value of each option by simply calculating the product of attributes of options:

$$EV_{gamble} = x_{win} \times p_{win} + x_{loss} \times (1 - p_{win})$$

$$EV_{sure} = (x) \times (1)$$

where x is the reward outcome (in units of gaining or losing token numbers) and p is the objective probability of receiving the corresponding outcome.

The expected value difference between the two options is then transformed into choice probabilities via a softmax function with terms of slope s and bias b:

$$P(Gamble) = \frac{1}{1 + e^{-s(\Delta EV - bias)}}$$

where $\Delta EV = EV_{gamble} - EV_{sure}$, s determines the sensitivity of choices to the ΔEV, and $bias$ is the directional bias of choosing gamble.

This model assumes the subjects are risk-neutral since they should have no preference when facing a risky option and a certain option with an identical expected value. Thus, the behavioral results that monkeys showed specific risk attitudes when facing a gamble and a sure option in different contexts can only be attributed to the two free parameters *s* and *bias*.

3.1.1.2 Expected utility model

Next, we tested the expected utility (EU) model that describes risk-attitude by a non-linear mapping between objective value (expected value) and subjective value (expected utility). The EU model describes the risk attitude of the subject mainly by the coefficient of the utility function (α). The utility function is in a form of power function that

$$u(x) = x^{\alpha}, for\ x > 0$$

in which x is the objective value of an option outcome, u is the utility of x, and α is the coefficient of the utility function. The α indicates not only the curvature of the utility function but also reflects the subject's risk attitude.

However, the traditional EU model only considers the utility function in gain context. To extend the utility function to the loss context, we test 2 different forms of the loss utility function:

1. $u(x) = (-x)^{\alpha}, for\ x < 0$

in which the utility function in loss share the same α with utility function in gain, so that the utility functions in gain and loss two curves symmetrical to the zero point ([0,0]).

2. $u(x) = -\lambda(-x)^{\alpha}, for\ x < 0$

in which the utility function in loss is a reflection of the utility function in gain, but with a modulation parameter λ. λ larger than 1 indicates losses loom larger than gains.

The EU is further calculated as:

$$EU = u(x) * p$$

in which u(x) is the utility of x and p is the objective probability of receiving the corresponding outcome (x). The expected utility difference between the two options is then transformed into

choice probabilities via a *softmax* function with terms of slope s and bias b as what we did in the EV model:

$$P(Gamble) = \frac{1}{1 + e^{-s(\Delta EU - bias)}}$$

where $\Delta EU = EU_{gamble} - EU_{sure}$, s determines the sensitivity of choices to the ΔSV, and $bias$ is the directional bias of choosing gamble. Overall, there are 4 parameters (α, λ, s, and $bias$) are included in the EU model.

3.1.1.3 Prospect theory model

The prospect theory (PT) model is derived from EU theory, whereas the PT model estimates the subjective value of an option with not only non-linear utilities in the gain and loss contexts but also a non-linear mapping of outcome probability. Thus, in addition to the parameter α proposed by the EU model, the PT model takes more parameters that can influence an individual's choice into account, including the coefficient of probability weighting function (γ), the coefficient that modulates the utility function in the loss context (λ), the response bias term of choice function (b), and the slope term of choice function (s).

The subjective utility is parameterized as:

$$u(x) = \begin{cases} x^{\alpha}, & for\ x > 0 \\ -\lambda(-x)^{\alpha}, & for\ x < 0 \end{cases}$$

where α is a free parameter determining the curvature of the utility function, u(x), and x is the reward outcome (in units of gaining or losing token numbers). The utility function in loss is modulated by a parameter λ in the original PT model.

The subjective probability of each option is computed by:

$$w(p) = \frac{p^{\gamma}}{(p^{\gamma} + (1-p)\gamma)1/r}$$

where γ is a free parameter determining the curvature of the probability weighting function, w(p), and p is the objective probability of receiving the corresponding outcome. U (x) and w(p) were followed with research(Juechems et al., 2017; Tversky & Kahneman, 1979).

The subjective value (SV, or say expected utility) of each option is computed by combining the output of u(x) and w(p) that map objective gains and losses relative to the reference point and objective probability onto subjective quantities, respectively:

$$SV_{gamble} = u(\, x_{\text{win}}) \times w(\, p_{\text{win}}) + u(x_{loss}) \times w(\, 1 - p_{win})$$

$$SV_{sure} = u(x) \times w(1)$$

The subjective value difference between the two options is then transformed into choice probabilities via a *softmax* function with terms of slope s and bias:

$$P(Gamble) = \frac{1}{1 + e^{-s(\Delta SV - bias)}}$$

where $\Delta SV = SV_{gamble} - SV_{sure}$, s determines the sensitivity of choices to the ΔSV, and $bias$ is the directional bias of choosing gamble. Overall, there are 5 parameters (α, λ, γ, *s*, and *bias*) included in the PT model.

Wealth-dependent models for expected value, expected utility, and prospect theory model

To know how token asset modulates monkey's choice in these models, we estimated corresponding parameters of EV, EU, and PT models for each start token number independently. In addition, we examined alternative wealth-dependent models by adding a Token term to the original PT model in different ways. We tested the wealth-dependent models in which the specific parameter *P* was modulated by the Token in the form:

$$P' = P + \theta * Token$$

where P could be α, λ, γ, *b*, or *s*. Overall, there are 6 parameters (α, λ, γ, *s*, *bias*, and θ) included in the wealth-dependent PT model.

3.1.1.4 Risk-value model

The risk-value model is derived from financial theory and decomposes the subjective value of each option into a weighted linear combination of Risk and Value. The Value was computed as the expected value (EV) of the option and the Risk was either computed as the variance (Var) of the gamble outcomes.

$$Var = (x_{win} - x_{loss})\ (\sqrt{p_{win}(1 - p_{win})})$$

with x_{win} denoting the potential winning token number, x_{loss} denoting the losing token number, p_{win} denoting the winning probability, p_{loss} and denoting the losing probability.

Comparing to the EU and PT model describes the risk attitude of the subject mainly by the coefficient of the utility function (α), the risk-value model attributes the risk attitude of the subject to the Risk-related term (Var). To know whether the difference of monkeys' risk attitudes in terms of gain and loss can be explained by the risk-value model, we modeled monkeys'

behaviors in gain and loss trials independently. Besides, we tested whether the risk-value model outperforms models using only the EV or the Var term to know whether the subjects made choices depending only on the Value, Risk, or both of options.

In these models, the subjective value difference between the two options is transformed into choice probabilities via a *softmax* function with terms of slope s:

$$P(Gamble) = \frac{1}{1 + e^{-(\Delta SV)}}$$

The subjective value of each option is computed by:

$$\Delta SV = \mu 0 + \mu 1(\Delta EV)$$

$$\text{Or} \quad \Delta SV = \mu 0 + \mu 1(\Delta Var)$$

$$\text{Or} \quad \Delta SV = \mu 0 + \mu 1(\Delta EV) + \mu 2(\Delta Var)$$

where $\Delta EV = EV_{gamble} - EV_{sure}$, $\Delta Var = Var_{gamble} - Var_{sure}$, μi is the coefficient for each variable.

Wealth-dependent risk-value model

Furthermore, to extend this model to describe how the token asset influences monkey's choice, we add the term Token, which is the start token number of each trial to the original risk-value model. Thus, the subjective value of each option was modeled as a weighted linear combination of ΔEV, ΔVar, and Token:

$$\Delta SV = \alpha 0 + \alpha 1(\Delta EV) + \alpha 2(\Delta Var) + \alpha 3(Token)$$

To ensure coefficients of variables within a model are comparable, ΔEV and ΔVar are normalized in the range of [-1,1] and Token is normalized in the range of [0,1]. Overall, there are 4 parameters ($\mu 1$, $\mu 2$, $\mu 3$, and *bias/* $\mu 0$) included in the full risk-value model.

3.1.1.5 Reward proximity model

In contrast to the EV, EU, PT, and risk-value models that assume monkey estimated subjective values (SVs) of options in a relative framework, the reward proximity (RP) model assumes monkeys estimated SVs of options closer to an absolute framework. In the relative framework, monkeys were supposed to be sensitive to the number of the token at the start of the trial (i.e. the reference point) as well as the "relative outcome" (a gain or a loss relative to the reference point) of option. Yet in the absolute framework, monkeys were supposed to be only sensitive to the expected end token number after choosing a given option, because the expected end token number directly indicated the probability of earning a reward in the near future. Thus, a monkey should be more likely to choose a sure option [+1] than a gamble option [+3,0; 75%,25%] when the start token number is equal to 5 since the probabilities of getting a reward after choosing the sure option and gamble option are 1 and 0.75, respectively.

This model uses the probability of getting a reward (P(Reward)) as the unit of subjective value estimation. Thus, the subjective value of each option is defined as the probability of getting a reward when choosing the given option under a specific token number:

$$SV_{option} = P(Reward|Token)$$

The SV of each option can be looked out in **Table3.1** when the option and start token number are known.

Table 3.1. Probability of getting a reward when choosing the specific option with given start token asset.

P(Reward)	Sure optin -3	-2	-1	0	1	2	3
Start token 0	0	0	0	0	0	0	0
1	0	0	0	0	0	0	0
2	0	0	0	0	0	0	0
3	0	0	0	0	0	0	1
4	0	0	0	0	0	1	1
5	0	0	0	0	1	1	1

P(Reward)	Gamble optin [-3,0; 0.9,0.1]	[-3,0; 0.5,0.5]	[-3,0; 0.25,0.75]	[0,3; 0.9,0.1]	[0,3; 0.5,0.5]	[0,3; 0.25,0.75]
Start token 0	0	0	0	0	0	0
1	0	0	0	0	0	0
2	0	0	0	0	0	0
3	0	0	0	0.1	0.5	0.75
4	0	0	0	0.1	0.5	0.75
5	0	0	0	0.1	0.5	0.75

The subjective value difference between the two options is then transformed into choice probabilities via a *softmax* function:

$$P(Gamble) = \frac{1}{1 + e^{-s(\Delta SV - bias)}}$$

where $\Delta SV = SV_{gamble} - SV_{sure}$, s determines the sensitivity of choices to the ΔSV, and $bias$ is the directional bias of choosing gamble. Since the reward proximity model takes both the start token number and the token can gain/loss when choosing a specific option into account, it is naturally a wealth-dependent model and includes only two free parameters *s* and *bias*.

3.1.1.6 Hybrid models

To examine whether monkeys can use multiple processes to make the decision, we tested a hybrid model that combines the original PT model (wealth-independent in a relative framework) with the reward proximity model (wealth-dependent in an absolute framework). The subjective value of each option is a linear combination of SV estimated by PT and SV estimated by RP model:

$$SV_{Option\ by\ PT} = u(\ x_{\text{win}}) \times w(\ p_{\text{win}}) + u(x_{loss}) \times w(\ 1 - p_{win})$$

$$SV_{Option\ by\ RP} = P(Reward|Token)$$

$$SV_{option} = \omega(SV\ by\ PT) + (1 - \omega)(SV\ by\ RP)$$

where u(x) and w(p) are the subjective mappings of x and p, and ω indicates the weightings of two-component models.

The subjective value difference between the two options is again transformed into choice probabilities via a *softmax* function:

$$P(Gamble) = \frac{1}{1 + e^{-s(\Delta SV - bias)}}$$

where $\Delta SV\ =\ SV_{gamble} - SV_{sure}$, s determines the sensitivity of choices to the ΔSV, and $bias$ is the directional bias of choosing gamble. Overall, there are 6 parameters (α, λ or β, γ, *s*, *bias*, and *ω*) included in this hybrid model.

3.1.3 Model comparison

3.1.3.1 Negative log likelihoods, AIC, BIC, and cross-validation

We optimized model parameters by minimizing the negative log likelihoods (-LL) of the data given different parameters setting using Matlab's *fmincon* function, initialized at multiple starting points of the parameter space as follows:

$$0 < \alpha, \lambda, \beta, \gamma < 5$$

$$-10 < bias < 10$$

$$0 < s < 20$$

$$-10 < \mu < 10$$

$$0 < \omega < 1$$

There are parameters (1) *slope* and *bias* in EV model, (2) α, λ (or β), *slope*, and *bias* in EU model, (3) α, λ (or β), γ, *slope*, and *bias* in PT model, (4) α, λ (or β), γ, *slope*, *bias*, and θ in wealth-dependent PT models, (5) $\mu 0$, $\mu 1$, $\mu 2$, $\mu 3$, and *slope* in wealth-dependent risk-value models, (6) *slope* and *bias* in reward proximity model, and (7) α, λ (or β), γ, *slope*, *bias*, and ω in the hybrid PT and RP model. Negative log-likelihoods were used to compute classical model selection criteria.

With data combined all trials across different experiment sessions form each monkey (Monkey G, 37 session, 23323 trials; Monkey O, 37 sessions, 19932 trials), we computed the Akaike's information criterion (AIC),

$$\mathrm{AIC} = 2\,\mathrm{k} + 2(-\mathrm{LL})$$

and the Bayesian information criterion (BIC),

$$\mathrm{BIC} = \mathrm{k}(\log(\mathrm{n})) + 2(-\mathrm{LL})$$

where –LL is the negative log-likelihood (-LL) of the model, n is the number of trials used for the modeling, k is the number of free parameters to be estimated.

In addition, we also performed a five-fold cross-validation method for each model. During cross-validation, we randomly divided all trials into 80% training set and 20% testing set. We used a training set to optimize the parameters for a given model, and use the testing set to calculate -LL to evaluate the model.

3.1.3.2 Model simulations

Next, we examined the generative performance by running the model simulation of the data after the optimized model's parameters. Model estimates of choice probability were generated trial-by-trial using the best-estimated parameters and then compared with the actual choices. The accuracy of the best model was calculated by finding the matching rate between model-predicted choices and empirical choices.

3.2 Results

3.2.1 Model comparison

Prospect theory model

Among the classical economic models (wealth-independent EV, EU, and PT model), we found that the PT model had the best fit for monkeys' behaviors (comparison of -LL from cross-validation in **Table 3.2**). This wealth-independent PT model still outperformed EV and EU models when adding a penalty term for the greater complexity of the model (AIC and BIC in **Table 3.2**). The optimized parameters for this best model were plotted in **Figure 3.1** (details of parameters for all models were list in **Table3.3).**

As in classical expected value theory in economics (Lattimore et al., 1992), a convex utility function ($\alpha > 1$) implies risk seeking, because in this scenario, the subject values large reward amounts disproportionally more than small reward amounts. Gain from winning the gamble thus has a stronger influence on choice than the loss from losing the gamble. In the same way, a concave utility function ($\alpha < 1$) implies risk-seeking because large reward amounts are valued disproportionally less than small ones. The λ can further influence the subject's risk-attitude in the context of gain or loss because it modulates the curvature of the utility function in the loss context. With a $\lambda > 1$, the utility function in the loss context will be steeper than that in the gain context, indicating the subject is more sensitive to the value change in the loss context. Alternatively, with a $\lambda < 1$, the utility function in the loss context will be flatter than that in the gain context, indicating the subject is less sensitive to the value change in the loss context. We found that for both monkeys, the best-fitting utility functions in the gain context were convex (**Figure 3.1**; 1-tailed t-test, $H1$: $\alpha > 1$; monkey G: $\alpha = 1.33$, $p < 10^{-4}$; monkey O: $\alpha = 1.38$, $p < 10^{-4}$), indicating that both monkeys were risk-seeking in the gain context. Also, the utility functions

in the loss context were steeper than the one in the gain context (**Figure 3.1**; 1-tailed t-test, *H*1: $\lambda > 1$; monkey G: $\lambda = 3.16$, $p < 10^{-4}$; monkey O: $\lambda = 1.04$, $p < 10^{-3}$), indicating that subjectively losses loom larger than gains for both monkeys.

In addition, a non-linear weighting of probabilities can also influence risk attitude. For example, an S-shaped probability weighting function ($\gamma < 1$) implies that the subject overweighs small probabilities and underweights large probabilities. This would lead to a higher willingness to accept a risky gamble because small probabilities to win large amounts would be overweighed relative to high probabilities to win moderate amounts. We found that both monkeys significantly over-weighted low probabilities and under-weighted high probabilities (**Figure 3.1**; 1-tailed t-test, *H*1: $\gamma < 1$; monkey G: $\gamma = 0.55$, $p < 10^{-4}$; monkey O: $\gamma = 0.74$, $p < 10^{-4}$). Therefore, the monkeys were attracted disproportionally to large reward amounts and overestimated the likelihood of obtaining them when the winning probability was low, again leading to risk-seeking behavior.

Moreover, the bias term in the softmax function can also influence the frequency of a subject's risky choices independent of the subjective value of the options. A negative bias will result in risk-seeking behavior because the subject tends to choose the gamble option, even if the SVs of gamble and sure option are identical. On the other hand, a positive bias will result in risk-averse behavior. We found strong evidence for negative bias in favor of gamble options (**Figure 3.1**; 1-tailed t-test, *H*1: *bias* <0; monkey G: *bias* = -1.13, $p < 10^{-4}$; monkey O: *bias* = -1.35, $p < 10^{-4}$). It suggested the monkeys had a strong preference for the risky options independent of the specific reward amount and outcome probability associated with the options.

Finally, we found that several wealth-dependent PT models outperformed the best-fitting PT model without the Token term (model comparison in **Table 3.2**). This indicated that the effect of

token assets on the monkeys' choice behavior was so strong that it required a model that explicitly incorporate it, such as wealth-dependent PT models, to best describe behavior despite the increase in model complexity. Across all wealth-dependent models, the effect of token assets was best explained by updating the α term in the utility function as a function of the token assets at the start of each trial. However, a wealth-dependent model in which α was modulated linearly proportional to the start token number resulted in some extreme estimates. We therefore also fitted a wealth-dependent model independently for trials with different start token numbers the estimated parameters in this model (marked in blue in **Table 3.3**) were less extreme. The better results for the independent fits suggest that the modulation by token assets might be non-linear and disproportional across the range of token assets.

To examine how each parameter was modulated by current token numbers, we plotted the estimated parameters (listed in **Table 3.4**) in **Figure 3.2**. First, we found that both monkeys were risk-seeking ($\alpha > 1$) when the start token number was low, but they became risk-neutral or risk-averse when the start token number increased (**Figure 3.2**; light to dark green lines indicate increasing start token number). The estimated α was negatively modulated by the start token number (regression analysis; Monkey G, $\beta = -0.16$, $p<10^{-4}$; Monkey O, $\beta = -0.14$, $p<10^{-4}$). Second, there was no significant difference for the estimated λ across different start token numbers for either monkey (regression analysis; Monkey G, $\beta = 0.03$, $p = 0.69$; Monkey O, $\beta = 0.01$, $p=0.4$). Third, the S-shaped weighting of probabilities was slightly influenced by increasing start token numbers in one monkey (light blue to dark blue lines; regression analysis; Monkey G, $\beta = 0.02$, $p<10^{-4}$), but not at all in the other one (Monkey O, $\beta = 0.0004$, $p = 0.89$). Forth, the monkeys showed a consistent tendency to choose the gamble option independent of specific option attributes (**Figure 3.1**; the negative bias of the choice function; t-test: both monkeys,

$p<10^{-4}$ for all start token numbers). This tendency decreased when the start token number increased (**Figure 3.2**; light gray to black lines; regression analysis; Monkey G, $\beta = 0.32$, $p<10^{-4}$; Monkey O, $\beta = 0.28$, $p<10^{-4}$), indicating monkeys became less risk-seeking as their wealth levels increased. Finally, the choice functions became steeper, that is monkeys' choices became less stochastic when the start token number increased for both monkeys (regression analysis; Monkey G, $\beta = 0.23$, $p<10^{-4}$; Monkey O, $\beta = 0.22$, $p<10^{-4}$). This result, combined with the token effect on response time, indicates that choices became slower but less stochastic when token assets increased, which suggests a speed-accuracy tradeoff.

Thus, the effect of the token asset on monkeys' risk attitude was primarily explained by modulation of the utility curvature that was shared in both of the gain ($u(x) = x^{\alpha}$) and loss ($u(x) = -\lambda(-x)^{\alpha}$) context, as well as the bias and slope term of choice function. Overall, the wealth-dependent PT model well described the behavioral results that monkeys were risk-seeking in both gain and loss context, more risk-seeking in the gain than in the loss context, and became more risk-averse the more token assets they had accumulated.

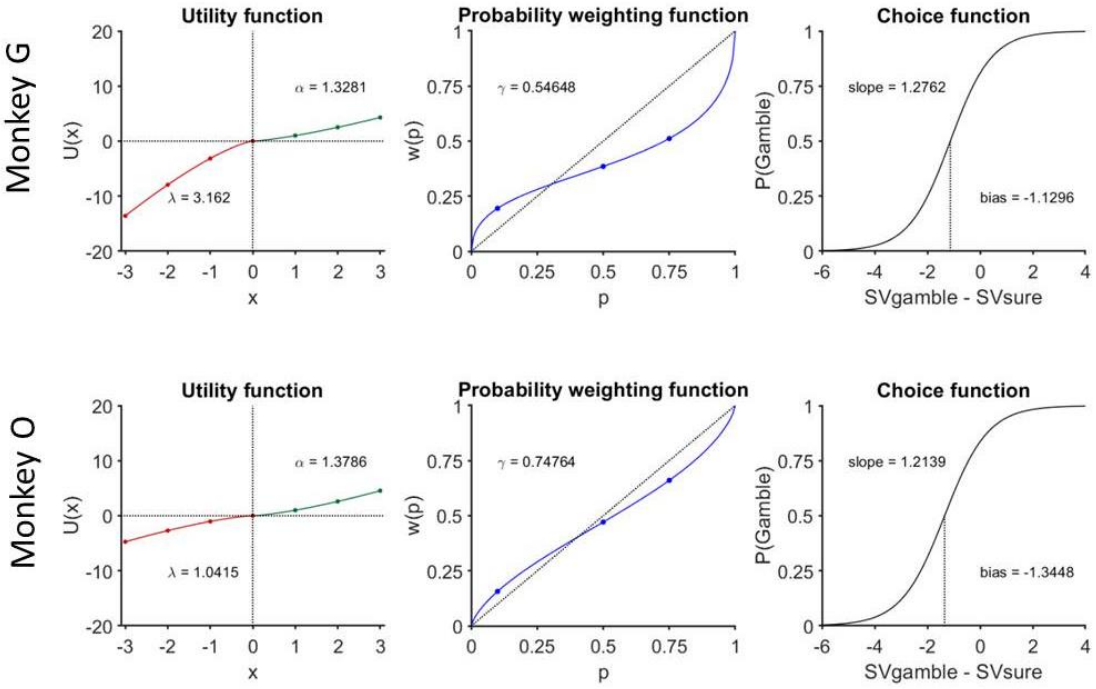

Figure 3.1. Modeling results for PT model that best-explained monkeys' behaviors among all wealth-independent models. The estimated parameters are estimated by models include data from all combined sessions (list in **Table 3.3**).

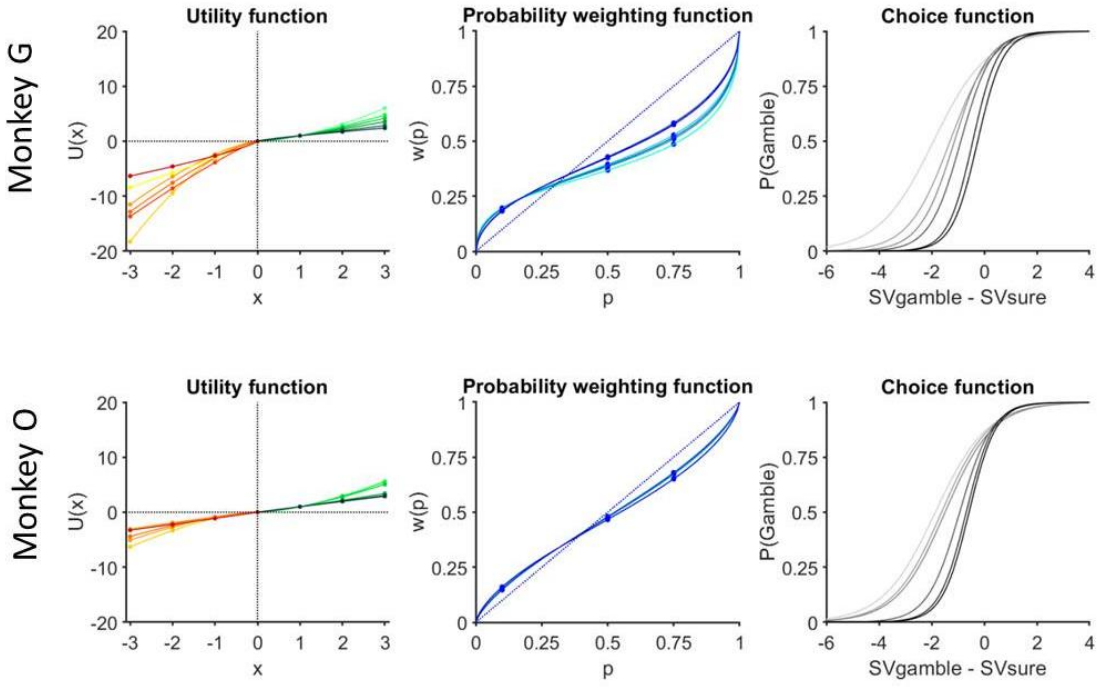

Figure 3.2. Modeling results for PT model that best-explained monkeys' behaviors among all wealth-dependent models. The estimated parameters are estimated by models include data from all combined sessions (list in **Table 3.3**). The color gradient indicates parameters for trials with different start token numbers (light to dark when the start token number increased).

Reward proximity model and hybrid model

We found the reward proximity provided a worse description of the monkeys' behavior than the best wealth-dependent PT model, as well as other models in the relative framework AIC, BIC, and -LL from cross-validation in **Table 3.2**). It implied that monkeys' behaviors were better described in a relative framework that takes both the starting point and relative gains and losses into account rather than an absolute framework, in which the monkey is assumed to only care about the end state of each choice.

Furthermore, the behavioral fit did not significantly improve even when we constructed a hybrid of the reward proximity model with the original wealth-independent PT model (AIC, BIC, and -LL from cross-validation in **Table 3.2**). This finding suggested that the effect of token assets on choice behavior is better explained by a wealth-dependent PT model in a relative framework than a wealth-dependent reward proximity model in an absolute framework. This provided additional strong support that the value estimation of the monkeys relied fundamentally on a relative framework.

Table 3.2. Akaike's information criterion (AIC), Bayesian information (BIC), and negative log-likelihood (-LL) for different models. AIC and BIC values are computed with all combined sessions for each monkey. –2*LL values are computed using five-fold cross-validation for each monkey. The wealth-dependent prospect theory model is the best model (blue) with the lowest AIC, BIC, and -2*LL values. The parameter in red indicates the parameter is modulated by the start token number (with parameter θ).

Wealth independent	EV *(b,s)*	EU *(α,λ,b,s)*	PT *(α,λ, γ, b,s)*
AIC	16692, 14896	15700, 14450	13762, 14205
BIC	16708, 14912	15732, 14482	13802, 14210
sum(-2LL)	16694, 14899	15702, 14453	13762, 14210

Wealth dependent	PT *(α ,λ, γ, b,s, θ)*	PT *(α, λ , γ, b,s, θ)*	PT *(α,λ, γ , b,s, θ)*	PT *(α,λ, γ, b ,s, θ)*	PT *(α,λ, γ, b, s , θ)*
AIC	11224, 10576	13761, 14207	13603, 14190	13764, 14207	18777, 19472
BIC	11272, 10624	13809, 14254	13651, 14238	13812, 14255	18826, 19519
sum(-2LL)	11267, 11274	13760, 14213	13159, 14194	109584, 108699	18782, 19470

	RP *(b,s)*	PT+RP *(α,λ, γ, b,s, ω)*	PT+RP *(α, β, γ, b,s, ω)*
AIC	29130, 23911	13603, 14142	13496, 14171
BIC	29146, 23927	13650, 14189	13544, 14218
sum(-2LL)	29134, 23910	13603, 14145	13500, 14175

Start token 0-5	EV *(b,s)*	EU *(α,λ,b,s)*	PT *(α,λ, γ, b,s)*
AIC	13246, 14028	13240, 14169	13223, 14213
BIC	13648, 14416	14043, 14944	14226, 15181
sum(-2LL)	13186, 13957	13039, 13958	12950, 13932

	Wealth independent RV *(ΔEV, Δvar,b)*	Wealth dependent RV *(ΔEV,Δvar,Tkn,b)*
AIC	13438, 12412	12846, 12226
BIC	14255, 13195	13939, 13270
sum(-2LL)	12994, 11968	12254, 11634

Table 3.3. The best-fit parameters for different models. The parameters are estimated by models include data from all combined sessions. The wealth-dependent prospect theory model that updates α with start token number is the best model (blue) with the lowest AIC, BIC, and -2*LL values (Table 3.2). The parameter in red indicates the parameter is modulated by the start token number (with parameter θ).

Wealth independent	EV *(b,s)*	EU *(α,λ,b,s)*	PT *(α,λ, γ, b,s)*
α	–	1.18, 1.41	1.33, 1.38
λ	–	1.81, 0.86	3.16, 1.04
γ	–	–	0.55, 0.75
bias	-0.57, -0.92	-0.82, -1.30	-1.13, -1.34
slope	1.93, 1.69	1.36, 1.19	1.28, 1.21

Wealth dependent	PT *(α ,λ, γ, b,s, θ)*	PT *(α, λ , γ, b,s, θ)*	PT *(α,λ, γ , b,s, θ)*	PT *(α,λ, γ, b ,s, θ)*	PT *(α,λ, γ, b, s , θ)*
α	5.00, 2.79	1.33, 1.38	1.35, 1.38	1.33, 1.38	2.43, 3.03
λ	5.00, 5.00	3.25, 1.05	3.03, 1.06	3.16, 1.04	1.28, 0.37
γ	0.00, 0.00	0.55, 0.75	0.59, 0.77	0.55, 0.75	0.56, 1.01
θ	-10, -3.50	-0.07, -0.01	-0.03, -0.02	0.48, 1.28	0.00, 0.04
bias	-10, -10	-1.13, -1.35	-1.13, -1.36	-1.13, -1.34	0.31, 0.16
slope	0.01, 0.06	1.27, 1.21	1.26, 1.20	10, 10	10, 9.95

	RP *(b,s)*	PT+RP *(α,λ, γ, b,s, ω)*
α	–	1.34, 1.39
λ	–	1.75, 0.61
γ	–	0.54, 0.73
ω	–	0.51, 0.55
bias	-0.14, -0.28	-0.61, -0.79
slope	2.99, 2.73	2.31, 2.08

PT	α	λ	γ	bias	slope
Start token 0	1.63, 1.58	3.04, 1.12	0.52, 0.73	-1.93, -1.86	0.96, 1.01
1	1.43, 1.55	2.40, 0.93	0.56, 0.79	-1.30, -1.62	1.26, 1.09
2	1.30, 1.48	3.07, 0.87	0.55, 0.77	-1.13, -1.49	1.52, 1.09
3	1.15, 1.11	3.86, 0.91	0.55, 0.78	-0.89, -0.93	1.69, 1.63
4	0.95, 1.01	2.96, 1.03	0.63, 0.78	-0.44, -0.68	2.11, 1.93
5	0.79, 0.97	2.65, 1.12	0.62, 0.73	-0.25, -0.58	2.05, 1.96

Risk-value model

The risk-value model is another classic economic model that is complementary to utility-based models, such as prospect theory. In the risk-value model, the subjective value of each option is a weighted linear combination of EV and variance (Var) of gamble outcome (as well as Token in the extended wealth-dependent model), which allows estimating the relative importance of different behavioral factors on choice behavior. We found that the wealth-dependent risk-value model best-described monkeys' behavior (AIC and BIC, and -LL from cross-validation in **Table 3.2**). The parameters of the best-fitting model are shown in **Figure 3.3.**

First, the monkeys behaved rationally and preferred the option with the higher EV in both gain and loss context (**Figure 3.3**; t-test, $H1$: $\beta_{\Delta EV} \neq 0$; monkey G: $\beta_{\Delta EV\ gain} = 5.30$, $\beta_{\Delta EV\ loss} = 14.64$, both $p < 10^{-4}$; monkey O: $\beta_{\Delta EV\ gain} = 5.99$, $\beta_{\Delta EV\ loss} = 7.47$, both $p < 10^{-4}$). Interestingly, the effect of EV difference on choice was significantly (or near significantly) stronger in the loss context than that in the gain context (**Figure 3.3**; paired t-test, $H1$: $\Delta\beta_{\Delta EV}$ ($\beta_{\Delta EV\ gain}$ - $\beta_{\Delta EV\ loss}$) $\neq 0$; monkey G: $\Delta\beta_{\Delta EV} = -9.33$, $p < 10^{-4}$; monkey O: $\Delta\beta_{\Delta EV} = -1.48$, $p = 0.0505$).

Second, we found that the coefficient of the risk term (ΔVar) was significantly negative for one monkey in both the gain and loss context (**Figure 3.3**; t-test, $H1$: $\beta_{\Delta Var} \neq 0$; monkey G: $\beta_{\Delta Var\ gain} = -0.55$, $\beta_{\Delta Var\ loss} = -3.60$, both $p < 10^{-4)}$; while significantly positive in the gain context and negative in the loss context for another monkey (**Figure 3.3**; t-test, $H1$: $\beta_{\Delta Var} \neq 0$; monkey O: $\beta_{\Delta Var\ gain} = 0.24$, $\beta_{\Delta Var\ loss} = -1.76$, both $p < 10^{-3}$). This suggested that monkeys were risk-averse. Furthermore, the coefficients of the risk term were significantly more negative for losses than for gains for both monkeys (**Figure 3.3**; paired t-test, $H1$: $\Delta\beta_{\Delta Var}$ ($\beta_{\Delta Var\ gain}$ - $\beta_{\Delta Var\ loss}$) $\neq 0$; monkey G: $\Delta\beta_{\Delta Var} = 3.05$, $p < 10^{-4}$; monkey O: $\Delta\beta_{\Delta Var} = 2.01$, $p < 10^{-4}$). This suggests a loss-aversion effect.

Third, the response bias terms were significantly positive in the gain and loss context for both monkeys (**Figure 3.3**; t-test, $H1$: $\beta_{Bias} \neq 0$; monkey G: $\beta_{Bias\ gain} = 1.70$, $p < 10^{-4,}$ $\beta_{Bias\ loss} = 0.09$, $p = 0.32$; monkey O: $\beta_{Bias\ gain} = 2.47$, $\beta_{Bias\ loss} = 0.77$, both $p < 10^{-4}$) i.e. the monkeys preferred the gamble option regardless of the option attributes (such as EV and risk), leading to risk-seeking behavior in the gain context. This "Bias effect" was stronger than the "Risk effect" so that monkeys exhibited an overall risk-seeking rather than a risk-averse behavior.

Finally, we found that the monkeys preferred the gamble option less for increasing token assets in the gain context (**Figure 3.3**; t-test, $H1$: $\beta_{Token} \neq 0$; monkey G: $\beta_{Token\ gain} = -1.80$, $p < 10^{-4}$; monkey O: $\beta_{Token\ gain} = -1.48$, $p < 10^{-4}$), but more (or equally) preferred the gamble for increasing token asset in the loss context (**Figure 3.3**; t-test, $H1$: : $\beta_{Token} \neq 0$; monkey G: : $\beta_{Token\ loss} = 1.68$, $p < 10^{-4}$; monkey O: : $\beta_{Token\ loss} = 0.12$, $p = 0.46$). This differential effect of token assets in the gain and loss context was significantly (**Figure 3.3**; paired t-test, $H1$: $\Delta\ \beta_{Token}$ ($\beta_{Token\ gain} - \beta_{Token\ loss}$) $\neq 0$; monkey G: $\Delta\ \beta_{Token} = -3.47$, $p < 10^{-4}$; monkey O: $\Delta\ \beta_{Token} = -1.60$, $p < 10^{-4}$). These results indicated the token assets had the opposite effect on the monkey's risk attitude in the gain and loss context. Compared with the other effects, the effect of token assets on choice behavior was weak but consistent with empirical monkeys' behaviors.

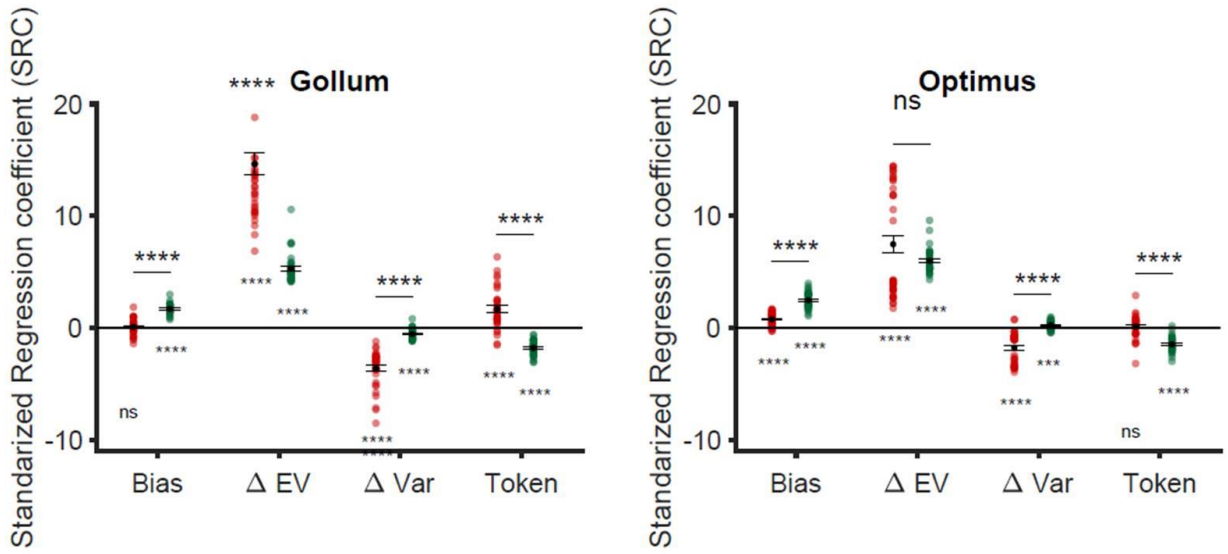

Figure 3.3. Coefficients in wealth-dependent risk-value model modeling for gain and loss trials. **** denotes $p < 10^{-4}$; ns denotes not significant.

3.2.2 Simulation results

To characterize how well our models predicted the contextual effects on risk attitude, we compared the predictions of the model with real behavior. We generated for each trial *t* the probability of choosing the gamble option according to the best-fitting model. For the best model (i.e. the wealth-dependent PT that estimated parameter for trials with different start token number independently), we calculated the accuracy by finding the matching rate between the model-estimated choices and actual choices (Monkey G: 0.89 for all trials; Monkey O: 0.82 for all trials).

Then we submitted the model-estimated choice probabilities to the same statistical analyses showed in **Figure 2.5** for the actual behavior. The model's estimated a probability higher than 0.5 to choose the gamble in both the gain and loss context (**Figure 3.4 left**). Moreover, the model-derived gamble choice probabilities were higher in the gain than that in the loss context

(**Figure 3.4left**). Finally, as the start token number increased, the choice probabilities predicted by the model decreased in the gain context and increased in the loss context (**Figure 3.4 right**). All of these predictions of the model were consistent with the results from actual choice behavior.

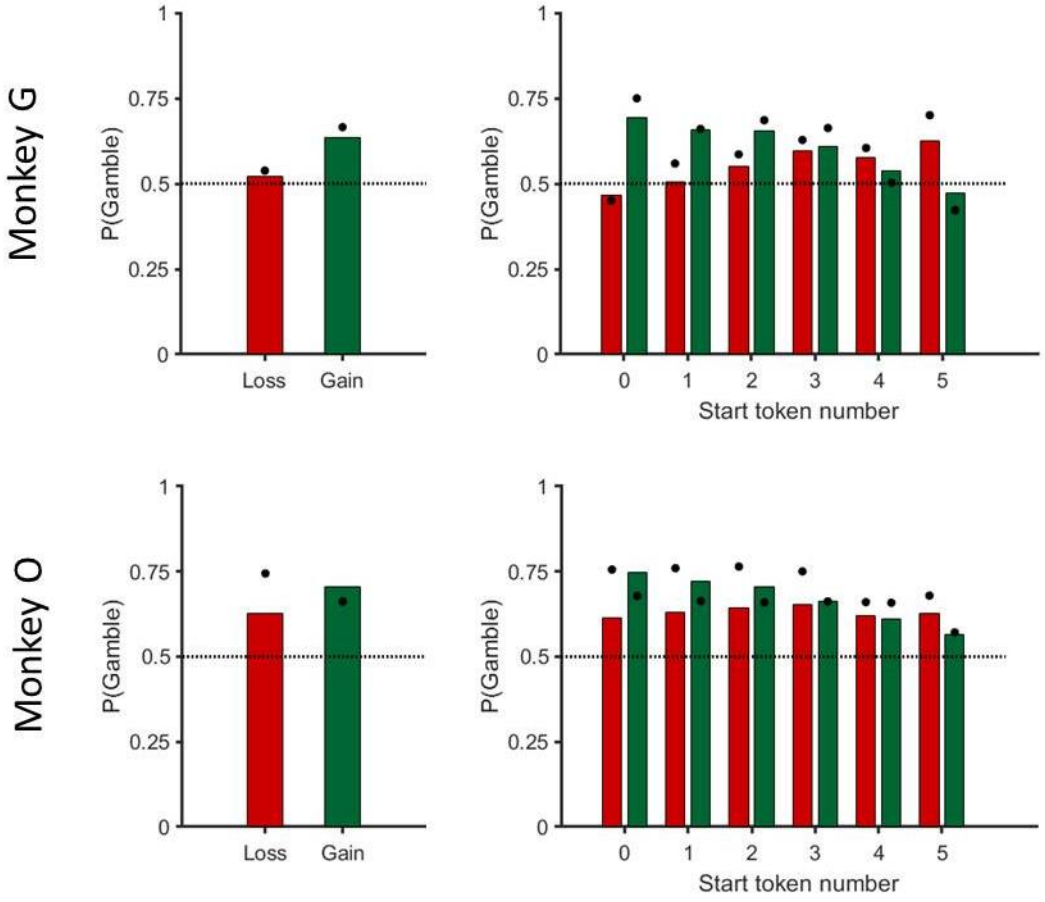

Figure 3.4. Behavioral results and model simulations from the best-fitted model.

3.3 Discussion

In sum, by comparing a range of variants of the prospect theory (PT) model, risk-value (RV) model, and reward proximity (RP) model, we found the wealth-dependent PT model best described the monkeys' behavioral data. The model-simulated choices showed the same contextual effects as found in the empirical data (**Figure 3.3**). Thus, the task developed in this study using monkeys generates behavior during decisions under risk that are similar to the one shown in humans. Thus, this task allowed us to investigate in the primate brain the neuronal computations of functional components of value estimation and representation postulated by prospect theory.

3.3.1 Constraints of current models and alternative model for the future direction

The wealth-dependent PT model, in which α was modulated by start token number, best-described monkeys' behavior. However, when we modeled behavior for each start token number independently, we found that most parameters in the original PT model (not only α, but also γ, *slope*, and *bias*) were influenced by the start token number (**Figure 3.3** and **Table 3.4**). This indicates that token assets can influence monkeys' risk-attitude in multiple ways. A more comprehensive examination of models with different parameter combinations that are influenced by token numbers may a good step in better understanding how the current wealth level influences monkeys' risky behaviors.

Moreover, one of the characteristics of this task was that the monkeys had to accumulate the necessary tokens (≥6) to receive a standard fluid reward (600μl water) over multiple trials (**Figure 2.3**). Therefore, models that take the past or future trials into account may provide a more natural description of behaviors in this task. For example, the reward proximity model, specifically fell short of predicting choice behaviors in the loss context because no matter what

the current token asset and the presented options are, the probability of getting a reward is always zero. Thus, it was not surprising that the fit of this model was much worse than of the other models. In the future, it might be interesting to extend the reward proximity model with variables that take future rewards (with specific weights) into account. Doing so might make this model more realistic and might provide better behavioral predictions.

Chapter 4

Neuronal correlates of decision-related variables in the anterior insular cortex

In the behavioral results, we found that macaques, like humans, change their risk attitude across wealth levels and gain/loss contexts. On the other hand, by constructing a series of behavioral models, we found the prospect theory model well-described monkeys' behaviors. Thus, to further investigated whether neurons in the anterior insular cortex (AIC) encoded the 'reference point' (i.e. the current wealth level of the monkey) and the 'loss aversion effect' (i.e. losses loom larger than gains) as postulated by prospect theory, we did single-unit recordings in the AIC. We first examined whether there were neuronal correlates in the AIC reflecting contextual factors including current token asset, the context of gain/loss, and the expected value of the option. Then we examined whether the neurons encoding value signals in context gain and loss in an asymmetrical manner. Finally, we checked whether changes in the activity of AIC neurons were correlated with the inter-trial fluctuations in choice and risk attitude.

4.1 Methods

4.1.1 Cortical localization and estimation of recording locations

We used T1 and T2 magnetic resonance images (MRIs) obtained for the monkey (3.0 T) to determine the location of the anterior insula. In primates, the insular cortex constitutes a separate cortical lobe, located on the lateral aspect of the forebrain, in the depth of the Sylvian or lateral fissure (LF)(Evrard, 2019; Reil, 1809) (**Figure 4.1**). It is adjoined anteriorly by the orbital

prefrontal cortex, and it is covered dorsally by the frontoparietal operculum and ventrally by the temporal operculum. The excision of the two opercula and part of the orbital prefrontal cortex reveals the insula proper, delimited by the anterior, superior, and inferior peri-insular (or limiting or circular) sulci. We used the known stereoscopic recording chamber location and recording depth of the electrode to estimate the location of each recorded neuron. The estimated recording locations were superimposed on the MRI scans of each monkey. Cortical areas were estimated using the second updated version of the macaque monkey brain atlas by Saleem and Logothetis (Reveley et al., 2017) with a web-based brain atlas(Bakker et al., 2015).

4.1.2 Surgical procedures and single-unit recording

Each animal was surgically implanted with a titanium head post and a hexagonal titanium recording chamber (29mm in diameter) 20.5 mm (Monkey G) and 16 mm (Monkey O) lateral to the midline, and 30 mm (Monkey G) and 34.5 mm (Monkey O) anterior of the interaural line. A craniotomy was then performed in the chambers on each animal, allowing access to the AIC. All sterile surgeries were performed under anesthesia. Post-surgical pain was controlled with an opiate analgesic (buprenex; 0.01 mg/kg IM), administered twice daily for 5 days postoperatively.

Single neuron activities were recorded extracellularly with single tungsten microelectrodes (impedance of 2-4 MΩs, Frederick Haer, Bowdoinham, ME). Electrodes were inserted through a guide tube positioned just above the surface of the dura mater and were lowered into the cortex under control of a self-built microdrive system. The electrodes penetrated perpendicular to the surface of the cortex. The depths of the neurons were estimated by their recording locations relative to the surface of the cortex. Electrophysiological data were collected using the TDT system (Tucker & Davis). Action potentials were amplified, filtered, and discriminated conventionally with a time-amplitude window discriminator. Spikes were isolated online if the

amplitude of the action potential was sufficiently above a background threshold to reliably trigger a time-amplitude window discriminator and the waveform of the action potential was invariant and sustained throughout the experimental recording. Spikes were then identified using principal component analysis (PCA) and the timestamps were collected at a sampling rate of 1,000 Hz.

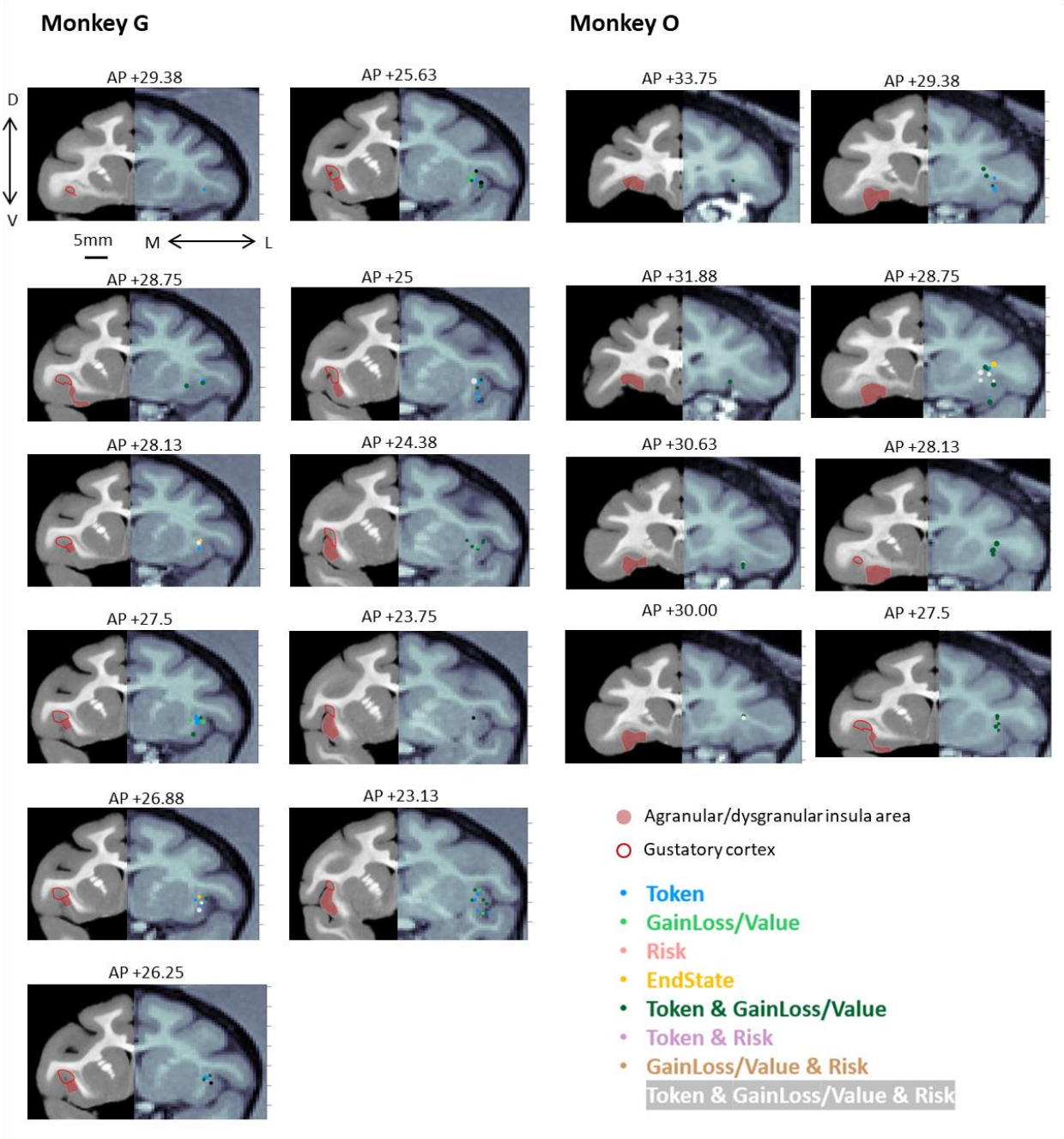
Monkey G
Monkey O
AP +29.38
AP +25.63
AP +33.75
AP +29.38
D
V
5mm
M
L
AP +28.75
AP +25
AP +31.88
AP +28.75
AP +28.13
AP +24.38
AP +30.63
AP +28.13
AP +27.5
AP +23.75
AP +30.00
AP +27.5
AP +26.88
AP +23.13
AP +26.25
Agranular/dysgranular insula area
Gustatory cortex
Token
GainLoss/Value
Risk
EndState
Token & GainLoss/Value
Token & Risk
GainLoss/Value & Risk
Token & GainLoss/Value & Risk

Figure 4.1. Recording sites with the location of neurons of different functional types.
Coronal MRI sections for each monkey show the locations of recorded neurons. The right side of each section shows the MRI from the anatomical scan of each monkey performed before surgery. Superimposed on each section is the estimated location of each recorded neuron based on penetration coordinates and recording depth. Neuronal classification according to the regression model is marked in different colors. The dot size indicates the number of units recorded in the location. Different colors indicate different functional signals encoded by the neurons. The position of each section in stereotactic coordinates is indicated on top. The left side of each section shows the most similar section in the macaque brain atlas of Saleem and Logothetis (2012). The location of the agranular and dysgranular insula (filled pink area), and gustatory cortex (red outlined area) are indicated in each section.

4.1.3 Spike density function

To represent neural activity as a continuous function, we calculated spike density functions by convolving the peri-stimulus time histogram with a growth-decay exponential function that resembled a postsynaptic potential(Hanes et al., 1998). Each spike, therefore, exerts influence only forward in time. The equation describes rate (R) as a function of time (t): $R(t) = (1 - \exp(-t/\tau g)) * \exp(-t/\tau d)$, where τg is the time constant for the growth phase of the potential and τd is the time constant for the decay phase. Based on physiological data from excitatory synapses, we used 1 ms for the value of τg and 20 ms for the value of τd (Sayer et al., 1990).

4.1.4 Linear regression analysis of neuronal coding

To find AIC neurons whose activity reflects specific decision-related variable(s), we performed linear regression with mean firing rate (FR) within the choice period for each trial as the dependent variable, and a predictor derived from the decision-related variables as the independent variable:

$$FR = constant + \alpha * predictor$$

in which α was the coefficient of the predictor. A constant term was added as a baseline model.
To tested four different classes of decision-related variables: (1) “Token-asset” variables, (2) “Gain/Loss-Value” variables, (3) “Risk” variables, and (4) an “Absolute value” variable. In total, we considered 16 different potential decision-related variables, as well as a baseline model that consisted only of a constant term.

Token-asset variables were variables that represented the start token number in one of three different types. The first type, the *linear token signal*, encoded the start token number in a linear, continuous manner (monotonically rising or falling from 0 to 5). The second type, the *binary token signal*, encoded the start token number in a binary, discontinuous manner (with a value of

"1" for trials with start token number 0 to 3 and a value of "2" for trials with start token number 3-5). The third type, the *tuned token signal*, encoded the start token number with a peak in activity at one of the token numbers from 0 to 5, and the activity symmetrically falling for token numbers that were smaller or larger than the peak.

Gain/Loss-Value variables were variables that represented the gain/loss context, the expected value of options, or gain/loss context-dependent value signals. We tested five types of variables. The first type, the *gain/loss signal*, encoded the context of gain or loss in a binary manner. Trials in the gain domain were indicated with a "1", and trials in the loss domain with a "-1". The only exception was no-choice trials with a sure option with EV = 0, which were indicated with a "0". The second type, the *linear value signal*, encoded the expected value of options in a linear, continuous manner across both the gain and loss domain (with a range from -3 to 3). The remaining types also encoded the expected value of options, but contingent on the gain/loss context. The third type, the *gain value signal*, encoded the expected value of options in a linear manner, but only in the gain domain (options with EV larger than 0 were encoded as the original number, otherwise were encoded as "0"), while the fourth type, the *loss value signal*, encoded the expected value of options in a linear manner only in the loss domain (options with EV smaller than 0 were encoded as the original number, otherwise were encoded as "0"). The fifth type, the *behavioral salience signal*, encoded the expected value of options in a linear but asymmetric direction for the gain and loss domain. Thus, this signal encoded the absolute distance of the value from zero, independent of whether it represented a gain or a loss (e.g. both an option with EV = 1.5 and an option with EV = -1.5 would be encoded as "1.5").

Risk variables were variables that represented the variance of possible outcomes of an option (calculated by $\sqrt{p(1-p)}$, in which p was the winning probability of the option). We considered

two different types. The first type, the *linear risk signal*, encoded the variance of outcome in a linear manner proportional to the variance. The second type, the *binary risk signal*, encoded whether the outcome of the option was uncertain or not in a binary manner (with a value of "1" for all gamble options and a value of "0" for all sure options).

So far, value always was defined as a relative change of tokens, independent of the start token number. We also considered an a*bsolute value signal* (i.e., the sum of all possible end token numbers, weight by their probability). This signal took into account not only the possible change in token number but also the start token number. Thus, it represented the outcome of a choice in an absolute framework that reflected how close the monkey was to earning the fluid reward.

Mixed-selective neuronal coding with regression analysis

The regression analysis using the series of single-variable models indicated that many neurons encoded multiple decision-related variables. We therefore further investigated the contribution of decision-related variables to neural activity, by using multiple linear regression with the mean firing rate (FR) within the choice period for each trial as the dependent variable, and predictors derived from the decision-related variables as the independent variables.

$$FR = constant + \alpha 1 * predictor 1 + \ldots\ldots + \alpha i * predictor\ i$$

We fitted a family of regression models with all possible combinations of the basic decision-related variables described in the last section. This resulted in a total of 163 tested models. For each neuron, we determined the best-fitting model using the Akaike information criterion and classified it as belonging to different functional categories according to the variables that were included in the best-fitting model.

4.1.5 Receiver operating criterion (ROC) analysis

To determine whether the neural activity of the AIC neurons was correlated with the monkey's choice behavior or risk-attitude, we computed a receiver operating characteristic (ROC) for each cell and computed the area under the curve (AUC) as a measure of the cell's discrimination ability in a trial-by-trial manner. For each neuron, we first computed the AUC value of *choice probability* by comparing the distributions of firing rates associated with each of the two choices (i.e. choice of "gamble" or choice of "sure"). We also computed the AUC value of *risk-seeking probability* by comparing the two distributions of firing rates associated with risk-seeking and risk-avoidance behavior. Risk-seeking trials were defined as trials where the monkey chose the gamble even though the expected value of the gamble option was smaller than the expected value of the sure option. We did not include trials in which the monkey chose the gamble option and it had a higher expected value because in that case, the monkey's choice did not give any indication about his risk-attitude at that moment. Conversely, risk-avoiding trials were defined as trials where the monkey chose the sure option even though the expected value of the sure option was smaller than the expected value of the gamble option. Thus, trials used to compute the risk-seeking probability were a subset of the trials used to compute the choice probability, namely those in which the monkeys did not make choices that maximized the expected value of the chosen option.

4.2 Results

4.2.1 Anterior Insular neurons encode decision-related variables that affect risk-attitude

To determine the neuronal basis underlying prospect theory, we recorded 240 neurons in the AIC of two macaque monkeys (monkey G: 142 neurons; monkey O: 98 neurons) working in the token gambling task. The recording locations are shown in **Figure 4.2a** (more details in **Figure**

4.1). We analyzed the neuronal activity in the choice period (i.e., the time from target onset to saccade initiation) to determine if AIC neurons carried signals that could influence decision making. We began by analyzing activity during no-choice trials, in which only one option was presented. In general, the AIC neurons showed weak spatial selectivity. Only 7% (17/240) of all AIC neurons showed a significant effect of spatial location on neuronal activity (1-way ANOVA, $p<0.05$). We therefore ignored spatial target configuration for the remaining analysis.

To quantitatively characterize the variables that each AIC neuron encodes during the choice period, we examined the activity of each neuron using a series of linear regression models with all potential combinations of 3 basic variables (token assets, value, and risk) and a baseline term. This resulted in 8 families of models. Within each family, a basic variable could be represented by varying numbers of specific instantiations (3 forms of token-encoding, 5 forms of value-encoding, 2 forms of risk-encoding). This resulted in a total of 162 tested models, including a model that included only a baseline term (for details see Methods). For each neuron, we identified the best fitting model using the Akaike information criterion and classified it into different functional categories according to the variables that were most likely encoded by the neuronal activity.

The vast majority of recorded AIC neuron activity (146/240; 61%) encoded at least one decision-related variable (task-related neurons: $p < 0.05$ for the coefficient of a specific variable in the best-fitting multiple linear regression model; **Figure 4.2b,** more details in **Table 4.1**). Among these task-related neurons, 78 neurons (33%) carried gain/loss-modulated value signals, 109 neurons (45%) carried token signals, 19 neurons (8%) carried risk signals, and 9 neurons (4%) carried an absolute value signal. A substantial number of AIC neurons (53/146; 36%)

showed mixed selectivity and encoded more than one decision-related variable. The distributions of neural type classification were similar across the two monkeys (**Table 4.2**).

A large group of AIC neurons reflected information about the expected value of the options (value-encoding neurons). A subset of this group of AIC neurons, carrying a *Linear value signal* (example neuron in **Figure 4.2c**), encoded the expected value of all options in a monotonically rising (n=13) or falling (n=1) fashion, for both gains and losses. This kind of value signal is not gain/loss context-sensitive. However, we found the neuronal activity of other subsets of value-encoding neurons that varied largely as a function of the way they represented value across the Gain and the Loss context (**Figure 4.2d-e**). One group of these value-encoding neurons carried a binary *Gain/Loss signal* (**Figure 4.2d**) that categorized each option as gain or loss, regardless of the expected value. In addition, we found AIC neurons that represented value in both the gain and loss context, but with inverse correlations of neural activity and value (**Figure 4.2e**). These neurons likely carried a *Behavioral salience signal*. Most interestingly, we found two other groups of AIC neurons carrying *Loss value* (**Figure 4.2f**) or *Gain value signals* (**Figure 4.2g**), respectively. These neurons represented a value signal, but only in either the loss or the gain context. We encountered more Loss value neurons (n=29) than Gain value neurons (n=4). The larger number of neurons encoding Loss value fits with human neuroimaging findings that suggest a role for the anterior insula in encoding aversive stimuli and situations(Canessa et al., 2013; Kuhnen & Knutson, 2005).

The largest proportion of AIC neurons reflected information about the currently owned token number. These token-encoding neurons used three different frameworks for encoding token assets. The first group carried a *Linear token signal* (**Figure 4.2h**). These AIC neurons monotonically increased (n=11) or decreased (n=2) their activity with the number of token

assets. The second group carried a *Binary token signal* (**Figure 4.2i**). These AIC neurons categorized all possible token numbers into a high [3, 4, 5] and a low [0, 1, 2] token level. Likely, this reflects a fundamental distinction between a 'low' token level, for which it is impossible that the monkey will earn a reward at the end of the current trial (because the monkey can only earn a maximum of 3 tokens in one trial), and a 'high' token level that makes it possible to earn a reward in the current trial. The third, and the largest, group carried a *Numerical token signal*. These AIC neurons are number-selective and are tuned for a preferred number (here four, example neuron in **Figure 4.2j**). We used a Gaussian function to fit this activity pattern. The AIC neurons carrying a Numerical token signal covered the entire scale from 0-5 tokens with some neurons having each of the possible token amounts as their preferred number.

Based on human neuroimaging data (Bossaerts, 2010; Preuschoff et al., 2008), it has been suggested that the anterior insular cortex encodes the riskiness of options. We tested therefore if AIC neurons encoded risk-related signals. Here risk was defined as outcome variance. We found some AIC neurons (n=9) carrying a *Linear risk signal* (**Figure 4.2k**) that encoded the risk of the various options across both the gain and loss context in a parametric fashion. We also found another group of AIC neurons (n=10) encoding a *Binary risk signal* that categorized options into safe or uncertain. More details of the distribution of type of neuron can be found in **Table 4.2**and **Table 4.3**.

In the analysis so far, we have used a relative framework for value. The expected value was defined as token changes relative to a reference point (the start token number). However, the value could also be defined in an absolute framework (i.e., the final token number at the end of the trial). Such an absolute value framework is arguably better suited for capturing the interest of the monkey in ascertaining how close he is to collecting 6 tokens and reaping a reward. We

tested for AIC neurons that represented the expected absolute value, which is the expected end token number weighted by the probability of each outcome. However, we found only a very small number (9/240; 4%) carrying an *End token signal* (**Figure 4.2l).**

A significant number of AIC neurons showed activity patterns that matched several predictions of prospect theory. First, we found that many AIC neurons encode the wealth level of the monkey, i.e. the token number at the start of the trial. Within the context of our task, this variable represented the reference point relative to which the gain or loss options are measured. Simultaneously, this variable also indicates the current state of progress and indicates how close the monkey is to achieving the next reward. Second, many other AIC neurons reflect in their activity whether the offer is a gain or a loss. Some of them encoded the context, i.e., whether the options were presented in the gain or loss context. Other neurons represented a gain/loss-specific value signal in a parametric manner exclusively. Third, only very few neurons encode the expected absolute value. Taken together, these three findings strongly imply that the primate AIC uses a relative value encoding framework, anchored to a reference point that reflects the current state of the monkey, as suggested by prospect theory.

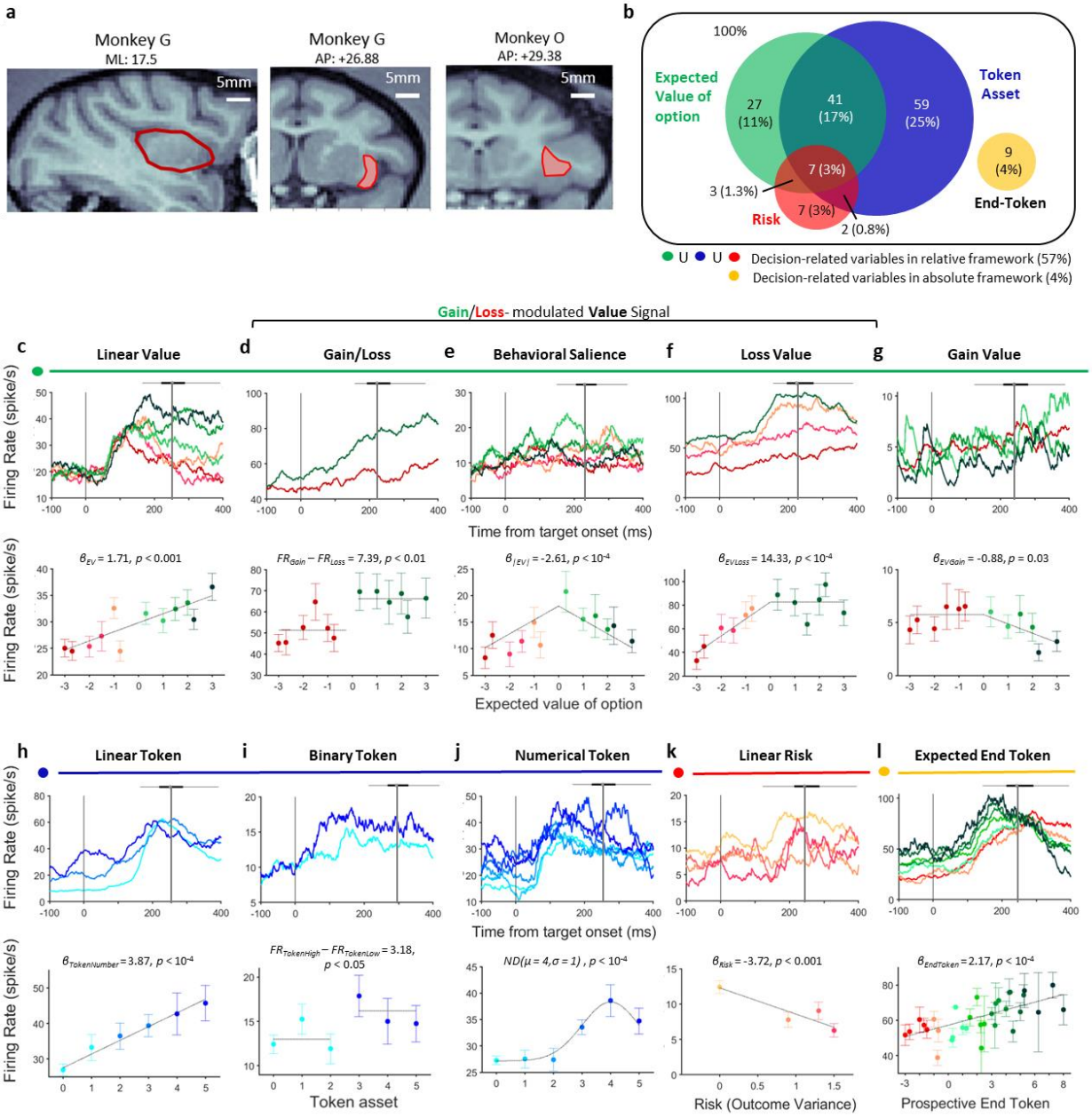
a
Monkey G
ML: 17.5
5mm
Monkey G
AP: +26.88
5mm
Monkey O
AP: +29.38
5mm
b
100%
Expected Value of option
Token Asset
27 (11%)
41 (17%)
59 (25%)
9 (4%)
End-Token
7 (3%)
3 (1.3%)
Risk
7 (3%)
2 (0.8%)
U U Decision-related variables in relative framework (57%)
Decision-related variables in absolute framework (4%)
Gain/Loss- modulated Value Signal
c Linear Value
d Gain/Loss
e Behavioral Salience
f Loss Value
g Gain Value
Firing Rate (spike/s)
Time from target onset (ms)
Expected value of option
h Linear Token
i Binary Token
j Numerical Token
k Linear Risk
l Expected End Token
Token asset
Risk (Outcome Variance)
Prospective End Token

Figure 4.2. AIC Neurons encode diverse task-related variables in forced-choice trials.

(a) MRI images showing the area of the recording of each monkey. Left and middle: sagittal (left) and coronal (middle) view of the insular cortex of monkey G. Right: coronal view of the insular cortex of monkey O.

(b) Venn diagram of the neurons encoding four task-related variables in the forced-choice trials. Green: the expected value of the option (EV); Blue: start token number; Red: risk (variability of potential outcomes); Yellow: end token number.

(c-g) Example neurons showing a variety of patterns by which the contextual information (gain vs. loss) and/or the EV were encoded. Upper panels: spike density function (SDF), aligned by the target onset (t=0). Lower panels: mean firing rate of each example neuron at different EV levels. The mean firing rate was calculated using the window from target onset to saccade initiation (varied across trials). The distribution of saccade timing was presented as a boxplot on top of each SDF. For clarity, when plotting the SDF, data of some EV levels were grouped together, as indicated by the color codes. (c) linear encoding of the EV across contexts; (d) binary encoding of gain/loss context; (e) linear encoding of the absolute value of the EV in both contexts; (f) linear encoding of the EV in the loss context; (g) linear encoding of the EV in the gain context.

(h-j) Example neurons showing a variety of patterns by which the token information was encoded. (h) linear; (i) binary encoding of the start token number; (j) encoding of a specific number of start token (=4). Conventions are as in (c-g).

(k) Example neuron showing linear encoding of the risk. Conventions are as in (c-g).

(l) Example neuron showing linear encoding of the end token number. Conventions are as in (c-g).

Table 4.1. Summary of the number and percentage of significant responding neurons in different subsets of neuron types for all recorded AIC neurons.

Gain/Loss-Value	**Gain/Loss** 13 (5%)	**Loss Value** 29 (12%)	**Gain Value** 4 (2%)	**Behavioral Salience** 13 (5%)	**Linear Value** 14 (6%)				**All** 73 (30%)
Token	**Linear Token** 13 (5%)	**Binary Token** 11 (5%)	**Token 0** 11 (5%)	**Token 1** 16 (7%)	**Token 2** 24 (10%)	**Token 3** 12 (5%)	**Token 4** 10 (4%)	**Token 5** 8 (3%)	**All** 105 (44%)
Risk	**Linear Risk** 9 (4%)	**Binary Risk** 10 (4%)							**All** 19 (8%)
Expected End Token	**End Token** 9 (4%)								**End Token** 9 (4%)

Table 4.2. Summary of the number and percentage of significant responding neurons in different subsets of neuron types for AIC neurons recorded from each monkey.

Gain/Loss-Value Monkey G (n=142) Monkey O (n=98)	**Gain/Loss** 4 (3%) 9 (9%)	**Loss Value** 9 (6%) 20 (20%)	**Gain Value** 1 (1%) 3 (3%)	**Behavioral Salience** 4 (3%) 9 (9%)	**Linear Value** 3 (2%) 11 (11%)				**All** 21 (15%) 52 (53%)
Token Monkey G (n=142) Monkey O (n=98)	**Linear Token** 7 (5%) 6 (6%)	**Binary Token** 9 (6%) 2 (2%)	**Token 0** 2 (1%) 9 (9%)	**Token 1** 9 (6%) 7 (7%)	**Token 2** 7 (5%) 14 (14%)	**Token 3** 6 (4%) 6 (6%)	**Token 4** 4 (3%) 6 (6%)	**Token 5** 4 (3%) 4 (4%)	**All** 48 (34%) 54 (55%)
Risk Monkey G (n=142) Monkey O (n=98)	**Linear Risk** 4 (3%) 5 (5%)	**Binary Risk** 6 (4%) 4 (4%)							**All** 10 (7%) 9 (9%)
Expected End Token Monkey G (n=142) Monkey O (n=98)	**End Token** 6 (4%) 3 (3%)								**End Token** 6 (4%) 3 (3%)

Table 4.3. Summary of the number and percentage of neurons positively or negatively correlated to different decision-related variables.

Gain/Loss-Value Positive correlation Negative correlation	**Gain/Loss** 8 (62%) 5 (38%)	**Loss Value** 27 (93%) 2 (7%)	**Gain Value** 0 (0%) 4 (100%)	**Behavioral Salience** 0 (0%) 13 (100%)	**Linear Value** 13 (93%) 1 (7%)				**All** 48 (66%) 25 (34%)
Token Positive correlation Negative correlation	**Linear Token** 11 (85%) 2 (15%)	**Binary Token** 4 (36%) 7 (64%)	**Token 0** 0 (0%) 11 (100%)	**Token 1** 8 (50%) 8 (50%)	**Token 2** 21 (88%) 3 (12%)	**Token 3** 12 (100%) 0 (0%)	**Token 4** 8 (80%) 2 (20%)	**Token 5** 5 (63%) 3 (37%)	**All** 69 (66%) 36 (34%)
Risk Positive correlation Negative correlation	**Linear Risk** 3 (33%) 6 (64%)	**Binary Risk** 3 (30%) 7 (70%)							**All** 6 (32%) 13 (68%)
Expected End Token Positive correlation Negative correlation	**End Token** 5 (56%) 4 (44%)								**End Token** 5 (56%) 4 (44%)

Table 4.4. The number of each signal during the choice period in the force choice trial recounted based upon the AUC for choice or risk-attitude.

	Token + Value + Risk	Token + Value	Token + Risk	Value + Risk	Token	Value	Risk	End Token	None
Both	0	0	1	0	3	0	0	0	0
Choice	0	0	3	0	5	0	2	1	4
Risk-attitude	0	1	3	0	8	0	3	0	1
Neither	3	12	23	1	104	5	16	9	32

4.2.2 Value-encoding neurons in AIC exhibit contextual modulation postulated by the Prospect theory

The majority of value-encoding AIC neurons were context-modulated (**Figure 4.2d-g**). A strong assumption of Prospect theory is that changes in relative value are not encoded symmetrically across gains and losses. Indeed, the monkeys' behavior indicated that they were more sensitive to objective value differences in the loss than the gain context (i.e. steeper utility functions in the loss than that in the gain context in **Figure 3.1**). We therefore investigated whether and how value signals across the AIC population showed matching differences in their sensitivity for gains and losses. We examined the absolute value of the standardized regression coefficients (SRC) of Loss-Value Neurons in the loss context and that of Gain-Value neurons in the gain context. At the population level, we found indeed that Loss value signals and Gain Value signals had different sensitivities to changes in value. Specifically, the normalized |SRC|s of Loss-Value Neurons in the loss context were larger than that of Gain-Value Neuron in the gain context (**Figure 4.3a,** permutation test; mean of $|SRC_{loss}|$= 2.978, mean of $|SRC_{gain}|$= 2.058, p = 0.054; unsigned SRC for losses and gains were indicated in red and green, respectively). This suggests that the AIC neurons encoding value signals were more sensitive to increasing loss than increasing gain (**Figure4. 3b**).

Moreover, the sensitivity of value change in gain or loss context was also influenced by the wealth level. Normalized |SRC| of Loss-Value Neurons in the loss context became smaller as the wealth level increased (**Figure 4.3c,** left; permutation test; mean of $|SRC_{loss}|$ in low wealth level = 3.49, mean of $|SRC_{loss}|$ with high wealth level= 2.47, p = 0.017; unsigned SRC in the loss context for low or high wealth levels were indicated in orange and red, respectively). Normalized |SRC| of Gain-Value Neurons in the gain context also became smaller as the wealth level

increased. However, this trend did not reach a significant level (**Figure 4.3c,** right; permutation test; mean of $|SRC_{Gain}|$ in low wealth level = 2.38, mean of $|SRC_{gain}|$ in high wealth level= 2.06, p = 0.29; unsigned SRC in the gain context in low or high wealth levels were indicated in light and dark green, respectively). Again, this wealth level-sensitive effect on AIC value coding (**Figure 3d**) is consistent with the fact that monkeys became less sensitive to objective value change when the wealth level increased (i.e., utility functions became flattered in both the loss and gain context when the wealth level increased; **Figure 3.2**).

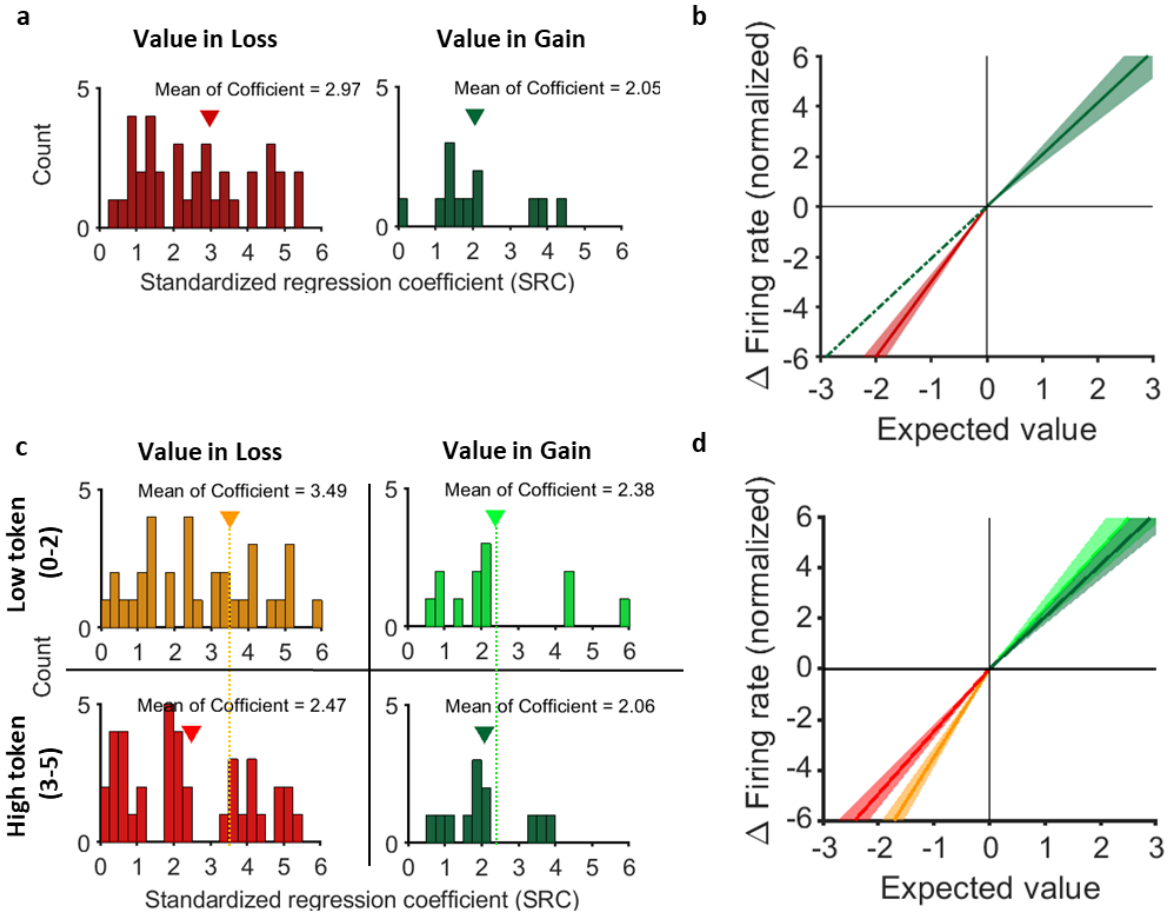
a
Value in Loss
Value in Gain
Mean of Cofficient = 2.97
Mean of Cofficient = 2.05
Count
Standardized regression coefficient (SRC)
b
Δ Firing rate (normalized)
Expected value
c
Value in Loss
Value in Gain
Low token (0-2)
High token (3-5)
Mean of Cofficient = 3.49
Mean of Cofficient = 2.38
Mean of Cofficient = 2.47
Mean of Cofficient = 2.06
Count
Standardized regression coefficient (SRC)
d
Δ Firing rate (normalized)
Expected value

Figure 4.3. Gain-Value and loss-Value neurons exhibit differential sensitivity to EV change in the gain and loss context.

(a-b) Linear regression was performed using the expected value of the option (EV) as the regressor, to account for the variability of firing rates for Loss-Value neurons (39 neurons) in loss-context trials; and for Gain-Value neurons (12 neurons) in gain-context trials. See Methods for details of the neuron selection.

(a) Distribution of the standardized regression coefficients (SRC). For cross-context comparison, the absolute values of SRCs (|SRCs|) were plotted. Left panel: data of those Loss-Value neurons in loss-context trials. Right panel: data of those Gain-Value neurons in gain-context trials. Each count represents one neuron. Inverted triangle: mean of the distribution.

(b) Replot the SRCs (as the slope of ΔFR to ΔEV) of Loss Value neurons (red) and those of Gain Value neurons (green) in loss- and gain-context, respectively. Noted that the slope of the red line is steeper than the slope of the green line ($p=0.053$, permutation test), indicating that as compared to the Gain Value neurons, the Loss Value neurons are more sensitive to EV change (in the loss context), mirroring the pattern observed from behavior (Fig.1g). The solid line and shadow area: mean ± S.E.M.

(c-d) Linear regression was performed using the expected value of the option (EV) as the regressor, to account for the variability of firing rates for Loss-Value neurons in loss-context trials in low or high token level; and for Gain-Value neurons in gain-context trials in low or high token level.

(c) Distribution of the |SRCs| of Loss Value neurons in loss-context (left column) and |SRCs| of Gain Value neurons in gain-context (right column), split by start token levels. Upper row: low token level (start token number = 0-2; Bottom row: high token level (start token number = 3-5). Conventions as in (a).

(d) Replot the SRCs from (c). Note that for both gain- and loss- contexts, the slope becomes shallower as the token level increases, consistent with the pattern observed from behavior (Fig.1g).

4.2.3 Choice probability of AIC neurons predict the internal states related to behavioral choices

The gain/loss-specific value signals and the wealth level signals in AIC were present before the choice was made and were therefore in a position to influence the monkey's decisions. To determine whether the neural activity of the AIC neurons correlates with choice behavior, we computed a receiver operating characteristic (ROC) for each cell and then computed the area under the curve (AUC) as a measure of the cell's discrimination ability. In this analysis, an AUC value significantly different from 0.5 indicates at least a partial discrimination between two conditions. For each AIC neuron, we calculated two AUC values. First, we compared the firing rate distributions on choice trials when the monkey chose the gamble versus the sure option. We used this AUC value as a measure of *choice probability*. Second, we compared the firing rate distributions on choice trials when the monkey was risk-seeking versus risk-avoiding. We used this AUC value as a measure of *risk-attitude probability*. Risk-seeking trials were defined as trials where the monkey chose the gamble, even when the expected value of the gamble option was smaller than the expected value of the sure option. We did not include trials, in which the monkey chose the gamble option and it had a higher expected value because in that case, the monkey's choice did not give any indication about his risk-attitude at that moment. Conversely, risk-avoiding trials were defined as trials where the monkey chose the sure option, even so, it had a lower expected value than the gamble option. Thus, trials used to compute the risk-seeking probability were the subset of the trials used to compute the choice probability, in which the monkeys did not make choices that maximized the expected value of the chosen option.

We found that trial-by-trial fluctuations in the activity of a subset of AIC neurons (35/240; 15%) significantly correlated with fluctuations of choice or risk-attitude. As shown in **Figure**

4.4, 19 neurons (8%) showed a significant choice probability (green), 20 neurons (8%) showed significant risk-attitude probability (purple), and 4 neurons (2%) showed both significant choice probability and risk-attitude probability (black). Across the AIC population (n=240), the ability of neural activity to predict choice and risk attitude showed a strong positive correlation (Pearson correlation; $r = 0.41$, $p<10^{-4}$).

AIC neurons encode contextual information that influences monkeys' choice and momentary risk-attitude, such as current wealth level, gain/loss, and the value of each option (**Figure 4.2**). It is therefore not surprising that the activity of many of these neurons is predictive of choice or risk-taking. To test whether neurons encoding specific behaviorally relevant variables were more likely to carry significant choice or risk-attitude probability signals (**Figure 4.5**), we used a chi-square test, which is used to determine whether there is a statistically significant difference between the expected frequencies and the observed frequencies in one or more categories. However, a chi-square test showed no significant dependency between the encoding of a specific decision-related variable and the likelihood that choice-predictive and/or risk-attitude-predictive signals were carried by a given AIC neuron (**Table4.4**, $\chi^2= 7.61$, $p = 0.67$, excluding neurons with AUROC that predict neither choice nor risk-attitude).

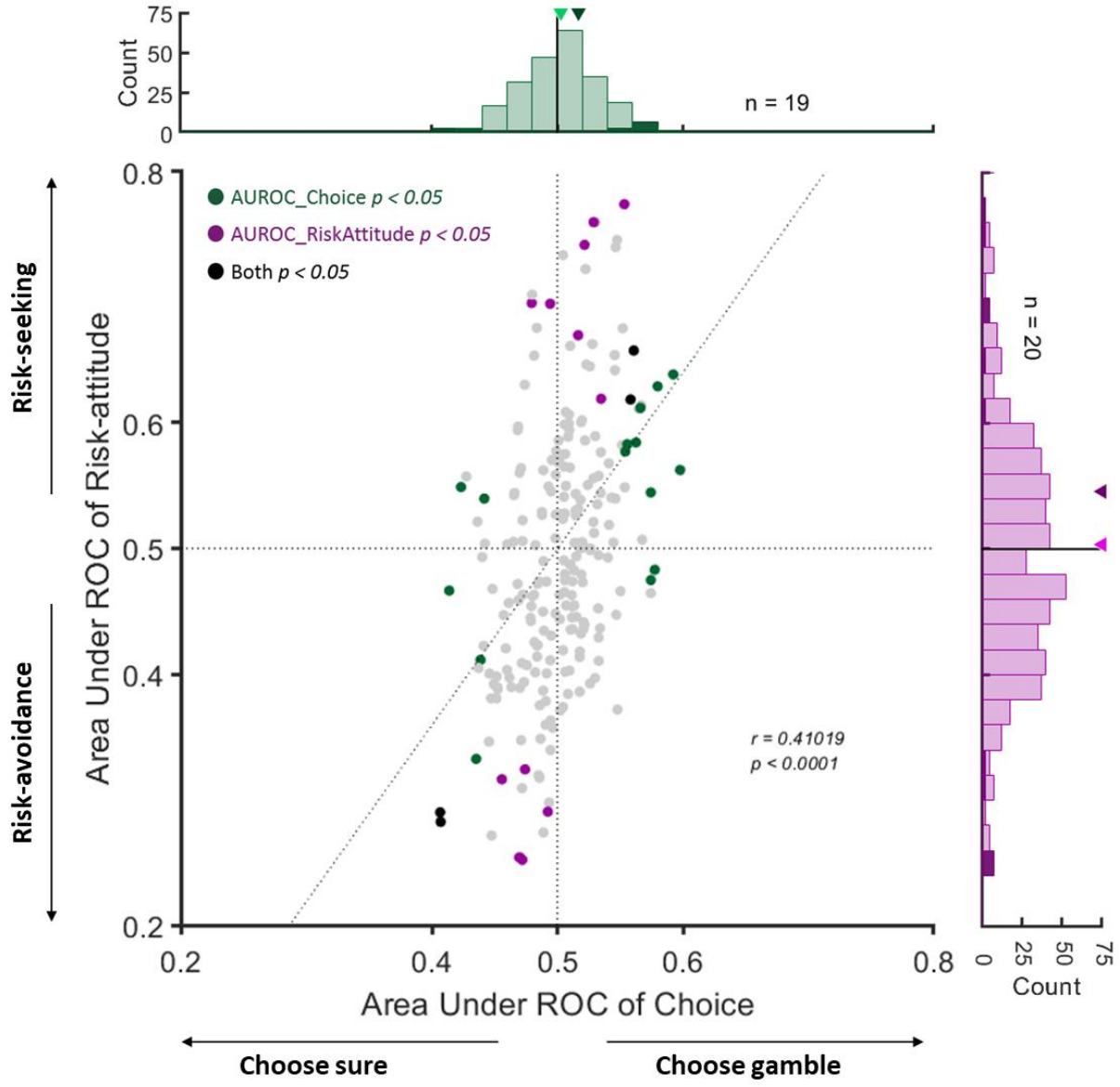
75
50
25
0
Count
n = 19
AUROC_Choice p < 0.05
AUROC_RiskAttitude p < 0.05
Both p < 0.05
Risk-seeking
Risk-avoidance
Area Under ROC of Risk-attitude
0.8
0.6
0.5
0.4
0.2
r = 0.41019
p < 0.0001
n = 20
0
25
50
75
Count
0.2
0.4
0.5
0.6
0.8
Area Under ROC of Choice
Choose sure
Choose gamble

Figure 4.4 Distribution of area under the curve (AUC) of receiver operating characteristic (ROC) for choice and risk-attitude in individual neurons.

AUC values capturing the covariation of each neuron with differences in choice (choosing gamble or sure) and risk-attitude (risk-seeking or risk-avoidance). Each point represents one neuron (n = 240), and colors indicate the significance of the two AUC values. In the marginal distributions, significant neurons are indicted in darker shades and the arrowheads indicate the average values across the entire distribution (light green or light purple) and the subset of neurons with significant AUC (dark green or dark purple), respectively. The gray vertical and horizontal dashed lines show the area of no significant discrimination ability (AUC of choice = 0.5 and AUC of risk-attitude = 0.5). The broken line represents the linear regression relating the AUC of choice and AUC of risk-attitude (r and p values refer to the regression slope).

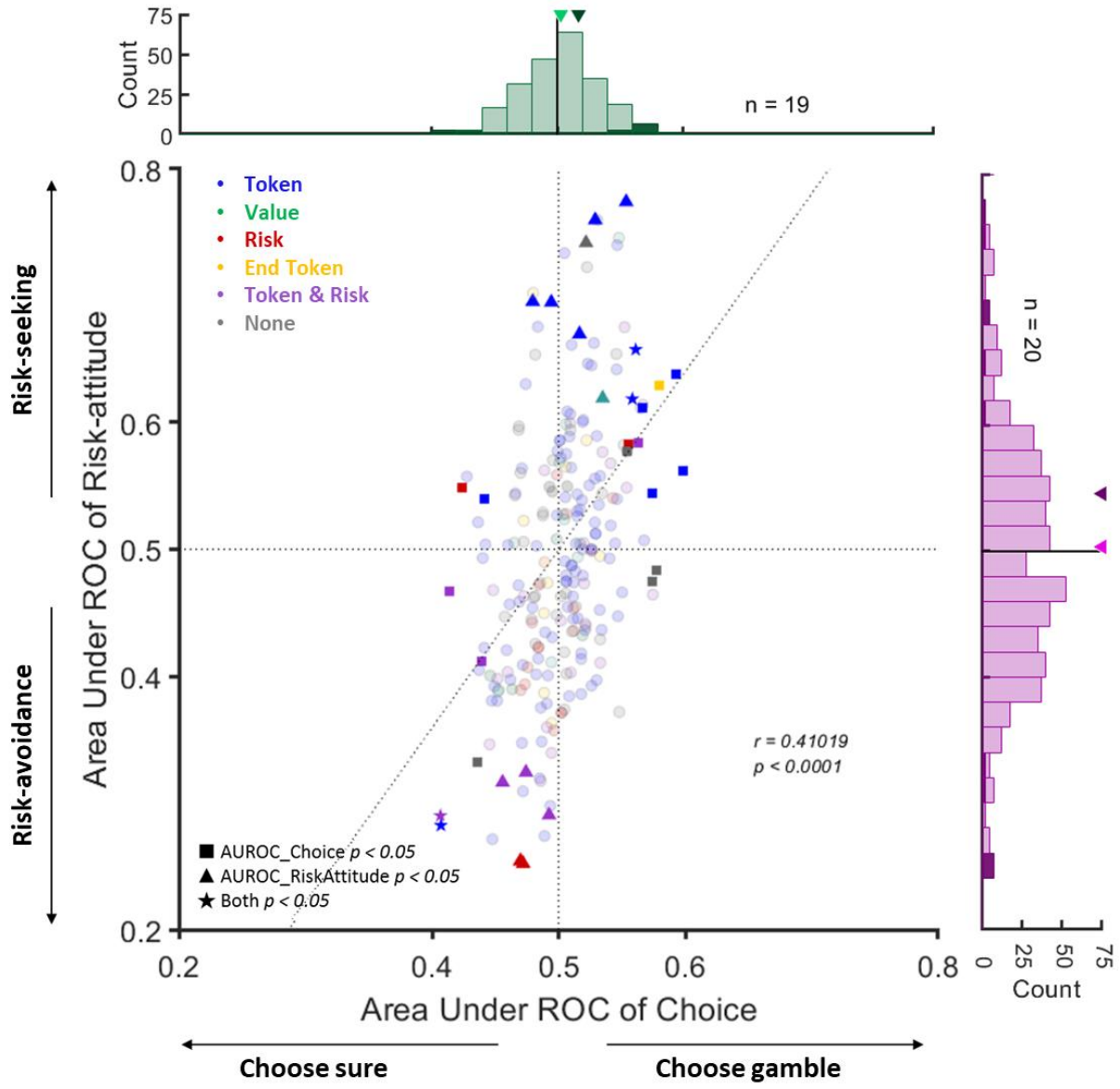
Count
75
50
25
0
n = 19
Token
Value
Risk
End Token
Token & Risk
None
Risk-seeking
Risk-avoidance
Area Under ROC of Risk-attitude
0.8
0.6
0.5
0.4
0.2
r = 0.41019
p < 0.0001
AUROC_Choice p < 0.05
AUROC_RiskAttitude p < 0.05
Both p < 0.05
n = 20
0
25
50
75
Count
0.2
0.4
0.5
0.6
0.8
Area Under ROC of Choice
Choose sure
Choose gamble

Figure 4.5. Distribution of area under the curve (AUC) of receiver operating characteristic (ROC) for choice and risk-attitude in neurons encode different kinds of decision-related signals.

AUC values capturing the covariation of each neuron with differences in choice (choosing gamble or sure) and risk-attitude (risk-seeking or risk-avoidance). Each point represents one neuron (n = 240). Shapes indicate the significance of the two AUC values. Colors indicate the functional signal encoded by the neuron. In the marginal distributions, significant neurons are indicted in darker shades and the arrowheads indicate the average values across the entire distribution (light green or light purple) and the subset of neurons with significant AUC (dark green or dark purple), respectively. The gray vertical and horizontal dashed lines show the area of no significant discrimination ability (AUC of choice = 0.5 and AUC of risk-attitude = 0.5). The broken line represents the linear regression relating the AUC of choice and AUC of risk-attitude (r and p values refer to the regression slope).

4.3 Discussion

4.3.1 Involvement of anterior insular cortex in the decision making under risk

The insular cortex is a large heterogeneous cortex that is typically divided into posterior granular, intermediate dysgranular, and anterior agranular sectors, based on cytoarchitectural differences. Our recordings were concentrated in the most anterior part of the insula and encompassed mostly agranular and some dysgranular areas (**Figure 4.1**). In addition, we also recorded some neurons in the border regions of the adjacent gustatory cortex. Importantly, we found no functional segregation or gradient with respect to the functional signals that were represented across the different cortical areas, we explored. This fits with a recent primate neuroimaging study that showed strong activation of this entire region by visual cues indicating reward, as well as reward delivery (Kaskan et al., 2017). Insula has long been known to be strongly connected with the neighboring gustatory cortex (Ogawa, 1994; Vincis et al., 2020). Recently, several lines of studies have demonstrated that neurons in the gustatory cortex not only engage the primary processing of gustatory inputs but also involve multisensory integration (Craig, 2002; Craig & Craig, 2009), as well as higher cognitive functions like decision-making (Kuhnen & Knutson, 2005; Vincis et al., 2020). This suggests that the primate insular cortex and the neighboring gustatory cortex are strongly interconnected and form an interacting distributed network during decision making.

4.3.2 Anterior insular neurons represent decision-related variables postulated by prospect theory

4.3.2.1 Anterior insular neurons encode the current wealth level

Prospect theory assumes that people make decisions based on the potential gain or losses relative to a reference point. In our experiment, the natural reference point against which the

monkey compared possible outcomes was the current token assets. Consistent with this idea, we found that the activity of a substantial number of AIC neurons (109/240; 45%) encoded start token number. The AIC has been suggested to represent the current physiological state of the subject (i.e., interoception) (Craig, 2002; Craig & Craig, 2009; Critchley & Garfinkel, 2018; Livneh et al., 2020). Our findings suggest that AIC also encodes more abstract state variables, such as current wealth level, which are important for economic decisions that will influence the future homeostatic state. Notably, we found some AIC neurons encode the start token number on a numerical scale, with their activity increased (or decreased) specifically when the monkey owned a particular number of tokens. Such a pattern of numerical encoding has been identified in the primate prefrontal and parietal cortex (Nieder, 2016; Nieder & Dehaene, 2009), medial temporal lobe (Kutter et al., 2018), and recently in AIC (L. Wang et al., 2015). It would be interesting for future studies to investigate whether these number-tuned neurons relate to the numerical abilities of primates.

4.3.2.2 Anterior insular neurons encode the value signal in a gain/loss-specific manner

Our results overwhelmingly support the notion that value-related signals in the brain operate in a relative framework. Only 4% of neurons in the AIC carried a value signal in an absolute framework. However, how the value of options is represented in a relative framework is an issue under debate. The core of the debate regards whether the value of gains and losses are represented in a single unitary system (Tom et al., 2007) or separately by two independent systems (Kahn et al., 2002; Knutson, Fong, et al., 2001; Yacubian et al., 2006). Some of the AIC neurons encoding a parametric value signal did continuously across gains and losses (14/47; 30%). However, most AIC neurons encoded gain or loss-specific value signals (33/47; 70%). Thus, while there is some evidence for both hypotheses, most AIC value-encoding neurons form

two independent representations that encode gains or losses, respectively. This functional separation is further supported by the presence of a large number of neurons carrying a categorical gain/loss signal. Interestingly, the number of loss-encoding neurons (29/33; 88%) is much larger than the number of gain-encoding AIC neurons (4/33; 12%). This may explain why human imaging studies often find a link between the AIC and the anticipation of aversive outcomes (Canessa et al., 2013; Kuhnen & Knutson, 2005). Thus, the AIC recordings show the presence of separate neuronal populations that encode value as a relative gain or loss. This could be the neuronal underpinning of the separate utility functions used in prospect theory.

4.3.3 Anterior insular cortex is engaged in monitoring 'risk' of option as well as 'risk-attitude' of subject

'Risk' is often formalized and quantified as the outcome variance, and the AIC has been implicated to play a role in monitoring risk(Bossaerts, 2010; Preuschoff et al., 2008). In line with this, we found 8% of the AIC neurons (n=19/240) whose activity correlates with the outcome variance. Moreover, the trial-by-trial variability of the monkeys' choice and risk attitude was correlated with activity changes in a subgroup of AIC neurons (**Figure 6**). All of this supports the hypothesis that AIC plays an important part in the process of decision-making under risk.

Chapter 5

Innovations and future directions

In the previous chapters, we described how contextual factors including current wealth level and gain/loss context influenced monkeys' risky behaviors as postulated by prospect theory and how the core concepts assumed in prospect theory were represented in the primate brain. In this chapter, we will highlight the innovations and significance of these findings and discuss a few lines of continuing/future research that, with my thesis work as the foundation, could enrich our knowledge about the neuronal network underlying decision-making under risk.

5.1 Innovations and significances of the current research

5.1.1 A behavioral model to investigate contextual-dependent risk attitude

The development of the token-based gambling task creates a situation in which the monkeys' risk attitude is not stable, but flexible and context-dependent. Specifically, both the token asset indicating the monkeys' current wealth level and the outcomes being gains and losses influence monkeys' preference toward risk. The use of tokens to this task allows investigating the monkeys' attitudes toward "economic losses" (reduction of the secondary reward) rather than "aversive stimuli" like intense light/sound, air-puff, foot-shock, bitter taste/odor that are directly delivered to the animals (primary punishment). Furthermore, it allows us to explore other behavioral effects that modulation of risk preference and economic choices, such as the endowment and framing effect.

5.1.2 Supporting evidence of prospect theory in behavioral, modeling, and neural levels

Prospect theory provides profound insights into how humans make risky decisions in a wide range of circumstances (Tversky & Kahneman, 1979, 1992). The behavioral hallmarks described by the theory have also been reported in old- and new-world monkeys, as well as in rats (M. K. Chen et al., 2006; Constantinople et al., 2019; Farashahi et al., 2018; Stauffer et al., 2015). This suggests that the neural circuits responsible for making risky decisions may have been evolutionarily conserved across mammals. Using a token-based gambling task, we demonstrated that monkeys exhibited different risk-attitudes when they were in different wealth levels and in different gain/loss contexts as described in the prospect theory. With a series of model examination, we further found the wealth-dependent prospect theory model well explained these behavioral effects. Finally, we found activity of AIC neurons in macaques exhibits critical characteristics including "reference-dependent" and "asymmetric value function in gain and loss" that are postulated by Prospect Theory. These behavioral, modeling, and neuronal findings provide further support that prospect theory is the result of neuronal circuits that are conserved in human and animals (at least in non-human primate).

5.1.3 Role of the anterior insular cortex in decision making under risk

To the best of our knowledge, this is the first study recording single neurons of the AIC in awake, behaving primates during risky decision-making. We interpreted the function of AIC from the perspective of economic, risky decisions (Kuhnen & Knutson, 2005) and within the framework of Prospect theory (Tversky & Kahneman, 1979). Decisions are likely not only guided by the rational, abstract processes depicted by economic models but are strongly influenced by emotional processes (Loewenstein et al., 2001). The AIC has been suggested to occupy a central position in regulating emotions as it receives interoceptive afferents from

visceral organs through the posterior granular insula area, representing contextual information (as demonstrated by this study), and is closely connected with the amygdala and autonomic nuclei (Craig, 2002; Evrard, 2019). This study took the first step to delineate how the decision context modulates economic value representation and thereby impacts the decision of subjects. Future work will further investigate the interacting functions of AIC in economic decisions, emotions, and autonomic regulation.

5.2 Future directions

5.2.1 Behavioral analyses across trials

In the current study, we developed the token-based gambling task, in which the monkey had to acquire multiple tokens (≥6 tokens) in successive trials to receive an immediate reward. Thus, the choice of each trial naturally dependents on the choices in previous trials and their results. Nevertheless, in the behavioral and modeling analyses so far, we only focused on how variables in the current trial (e.g. token asset, the context of gain/loss, and values of presented options) influenced monkeys' risky behavior. To better depict how monkeys made decisions in the token-based gambling task across trials, our next steps will be to examining how monkeys behave based on past events (e.g. different history effects) and the prospect of future events.

We can first investigate the history effect on a smaller scale by examining how monkeys' risky choices are influenced by the choice history or outcome history in the previous trial(s). We would like to test whether monkeys showed inclinations to switch or repeat their choices based on their choice in the previous trial and their outcome (choice history). One possibility is that monkeys use a 'win-stay and loose-shift' strategy (Blanchard et al., 2014; Constantinople et al., 2019). In this strategy, the monkeys would repeat a choice (e.g., a gamble), when that same choice resulted in a win (i.e., the better outcome of the gamble), but would switch to choosing

the sure option when they had lost the gamble in the past trial. In that case, the outcome history would be evaluated in a binary matter. Another possibility is that the monkeys adapted their behavior based on the token outcome (token numbers -3 to 3) they received in the previous trial. In that case, the outcome history would be evaluated in a parametric manner. Finally, if monkeys' behaviors are indeed biased by the choice and outcome history, we can ask how far back the effects be traced back and how the relative weight of their outcome on the present choice changes (Lau & Glimcher, 2005).

We can also investigate history effects on a larger time scale to see whether the monkeys' behavior is influenced by the fatigue effect (Süss & Schmiedek, 2000) or the satiation effect (Yamada et al., 2013). For example, within a session, the monkeys might be more cautious to maximize the value of the chosen option in the early phase while starting to use some heuristics like a repeated gamble or sure choice in the late phase. We can further examine whether this switch from rational choice to heuristic is directly related to the passage of time or the monkeys' satiation state indicated by the reward volume they have received. Furthermore, since monkeys can learn to collect enough tokens in a few trials to win an immediate reward, we might hypothesize that monkeys can represent the 'prospect' of future reward. In that case, we can examine whether the monkeys have the ability to plan actions across multiple trials to achieve future goals (collect at 6 tokens to exchange for a large amount of water). This is relevant to the reward proximity model described in chapter 4 that assumed monkeys were optimizing reward harvesting across trials.

5.2.2 Risk-seeking monkeys

Overall, monkeys in the present study were more prone to choose gamble options (**Figure. 2.5**). This is in line with similar findings of previous monkey experiments (Farashahi et al., 2018;

McCoy & Platt, 2005; So & Stuphorn, 2010; Stauffer et al., 2015), yet is inconsistent with most human studies (Fishburn & Kochenberger, 1979; Hershey & Schoemaker, 1980; Tversky & Kahneman, 1979, 1992). It is unclear whether such a discrepancy between humans and monkeys was due to species-specific differences, individual variability, or task design. Macaques have been shown to be risk-aversive, like humans, in a foraging task (Eisenreich et al., 2019) and in a risky decision-making task using animals' hydration state to index their non-monetary wealth level (Yamada et al., 2013). The observed tendency to choose gamble options was therefore likely due to task-specific factors, such as the small reward amount at stake and a large number of trials. Further studies that examine whether and how these potential factors can influence monkeys' risk attitude or perform an analog experiment in humans may provide a better understanding of this behavioral discrepancy.

5.2.3 Neuronal response after the choice

In the neural results showed in chapter 4, we focused on activities of AIC neurons specific during the choice period (from target onset to saccade initiation). This helped us to investigate how AIC neurons encoded decision-related variables that would finally guide monkeys' choices. However, it is of critical importance to know whether and how AIC neurons play a role in representing the reward expectation (Kaskan et al., 2017; Mizuhiki et al., 2012), actual reward (Wittmann et al., 2010), and risk or reward prediction error (RPE) (Preuschoff et al., 2008; Seymour et al., 2004).

We would like to first focus on neuronal activity during the period between choice onset to token outcome revealed, to examine whether the outcome expectation (estimated as the expected value of the chosen option) is represented by AIC neurons. After the token outcome revealed, we can further check whether the AIC neurons carry the information of (1) parametric token

outcome (numerical token outcome from -3 to 3), (2) categorical outcome (winning or losing the gamble, or receiving a certain outcome from the sure option), (3) reward prediction error (the discrepancy between outcome expectation and actual outcome), and (4) context-dependent token outcome (whether two identical token outcomes that gaining/losing 'zero token' resulted in a gain or loss trials are encoded differently), which is consistent to the reward prediction error framework that reflects the value of an outcome relative to its reward expectation.

We can thereafter extend the neuronal activities in the outcome period to discuss the issues (1) whether outcome values in loss or gain context were encoded differentially within the AIC, (2) whether both negative and positive prediction error signals can be found in the AIC and (3) what is the relationship between neuronal coding of negative/positive value and neuronal coding of negative/positive RPE.

To explore more on how these value signals and learning signals are represented or implemented in the brain, it is of critical importance to investigate brain areas that are known to highly engage in value-based decision making and reinforcement learning (Niv, 2009). Brain areas in the dopaminergic system, including the prefrontal cortex, basal ganglia, and the ventral tegmental area may be good candidates for future research (Glimcher, 2011; Schultz, 2015). Moreover, it is also interesting to take brain areas that are suggested to represent the negative reward-prediction error in either the dopaminergic system (e.g. habenula) (Matsumoto & Hikosaka, 2007; Salas et al., 2010) or serotoninergic system (Daw et al., 2002) into to future consideration.

5.2.4 Dynamic neuronal activity and population analyses

In the neural results showed in chapter 4, we found AIC neurons showed mix-selectivity to multiple variables in the choice period. It is plausible that AIC neurons can encode many task-

related signals in different dimensions. Furthermore, if we expanded the time scale to the whole trial, we can find more complicated dynamic multiplexed signals in the AIC neurons. For example, a neuron can carry the information of token asset in the ITI (before the token cue onset), sustained the information of token asset after token cue onset, encode the expected value of gamble option, and then encode the reward expectation after choice.

Besides the AIC, accumulating evidence has found that multiple brain areas including the prefrontal cortex (Aoi et al., 2020; Rigotti et al., 2013), orbitofrontal cortex (Abe & Lee, 2011; Hirokawa et al., 2019), and amygdala (Corder et al., 2019) have a multidimensional code for context, decisions, and both relevant and irrelevant sensory or motor information. Moreover, these representations can also evolve in time. The heterogeneous tunings to multiple variables in a single neuron level make it difficult to know the clear role of these neuronal representations. It thereafter led to the suggestion that representation in individual neurons in these higher cognitive brain areas are randomly mixed and can only be well understood at the neural population level. By combining multi-electrode recording with population analyses (e.g. clustering analyses and dimensionality reduction), we may gain more insight into how AIC neurons represent information (e.g. the state of current wealth or the task-relevant sensory information) dynamically in a multi-dimensional subspace in the future.

5.2.5 Role of frontal areas in this decision-making process

In the present study, we found that neurons in the anterior insular cortex (AIC) monitor the contextual factors that influence monkey's risk attitudes. Specifically, AIC neurons encode the wealth level of the monkey and option values in a gain/loss-specific manner, suggesting a potential neural basis for the reference point and the asymmetrical value functions proposed in prospect theory. These results support the hypothesis that the role of primate AIC in risky

decision-making is to provide the information of decision context, and by which the value representation of available options is modulated in support of the animal's choices. However, we only found changes in the activity of a minor group of AIC neurons directly predict inter-trial fluctuations in risky choice. It suggested the AIC neurons likely do not control risky choice directly, but rather modify ongoing choice processes in the frontal cortex by providing contextual input.

We are particularly interested in two frontal areas, the lateral prefrontal cortex (Paulus et al., 2001) and medial frontal cortex (Critchley et al., 2001; Ernst et al., 2004; Gehring & Willoughby, 2002) since their activity levels have been found to correlate with the probability that a subject chooses to seek or avoid risk. The first candidate, the supplementary eye field (SEF) is an oculomotor area in the medial frontal cortex that was found to represent action value signals in an oculomotor gambling task (So & Stuphorn, 2010; Stuphorn et al., 2010; Stuphorn & Schall, 2006). The second candidate, the lateral prefrontal cortex (LPFC) is known to be active during risky decisions (Paulus et al., 2001) and connect the AIC and SEF by receiving input from AIC and projecting to SEF. Thus, we hypothesize that (1) AIC neurons represent behaviorally relevant contextual information that influences the probability of choosing a particular risky reward option, (2) SEF neurons receives information about risk-attitude and uses it to influence decisions under risk, and (3) LPFC transforms risk-attitude signals in AIC into choice selection signals in SEF.

5.2.6 Causal role of these brain areas in the decision making under risk

In addition to recording the neuronal activity in the proposed brain areas (AIC, FEF, and LPFC) to search for the neuronal correlates of contextual variables that influence risk attitude or reflect the risky choice, we can further test whether these areas are causally necessary for

decision making under risk by reversible inactivation techniques. At the behavioral level, we can examine how monkeys' risk attitudes in token-based gambling are affected after the inactivation of one of these areas. At the neuronal level, we can also monitor how the inactivation of one area affects the neural activity recorded simultaneously in other non-inactivated areas.

These experiments will provide novel approaches to understanding the competition between risk-seeking and risk-avoidance behavior at the neuronal level, and gain more understanding of the neural mechanisms controlling risk attitude.

Reference

Abe, H., & Lee, D. (2011). Distributed coding of actual and hypothetical outcomes in the orbital and dorsolateral prefrontal cortex. *Neuron*, *70*(4), 731–741.

Allais, M. (1953). Le comportement de l'homme rationnel devant le risque: Critique des postulats et axiomes de l'école américaine. *Econometrica: Journal of the Econometric Society*, 503–546.

Amiez, C., Joseph, J.-P., & Procyk, E. (2006). Reward encoding in the monkey anterior cingulate cortex. Cerebral Cortex, 16(7), 1040–1055.

Aoi, M. C., Mante, V., & Pillow, J. W. (2020). Prefrontal cortex exhibits multidimensional dynamic encoding during decision-making. *Nature Neuroscience*, 1–11.

Arrow, K. J. (1965). Aspects of the theory of risk-bearing. Yrjö Jahnssonin Säätiö.

Asaad, W. F., & Eskandar, E. N. (2008). A flexible software tool for temporally-precise behavioral control in Matlab. Journal of Neuroscience Methods, 174(2), 245–258.

Bakker, R., Tiesinga, P., & Kötter, R. (2015). The scalable brain atlas: Instant web-based access to public brain atlases and related content. Neuroinformatics, 13(3), 353–366.

Barron, G., & Erev, I. (2003). Small feedback-based decisions and their limited correspondence to description-based decisions. Journal of Behavioral Decision Making, 16(3), 215–233.

Bechara, A., Tranel, D., Damasio, H., & Damasio, A. R. (1996). Failure to respond autonomically to anticipated future outcomes following damage to prefrontal cortex. Cerebral Cortex, 6(2), 215–225.

Berns, G. S., Capra, C. M., Chappelow, J., Moore, S., & Noussair, C. (2008). Nonlinear neurobiological probability weighting functions for aversive outcomes. Neuroimage, 39(4), 2047–2057.

Blais, A.-R., & Weber, E. U. (2006). A domain-specific risk-taking (DOSPERT) scale for adult populations. Judgment and Decision Making, 1(1).

Blanchard, T. C., Wilke, A., & Hayden, B. Y. (2014). Hot-hand bias in rhesus monkeys. Journal of Experimental Psychology: Animal Learning and Cognition, 40(3), 280.

Bossaerts, P. (2010). Risk and risk prediction error signals in anterior insula. Brain Structure and Function, 214(5–6), 645–653.

Breiter, H. C., Aharon, I., Kahneman, D., Dale, A., & Shizgal, P. (2001). Functional imaging of neural responses to expectancy and experience of monetary gains and losses. Neuron, 30(2), 619–639.

Abe, H., & Lee, D. (2011). Distributed coding of actual and hypothetical outcomes in the orbital and dorsolateral prefrontal cortex. *Neuron*, *70*(4), 731–741.

Allais, M. (1953). Le comportement de l'homme rationnel devant le risque: Critique des postulats et axiomes de l'école américaine. *Econometrica: Journal of the Econometric Society*, 503–546.

Amiez, C., Joseph, J.-P., & Procyk, E. (2006). Reward encoding in the monkey anterior cingulate cortex. Cerebral Cortex, 16(7), 1040–1055.

Aoi, M. C., Mante, V., & Pillow, J. W. (2020). Prefrontal cortex exhibits multidimensional dynamic encoding during decision-making. *Nature Neuroscience*, 1–11.

Arrow, K. J. (1965). Aspects of the theory of risk-bearing. Yrjö Jahnssonin Säätiö.

Asaad, W. F., & Eskandar, E. N. (2008). A flexible software tool for temporally-precise behavioral control in Matlab. Journal of Neuroscience Methods, 174(2), 245–258.

Bakker, R., Tiesinga, P., & Kötter, R. (2015). The scalable brain atlas: Instant web-based access to public brain atlases and related content. Neuroinformatics, 13(3), 353–366.

Barron, G., & Erev, I. (2003). Small feedback-based decisions and their limited correspondence to description-based decisions. Journal of Behavioral Decision Making, 16(3), 215–233.

Bechara, A., Tranel, D., Damasio, H., & Damasio, A. R. (1996). Failure to respond autonomically to anticipated future outcomes following damage to prefrontal cortex. Cerebral Cortex, 6(2), 215–225.

Berns, G. S., Capra, C. M., Chappelow, J., Moore, S., & Noussair, C. (2008). Nonlinear neurobiological probability weighting functions for aversive outcomes. Neuroimage, 39(4), 2047–2057.

Blais, A.-R., & Weber, E. U. (2006). A domain-specific risk-taking (DOSPERT) scale for adult populations. Judgment and Decision Making, 1(1).

Blanchard, T. C., Wilke, A., & Hayden, B. Y. (2014). Hot-hand bias in rhesus monkeys. Journal of Experimental Psychology: Animal Learning and Cognition, 40(3), 280.

Bossaerts, P. (2010). Risk and risk prediction error signals in anterior insula. Brain Structure and Function, 214(5–6), 645–653.

Breiter, H. C., Aharon, I., Kahneman, D., Dale, A., & Shizgal, P. (2001). Functional imaging of neural responses to expectancy and experience of monetary gains and losses. Neuron, 30(2), 619–639.

Critchley, H. D., Mathias, C. J., & Dolan, R. J. (2001). Neural activity in the human brain relating to uncertainty and arousal during anticipation. *Neuron*, *29*(2), 537–545.

Daw, N. D., Kakade, S., & Dayan, P. (2002). Opponent interactions between serotonin and dopamine. Neural Networks, 15(4–6), 603–616.

De Martino, B., Camerer, C. F., & Adolphs, R. (2010). Amygdala damage eliminates monetary loss aversion. Proceedings of the National Academy of Sciences, 107(8), 3788–3792.

Dohmen, T., Falk, A., Huffman, D., Sunde, U., Schupp, J., & Wagner, G. G. (2011). Individual risk attitudes: Measurement, determinants, and behavioral consequences. Journal of the European Economic Association, 9(3), 522–550.

Eckel, C. C., & Grossman, P. J. (2008). Men, women and risk aversion: Experimental evidence. Handbook of Experimental Economics Results, 1, 1061–1073.

Eisenreich, B. R., Hayden, B. Y., & Zimmermann, J. (2019). Macaques are risk-averse in a freely moving foraging task. Scientific Reports, 9(1), 1–12.

Ernst, M., Bolla, K., Mouratidis, M., Contoreggi, C., Matochik, J. A., Kurian, V., Cadet, J.-L., Kimes, A. S., & London, E. D. (2002). Decision-making in a risk-taking task: A PET study. Neuropsychopharmacology, 26(5), 682–691.

Ernst, M., Nelson, E. E., McClure, E. B., Monk, C. S., Munson, S., Eshel, N., Zarahn, E., Leibenluft, E., Zametkin, A., & Towbin, K. (2004). Choice selection and reward anticipation: An fMRI study. Neuropsychologia, 42(12), 1585–1597.

Evrard, H. C. (2019). The organization of the primate insular cortex. Frontiers in Neuroanatomy, 13, 43.

Farashahi, S., Azab, H., Hayden, B., & Soltani, A. (2018). On the flexibility of basic risk attitudes in monkeys. Journal of Neuroscience, 38(18), 4383–4398.

Fiorillo, C. D., Tobler, P. N., & Schultz, W. (2003). Discrete coding of reward probability and uncertainty by dopamine neurons. Science, 299(5614), 1898–1902.

Fishburn, P. C., & Kochenberger, G. A. (1979). Two-piece von Neumann-Morgenstern utility functions. Decision Sciences, 10(4), 503–518.

Frank, M. J., Seeberger, L. C., & O'reilly, R. C. (2004). By carrot or by stick: Cognitive reinforcement learning in parkinsonism. Science, 306(5703), 1940–1943.

Fujimoto, A., & Minamimoto, T. (2019). Trait and state-dependent risk attitude of monkeys measured in a single-option response task. Frontiers in Neuroscience, 13.

Gehring, W. J., & Willoughby, A. R. (2002). The medial frontal cortex and the rapid processing of monetary gains and losses. Science, 295(5563), 2279–2282.

Gianotti, L. R., Knoch, D., Faber, P. L., Lehmann, D., Pascual-Marqui, R. D., Diezi, C., Schoch, C., Eisenegger, C., & Fehr, E. (2009). Tonic activity level in the right prefrontal cortex predicts individuals' risk taking. Psychological Science, 20(1), 33–38.

Gilaie-Dotan, S., Tymula, A., Cooper, N., Kable, J. W., Glimcher, P. W., & Levy, I. (2014a). Neuroanatomy predicts individual risk attitudes. Journal of Neuroscience, 34(37), 12394–12401.

Gilaie-Dotan, S., Tymula, A., Cooper, N., Kable, J. W., Glimcher, P. W., & Levy, I. (2014b). Neuroanatomy Predicts Individual Risk Attitudes. The Journal of Neuroscience, 34(37), 12394. https://doi.org/10.1523/JNEUROSCI.1600-14.2014

Glimcher, P. W. (2008). Understanding risk: A guide for the perplexed. Cognitive, Affective, & Behavioral Neuroscience, 8(4), 348–354.

Glimcher, P. W. (2011). Understanding dopamine and reinforcement learning: The dopamine reward prediction error hypothesis. Proceedings of the National Academy of Sciences, 108(Supplement 3), 15647–15654.

Gonzalez, C., Dana, J., Koshino, H., & Just, M. (2005). The framing effect and risky decisions: Examining cognitive functions with fMRI. Journal of Economic Psychology, 26(1), 1–20.

Hanes, D. P., Patterson, W. F., & Schall, J. D. (1998). Role of frontal eye fields in countermanding saccades: Visual, movement, and fixation activity. Journal of Neurophysiology, 79(2), 817–834.

Hayden, B. Y., Heilbronner, S. R., Nair, A. C., & Platt, M. L. (2008). Cognitive influences on risk-seeking by rhesus macaques. Judgment and Decision Making, 3(5), 389.

Hayden, B. Y., & Platt, M. L. (2007). Temporal discounting predicts risk sensitivity in rhesus macaques. Current Biology, 17(1), 49–53.

Hershey, J. C., & Schoemaker, P. J. (1980). Prospect theory's reflection hypothesis: A critical examination. Organizational Behavior and Human Performance, 25(3), 395–418.

Hertwig, R., Barron, G., Weber, E. U., & Erev, I. (2004). Decisions from experience and the effect of rare events in risky choice. Psychological Science, 15(8), 534–539.

Hirokawa, J., Vaughan, A., Masset, P., Ott, T., & Kepecs, A. (2019). Frontal cortex neuron types categorically encode single decision variables. Nature, 576(7787), 446–451.

Hsu, M., Bhatt, M., Adolphs, R., Tranel, D., & Camerer, C. F. (2005). Neural systems responding to degrees of uncertainty in human decision-making. Science, 310(5754), 1680–1683.

Hsu, M., Krajbich, I., Zhao, C., & Camerer, C. F. (2009). Neural response to reward anticipation under risk is nonlinear in probabilities. Journal of Neuroscience, 29(7), 2231–2237.

Huettel, S. A., Stowe, C. J., Gordon, E. M., Warner, B. T., & Platt, M. L. (2006). Neural signatures of economic preferences for risk and ambiguity. Neuron, 49(5), 765–775.

Ishii, H., Ohara, S., Tobler, P. N., Tsutsui, K.-I., & Iijima, T. (2012). Inactivating anterior insular cortex reduces risk taking. Journal of Neuroscience, 32(45), 16031–16039.

Juechems, K., Balaguer, J., Ruz, M., & Summerfield, C. (2017). Ventromedial prefrontal cortex encodes a latent estimate of cumulative reward. Neuron, 93(3), 705-714. e4.

Jung, W. H., Lee, S., Lerman, C., & Kable, J. W. (2018). Amygdala functional and structural connectivity predicts individual risk tolerance. Neuron, 98(2), 394-404. e4.

Kahn, I., Yeshurun, Y., Rotshtein, P., Fried, I., Ben-Bashat, D., & Hendler, T. (2002). The role of the amygdala in signaling prospective outcome of choice. Neuron, 33(6), 983–994.

Kaskan, P. M., Costa, V. D., Eaton, H. P., Zemskova, J. A., Mitz, A. R., Leopold, D. A., Ungerleider, L. G., & Murray, E. A. (2017). Learned value shapes responses to objects in frontal and ventral stream networks in macaque monkeys. Cerebral Cortex, 27(5), 2739–2757.

Knoch, D., Gianotti, L. R., Pascual-Leone, A., Treyer, V., Regard, M., Hohmann, M., & Brugger, P. (2006). Disruption of right prefrontal cortex by low-frequency repetitive transcranial magnetic stimulation induces risk-taking behavior. Journal of Neuroscience, 26(24), 6469–6472.

Knutson, B., Adams, C. M., Fong, G. W., & Hommer, D. (2001). Anticipation of increasing monetary reward selectively recruits nucleus accumbens. Journal of Neuroscience, 21(16), RC159–RC159.

Knutson, B., Fong, G. W., Adams, C. M., Varner, J. L., & Hommer, D. (2001). Dissociation of reward anticipation and outcome with event-related fMRI. Neuroreport, 12(17), 3683–3687.

Knutson, B., & Greer, S. M. (2008). Anticipatory affect: Neural correlates and consequences for choice. Philosophical Transactions of the Royal Society B: Biological Sciences, 363(1511), 3771–3786.

Krain, A. L., Wilson, A. M., Arbuckle, R., Castellanos, F. X., & Milham, M. P. (2006). Distinct neural mechanisms of risk and ambiguity: A meta-analysis of decision-making. NeuroImage, 32(1), 477–484.

Kuhnen, C. M., & Knutson, B. (2005). The neural basis of financial risk taking. Neuron, 47(5), 763–770.

Kutter, E. F., Bostroem, J., Elger, C. E., Mormann, F., & Nieder, A. (2018). Single neurons in the human brain encode numbers. Neuron, 100(3), 753-761. e4.

Lattimore, P. K., Baker, J. R., & Witte, A. D. (1992). The influence of probability on risky choice: A parametric examination. National Bureau of Economic Research.

Lau, B., & Glimcher, P. W. (2005). Dynamic response-by-response models of matching behavior in rhesus monkeys. Journal of the Experimental Analysis of Behavior, 84(3), 555–579.

Lauriola, M., & Levin, I. P. (2001). Personality traits and risky decision-making in a controlled experimental task: An exploratory study. Personality and Individual Differences, 31(2), 215–226.

Levin, I. P., & Hart, S. S. (2003). Risk preferences in young children: Early evidence of individual differences in reaction to potential gains and losses. Journal of Behavioral Decision Making, 16(5), 397–413.

Levin, I. P., Xue, G., Weller, J. A., Reimann, M., Lauriola, M., & Bechara, A. (2012). A neuropsychological approach to understanding risk-taking for potential gains and losses. Frontiers in Neuroscience, 6, 15.

Livneh, Y., Sugden, A. U., Madara, J. C., Essner, R. A., Flores, V. I., Sugden, L. A., Resch, J. M., Lowell, B. B., & Andermann, M. L. (2020). Estimation of Current and Future Physiological States in Insular Cortex. Neuron, Journal Article.

Loewenstein, G. F., Weber, E. U., Hsee, C. K., & Welch, N. (2001). Risk as feelings. Psychological Bulletin, 127(2), 267.

Machina, M. J. (1987). Decision-making in the presence of risk. Science, 236(4801), 537–543.

Manes, F., Sahakian, B., Clark, L., Rogers, R., Antoun, N., Aitken, M., & Robbins, T. (2002). Decision-making processes following damage to the prefrontal cortex. Brain, 125(3), 624–639.

March, J. G., & Shapira, Z. (1987). Managerial perspectives on risk and risk taking. Management Science, 33(11), 1404–1418.

Markowitz, H. (1952). The utility of wealth. Journal of Political Economy, 60(2), 151–158.

Matsumoto, M., & Hikosaka, O. (2007). Lateral habenula as a source of negative reward signals in dopamine neurons. Nature, 447(7148), 1111–1115.

McCoy, A. N., & Platt, M. L. (2005). Risk-sensitive neurons in macaque posterior cingulate cortex. Nature Neuroscience, 8(9), 1220–1227.

Mizuhiki, T., Richmond, B. J., & Shidara, M. (2012). Encoding of reward expectation by monkey anterior insular neurons. Journal of Neurophysiology, 107(11), 2996–3007.

Nieder, A. (2016). The neuronal code for number. Nature Reviews Neuroscience, 17(6), 366.

Nieder, A., & Dehaene, S. (2009). Representation of number in the brain. Annual Review of Neuroscience, 32(Journal Article), 185–208.

Niv, Y. (2009). Reinforcement learning in the brain. Journal of Mathematical Psychology, 53(3), 139–154.

Ogawa, H. (1994). Gustatory cortex of primates: Anatomy and physiology. Neuroscience Research, 20(1), 1–13.

Ojala, K. E., Janssen, L. K., Hashemi, M. M., Timmer, M. H., Geurts, D. E., Ter Huurne, N. P., Cools, R., & Sescousse, G. (2018). Dopaminergic drug effects on probability weighting during risky decision making. Eneuro, 5(2).

O'Neill, M., & Schultz, W. (2010). Coding of reward risk by orbitofrontal neurons is mostly distinct from coding of reward value. Neuron, 68(4), 789–800.

Paulus, M. P., Hozack, N., Zauscher, B., McDowell, J. E., Frank, L., Brown, G. G., & Braff, D. L. (2001). Prefrontal, parietal, and temporal cortex networks underlie decision-making in the presence of uncertainty. Neuroimage, 13(1), 91–100.

Paulus, M. P., Rogalsky, C., Simmons, A., Feinstein, J. S., & Stein, M. B. (2003). Increased activation in the right insula during risk-taking decision making is related to harm avoidance and neuroticism. Neuroimage, 19(4), 1439–1448.

Payne, J. W., Bettman, J. R., & Johnson, E. J. (1992). Behavioral decision research: A constructive processing perspective. Annual Review of Psychology, 43(1), 87–131.

Pedroni, A., Frey, R., Bruhin, A., Dutilh, G., Hertwig, R., & Rieskamp, J. (2017). The risk elicitation puzzle. Nature Human Behaviour, 1(11), 803–809.

Pietras, C. J., & Hackenberg, T. D. (2001). Risk-sensitive choice in humans as a function of an earnings budget. Journal of the Experimental Analysis of Behavior, 76(1), 1–19.

Powell, M., & Ansic, D. (1997). Gender differences in risk behaviour in financial decision-making: An experimental analysis. Journal of Economic Psychology, 18(6), 605–628.

Preuschoff, K., Quartz, S. R., & Bossaerts, P. (2008). Human insula activation reflects risk prediction errors as well as risk. Journal of Neuroscience, 28(11), 2745–2752.

Rao, H., Korczykowski, M., Pluta, J., Hoang, A., & Detre, J. A. (2008). Neural correlates of voluntary and involuntary risk taking in the human brain: An fMRI Study of the Balloon Analog Risk Task (BART). NeuroImage, 42(2), 902–910.

Reil, J. C. (1809). Die sylvische Grube. Arch Physiol, 9, 195–208.

Reveley, C., Gruslys, A., Ye, F. Q., Glen, D., Samaha, J., E. Russ, B., Saad, Z., K. Seth, A., Leopold, D. A., & Saleem, K. S. (2017). Three-dimensional digital template atlas of the macaque brain. Cerebral Cortex, 27(9), 4463–4477.

Rigotti, M., Barak, O., Warden, M. R., Wang, X.-J., Daw, N. D., Miller, E. K., & Fusi, S. (2013). The importance of mixed selectivity in complex cognitive tasks. Nature, 497(7451), 585–590.

Salas, R., Baldwin, P., De Biasi, M., & Montague, R. (2010). BOLD responses to negative reward prediction errors in human habenula. Frontiers in Human Neuroscience, 4, 36.

Sayer, R. J., Friedlander, M. J., & Redman, S. J. (1990). The time course and amplitude of EPSPs evoked at synapses between pairs of CA3/CA1 neurons in the hippocampal slice. Journal of Neuroscience, 10(3), 826–836.

Schultz, W. (2015). Neuronal reward and decision signals: From theories to data. Physiological Reviews, 95(3), 853–951.

Schutter, D. J., & Van Honk, J. (2005). Electrophysiological ratio markers for the balance between reward and punishment. Cognitive Brain Research, 24(3), 685–690.

Sela, T., Kilim, A., & Lavidor, M. (2012). Transcranial alternating current stimulation increases risk-taking behavior in the balloon analog risk task. Frontiers in Neuroscience, 6, 22.

Seo, H., & Lee, D. (2009). Behavioral and neural changes after gains and losses of conditioned reinforcers. Journal of Neuroscience, 29(11), 3627–3641.

Seymour, B., O'Doherty, J. P., Dayan, P., Koltzenburg, M., Jones, A. K., Dolan, R. J., Friston, K. J., & Frackowiak, R. S. (2004). Temporal difference models describe higher-order learning in humans. Nature, 429(6992), 664–667.

Sharpe, W. F. (1964). Capital asset prices: A theory of market equilibrium under conditions of risk. The Journal of Finance, 19(3), 425–442.

Shiv, B., Loewenstein, G., & Bechara, A. (2005). The dark side of emotion in decision-making: When individuals with decreased emotional reactions make more advantageous decisions. Cognitive Brain Research, 23(1), 85–92.

Slovic, P. (1995). The construction of preference. American Psychologist, 50(5), 364.

Smith, B. W., Mitchell, D. G., Hardin, M. G., Jazbec, S., Fridberg, D., Blair, R. J. R., & Ernst, M. (2009). Neural substrates of reward magnitude, probability, and risk during a wheel of fortune decision-making task. Neuroimage, 44(2), 600–609.

So, N.-Y., & Stuphorn, V. (2010). Supplementary eye field encodes option and action value for saccades with variable reward. Journal of Neurophysiology, 104(5), 2634–2653.

Stauffer, W. R., Lak, A., Bossaerts, P., & Schultz, W. (2015). Economic choices reveal probability distortion in macaque monkeys. Journal of Neuroscience, 35(7), 3146–3154.

Stearns, S. C. (2000). Daniel Bernoulli (1738): Evolution and economics under risk. Journal of Biosciences, 25(3), 221–228.

Stephens, D. W. (1981). The logic of risk-sensitive foraging preferences.

Stephens, D. W. (2008). Decision ecology: Foraging and the ecology of animal decision making. Cognitive, Affective, & Behavioral Neuroscience, 8(4), 475–484.

Stevens, S. S. (2017). Psychophysics: Introduction to its perceptual, neural and social prospects. Routledge.

Stuphorn, V., Brown, J. W., & Schall, J. D. (2010). Role of supplementary eye field in saccade initiation: Executive, not direct, control. Journal of Neurophysiology, 103(2), 801–816.

Stuphorn, V., & Schall, J. D. (2006). Executive control of countermanding saccades by the supplementary eye field. Nature Neuroscience, 9(7), 925–931.

Sugrue, L. P., Corrado, G. S., & Newsome, W. T. (2004). Matching behavior and the representation of value in the parietal cortex. Science, 304(5678), 1782–1787.

Süss, H. M., & Schmiedek, F. (2000). Fatigue and practice effects during cognitive tasks lasting several hours. Zeitschrift Fur Experimentelle Psychologie: Organ Der Deutschen Gesellschaft Fur Psychologie, 47(3), 162.

Symmonds, M., Emmanuel, J. J., Drew, M. E., Batterham, R. L., & Dolan, R. J. (2010). Metabolic state alters economic decision making under risk in humans. PloS One, 5(6), e11090.

Takahashi, H., Matsui, H., Camerer, C., Takano, H., Kodaka, F., Ideno, T., Okubo, S., Takemura, K., Arakawa, R., & Eguchi, Y. (2010). Dopamine D1 receptors and nonlinear probability weighting in risky choice. Journal of Neuroscience, 30(49), 16567–16572.

Tobler, P. N., O'Doherty, J. P., Dolan, R. J., & Schultz, W. (2007). Reward value coding distinct from risk attitude-related uncertainty coding in human reward systems. Journal of Neurophysiology, 97(2), 1621–1632.

Tom, S. M., Fox, C. R., Trepel, C., & Poldrack, R. A. (2007). The neural basis of loss aversion in decision-making under risk. Science, 315(5811), 515–518.

Trepel, C., Fox, C. R., & Poldrack, R. A. (2005). Prospect theory on the brain? Toward a cognitive neuroscience of decision under risk. Cognitive Brain Research, 23(1), 34–50.

Tversky, A., & Kahneman, D. (1979). Prospect theory: An analysis of decision under risk. Econometrica, 47(2), 263–291.

Tversky, A., & Kahneman, D. (1992). Advances in prospect theory: Cumulative representation of uncertainty. Journal of Risk and Uncertainty, 5(4), 297–323.

van Duuren, E., van der Plasse, G., Lankelma, J., Joosten, R. N., Feenstra, M. G., & Pennartz, C. M. (2009). Single-cell and population coding of expected reward probability in the orbitofrontal cortex of the rat. Journal of Neuroscience, 29(28), 8965–8976.

Vermeer, A. B. L., Boksem, M. A., & Sanfey, A. G. (2014). Neural mechanisms underlying context-dependent shifts in risk preferences. NeuroImage, 103(Journal Article), 355–363.

Vermeer, A. B. L., & Sanfey, A. G. (2015). The effect of positive and negative feedback on risk-taking across different contexts. PloS One, 10(9), e0139010.

Vincis, R., Chen, K., Czarnecki, L., Chen, J., & Fontanini, A. (2020). Dynamic representation of taste-related decisions in the gustatory insular cortex of mice. Current Biology, Journal Article.

Von Neumann, J., & Morgenstern, O. (1947). Theory of games and economic behavior, 2nd rev.

Wang, L., Uhrig, L., Jarraya, B., & Dehaene, S. (2015). Representation of numerical and sequential patterns in macaque and human brains. Current Biology, 25(15), 1966–1974.

Wang, M., Rieger, M. O., & Hens, T. (2017). The impact of culture on loss aversion. Journal of Behavioral Decision Making, 30(2), 270–281.

Weber, B. J., & Chapman, G. B. (2005). Playing for peanuts: Why is risk seeking more common for low-stakes gambles? Organizational Behavior and Human Decision Processes, 97(1), 31–46.

Weber, E. U., Blais, A., & Betz, N. E. (2002). A domain-specific risk-attitude scale: Measuring risk perceptions and risk behaviors. Journal of Behavioral Decision Making, 15(4), 263–290.

Weber, E. U., & Hsee, C. (1998). Cross-cultural differences in risk perception, but cross-cultural similarities in attitudes towards perceived risk. Management Science, 44(9), 1205–1217.

Weber, E. U., Shafir, S., & Blais, A.-R. (2004). Predicting risk sensitivity in humans and lower animals: Risk as variance or coefficient of variation. Psychological Review, 111(2), 430.

Weller, J. A., Levin, I. P., & Denburg, N. L. (2011). Trajectory of risky decision making for potential gains and losses from ages 5 to 85. Journal of Behavioral Decision Making, 24(4), 331–344.

Weller, J. A., Levin, I. P., Shiv, B., & Bechara, A. (2009). The effects of insula damage on decision-making for risky gains and losses. Social Neuroscience, 4(4), 347–358.

Wittmann, M., Lovero, K. L., Lane, S. D., & Paulus, M. P. (2010). Now or later? Striatum and insula activation to immediate versus delayed rewards. Journal of Neuroscience, Psychology, and Economics, 3(1), 15.

Xue, G., Lu, Z., Levin, I. P., Weller, J. A., Li, X., & Bechara, A. (2009). Functional dissociations of risk and reward processing in the medial prefrontal cortex. Cerebral Cortex, 19(5), 1019–1027.

Yacubian, J., Gläscher, J., Schroeder, K., Sommer, T., Braus, D. F., & Büchel, C. (2006). Dissociable systems for gain-and loss-related value predictions and errors of prediction in the human brain. Journal of Neuroscience, 26(37), 9530–9537.

Yamada, H., Tymula, A., Louie, K., & Glimcher, P. W. (2013). Thirst-dependent risk preferences in monkeys identify a primitive form of wealth. Proceedings of the National Academy of Sciences, 110(39), 15788–15793.

Ye, H., Chen, S., Huang, D., Wang, S., & Luo, J. (2015). Modulating activity in the prefrontal cortex changes decision-making for risky gains and losses: A transcranial direct current stimulation study. Behavioural Brain Research, 286, 17–21.

Ye, H., Huang, D., Wang, S., Zheng, H., Luo, J., & Chen, S. (2016). Activation of the prefrontal cortex by unilateral transcranial direct current stimulation leads to an asymmetrical effect on risk preference in frames of gain and loss. Brain Research, 1648, 325–332.

Zandbelt, B. (2014). Exgauss: A MATLAB toolbox for fitting the ex-Gaussian distribution to response time data. Figshare.

Curriculum Vitae

You-Ping Yang

The Johns Hopkins University

Phone: 202-848-3076
Email: ypyang.tw@gmail.com

Education

Ph.D. in Psychological and Brain Sciences 2021
Johns Hopkins University Baltimore, MD
Thesis Advisor: Veit Stuphorn Ph.D.
Thesis Title: Primate Anterior Insular Cortex Represents Economic Decision Variables Postulated by Prospect Theory

M.A. in Psychological and Brain Sciences 2017
Johns Hopkins University Baltimore, MD
Thesis Advisor: Veit Stuphorn Ph.D.

M.S. in Biological Psychology 2011
National Taiwan University, NTU Taipei, Taiwan
Thesis Advisor: Prof. Keng-Chen Liang, Ph.D.
Thesis Title: c-Fos Expression in Rat's Brain Following Acquisition and Expression of Recent or Remote Memory in an Inhibitory Avoidance Task

B.A. in Psychology 2007
National Taiwan University, NTU Taipei, Taiwan
Certification in Neurobiology and Cognitive Science Program

Research/Work Experience

Research Assistant 2012 – 2015
Department of Physical Medicine and Rehabilitation Taoyuan, Taiwan
Chang Gung Memorial Hospital
Research Advisor: Yu-Cheng Pei, M.D.- Ph.D.

Research Assistant 2011 – 2012
Department of Psychology Taipei, Taiwan
National Chengchi University, NCCU
Research Advisor: Ruey-Ming Liao, Ph.D.

Honors and Awards

Government Scholarship for Overseas Study 2015-2019
Cognitive Neuroscience, Ministry of Education Taiwan

Excellent Teaching Assistant 2010
Outstanding Teaching Assistant 2010
Outstanding Teaching Assistant 2009
Center for Teaching and Learning Development, National Taiwan University Taipei, Taiwan

Publications

Yang, Y. P., Li, X., & Stuphorn, V. Primate anterior insular cortex represents economic decision variables postulated by Prospect theory. (in review). *bioRxiv*.

Sampson, A.L., **Yang, Y. P.**, Usher, M., Levy, D., Stuphorn, V., & Niebur E. Supplementary motor area activity in macaques performing a multi-attribute decision-making task. (in preparation).

Conference presentations

Yang, Y. P., Li, X., & Stuphorn, V. *Primate insular cortex represents contextual information that modulates risk-attitude.* Society for Neuroscience, 2019: Nanosymposium.

Yang, Y. P., Li, X., & Stuphorn, V. *Primate insular cortex represents contextual information that modulates risk-attitude.* Society for Neuroscience, 2018: Poster.

Yang, Y. P., Stuphorn, V. , & Niebur, E. *Neural Mechanism underlying multi-attribute decision making in primates.* Society for Neuroscience, 2017: Poster.

Yang, Y. P., Li, X., & Stuphorn, V. *Token asset effect on monkey's decision making involving risky gains and losses.* Society for Neuroeconomics, 2017: Poster.

Yang, Y. P., Li, X., & Stuphorn, V. *Token asset effect on monkey's decision making involving risky gains and losses.* Society for Neuroscience, 2016: Poster.

Yang, Y. P., Change, T. Y., Lai, H. Y., & Pei, Y. C. *Proprioceptive input of hand conformation is a constraint of multi-digit motion processing.* Society for Neuroscience, 2014: Poster.

Yang, Y. P., & Liang, K. C. *Regional Specific c-Fos expression in formation and expression of inhibitory avoidance memory.* Society for Neuroscience, 2012: Poster.